INFLUENCE OF SOURCE PARAMETERS ON THE PROPERTIES OF A PLASMA JET

by

GRETCHEN ELYSE GRAHAM EDELMON, B.S.E.E.

A THESIS

IN

ELECTRICAL ENGINEERING

Submitted to the Graduate Faculty
of Texas Tech University in
Partial Fulfillment of
the Requirements for
the Degree of

MASTER OF SCIENCE

IN

ELECTRICAL ENGINEERING

Approved

Accepted

May, 1991

ACKNOWLEDGEMENTS

I would like to express my gratitude to Dr. Klaus W. Zieher for the opportunity to work on this project. I appreciate his leadership and support throughout the duration of this endeavor. I also thank Dr. M. K. Kristiansen and Dr. Carlton Whitehead for serving on my committee. I must also thank Dr. Tommy Burkes and Dr. Glenn McDuff for helping me to realize the importance of an advanced degree in the first place, without them I would not have continued into graduate school. The financial support from the Air Force Office of Scientific Research is greatly appreciated.

I am most appreciative of the Pulsed Power Lab staff who are always willing to give assistance and advice. I especially thank Mr. Lonnie Stevenson for his invaluable assistance in the machine shop. Mike Grothaus and David Buraczyk were inexpressibly helpful. They were always there to answer any questions and help with any problems when I started working on this project. I would like to thank my fellow graduate students for their support and I wish them all continued success. Without them it would not have been nearly as much fun. I especially miss "the old group": Tommy Cavazos, Kevin Harris, Gordon Masten, Michele Wofford and Ken Bynum.

Finally, I want to sincerely thank my whole family for their love and support throughout my college years. The encouragement from them always motivated me to keep in good spirits even when things didn't seem so great. I save my warmest regards for my husband and best friend, Brian.

TABLE OF CONTENTS

ABSTRACT

In the Plasma Edge Cathode scheme, a nearly stationary plasma cathode is formed by partially obstructing a well directed plasma with a material edge. Electrons are extracted in a direction normal to the flow of plasma. An electron current density of 100 A/cm^2 is theoretically possible. In order to achieve this desired current density, certain temperature, density, and ionization levels are required in the plasma.

The motivation for the work discussed in this thesis, is to determine how changes in the source parameters affect these plasma characteristics. The plasma source consists of an RC storage circuit charged to 20 kV and a triggered switch. When the switch is triggered, a surface flashover occurs over a coaxially arranged dielectric to produce the plasma. The source dielectric material and geometry, charging voltage polarity, and the charge circuit inductance are the parameters which will be varied.

The emphasis in this work has been on the development of a triple Langmuir probe and the corresponding circuitry to diagnose the temperature of the plasma. Faraday cup probes and a time of flight mass spectrometer are also used as diagnostics to find the plasma composition and velocity of the various species. The data acquisition is automated by the use of an HP Vectra computer and three HP digital oscilloscopes. The program sets up the oscilloscopes to perform the measurements and then transfers the data to the computer for analysis.

The resulting data are compared in order to better understand the optimum source arrangement for the Plasma Edge Cathode system.

LIST OF TABLES

LIST OF FIGURES

CHAPTER I

INTRODUCTION

The plasma which has been studied in this work is generated by a surface flashover in vacuum. A triggered spark gap discharges stored energy from a capacitor bank across a coaxially arranged dielectric surface. The Plasma Edge Cathode (PEC) scheme [1,2,3] creates a stationary plasma cathode by partially blocking the flow of the plasma jet with a straight edged obstacle. A stationary plasma cathode is formed by blocking the flow of a well directed plasma with a straight edged obstacle. Electrons are extracted transversely to the plasma flow from the resulting cathode created by the stationary plasma edge. Current densities of up to 100 A/cm^2 are theoretically possible [1,2]. The concept of the Plasma Edge Cathode is shown in Fig. 1.

In order for the PEC to achieve the high electron current density which is promised by the theory, certain conditions must be met. First, the velocity of the plasma must be great enough to allow for a stationary boundary. With higher velocities, the plasma edge will exhibit less curvature over the axial distance. Second, the ion species should have a high mass to charge ratio. Heavier ions will have greater momentum, suffering less deflection behind the edge. Finally, the plasma must have a sufficient density to allow for electrons to be extracted and still maintain space charge limitations.

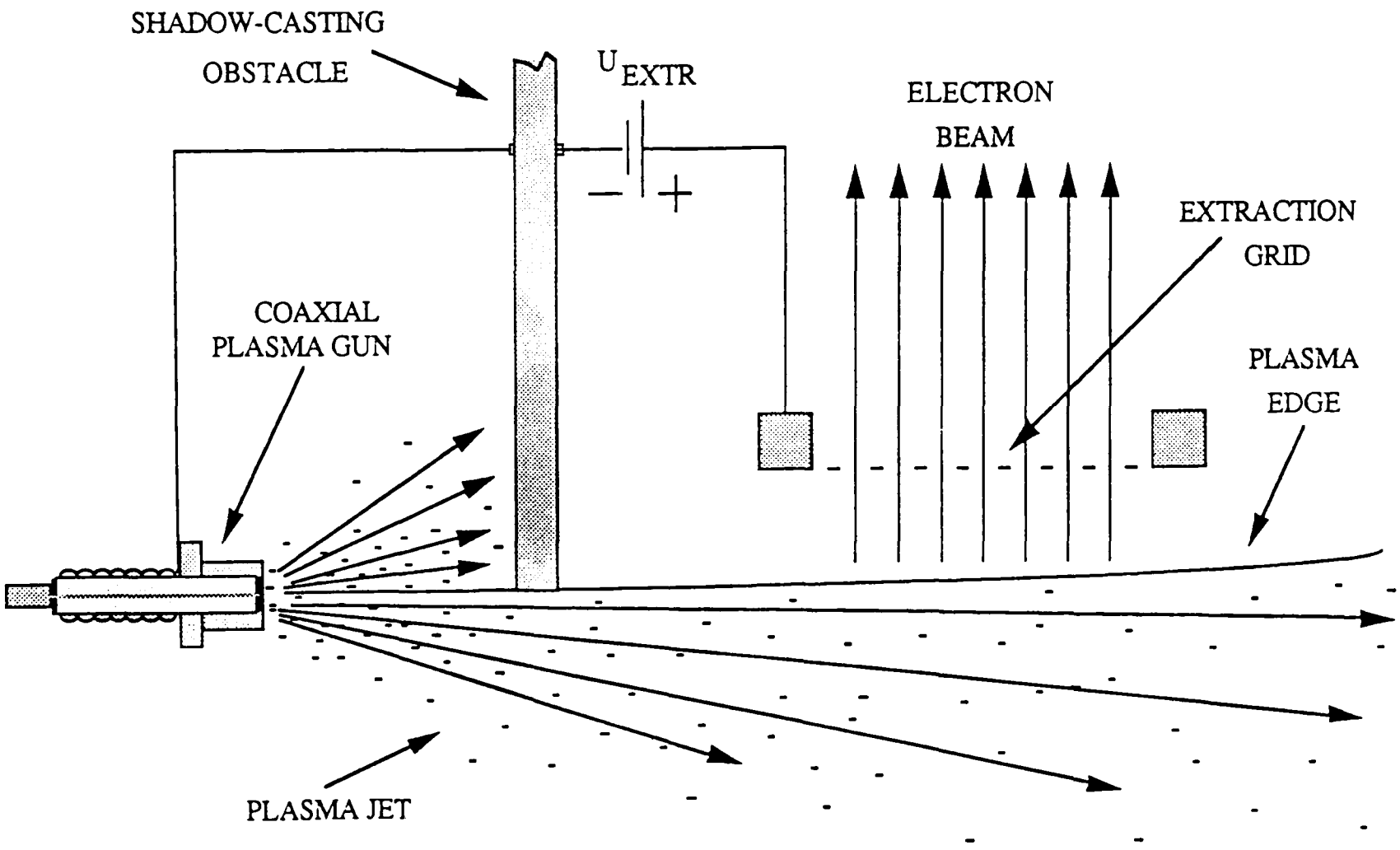

Fig. 1
Concept of a Plasma Edge Cathode [3]

The following relationship between the source limited current density, j_{max}, and the plasma density, n, can be derived [3]:

$$n \geq \frac{j_{max}}{e} \left(\frac{k\, T_e}{2\, \pi\, m_e} \right)^{\frac{1}{2}} \quad , \tag{1.1}$$

where k is the Boltzmann's constant, T_e is the electron temperature, and e and m are the electron charge and mass, respectively. Thus, for a current density of 100 A/cm^2 to be achieved at a temperature of kT_e = 1 eV, the density must be 4 x 10^{13} cm^{-3}.

The plasma boundary motion can be approximated in the moving reference frame by investigating a one-fluid, one-dimensional plasma expansion. The momentum conservation and the continuity equations describe the motion [2,3].

$$\rho \frac{d\,\vec{v}}{dt} = -\Delta\, p \tag{1.2}$$

$$\frac{\partial n}{\partial t} = -\Delta(n\vec{v}) \quad . \tag{1.3}$$

These equations can be written in one dimension as

$$\frac{dv_x}{dt} = \frac{-(1 + z)\, k\, T_e}{M_i} \gamma \left(\frac{n}{n_o} \right)^{(\gamma - 2)} \frac{\partial \left(\frac{n}{n_o} \right)}{\partial x} \quad , \tag{1.4}$$

and

$$\frac{\partial n}{\partial t} = -v_x \left(\frac{\partial n}{\partial x} \right) - n \left(\frac{\partial v_x}{\partial x} \right) \quad , \tag{1.5}$$

where $\gamma = (2 + N)/N$, with N being the number of degrees of freedom and z is the charge state. For adiabatic expansion, γ is 5/3. The expression in Eq. (1.4) is of the form F=ma. Since distance can be related to acceleration by

$$s = \frac{1}{2} a t^2 \quad , \tag{1.6}$$

where s is the distance that the boundary expands in the transverse direction during the time t. With t written as D/v_z, where D is the distance the particle will travel in the axial direction due to its velocity in that direction, v_z, the following expression can be obtained.

$$\Delta s = \left(- \frac{(1 + z)\, k\, T_e\, 1.67\, \frac{1}{2}}{M_i\, 10^{-2}} \right) \left(\frac{D}{v_z} \right)^2 \quad . \tag{1.7}$$

From Eq. (1.7), it can be seen that Δs is proportional to one plus the charge state divided by the kinetic energy of the plasma. Thus, the higher the kinetic energy, the smaller the expansion. In order to make an estimate of required particle energies from Eq. (1.7), the half density point, or $n/n_o \sim .5$, can be combined with a typical temperature of $kT_e = 1$ eV and

$$\frac{\partial \left(\frac{n}{n_o} \right)}{\partial x} \sim \frac{1}{1\ cm} \quad .$$

Further, it is desired that $\Delta s \leq .5$ cm and the travel distance can be taken as ~5 cm. With these assumptions, one can determine the minimum velocity that a particular ion species must have in order to successfully traverse the extraction gap. The minimum energy required is approximated by Eq. (1.8).

$$\frac{1}{2} M_i v_z^2 \geq (1 + z) (6.667 X 10^{-19}) \quad [J] \tag{1.8}$$

For O^{3+}, an ion typically found in this plasma, this expression translates to a minimum velocity of 1.41 cm/μs. This requirement will be considered again when the velocities and species are known for each of the source configurations in order to make an assessment of the optimum set-up.

The objective for this diagnostic work was to gather information about how changes in the source parameters affect the physical plasma parameters of interest. Specifically, the gun geometry, arc current polarity, and stored energy were varied. Probes for measuring density, temperature and plasma species were used which are based on particle flux measurements [4]. Biased Faraday cup probes were used to detect plasma density and velocity, a triple Langmuir probe was used to measure electron temperature, and a time-of-flight arrangement was used to determine the plasma ion species and their initial velocity [5]. The Faraday cup probes and the time-of-flight measurements will be discussed along with the overall system set-up in Chapter II. The triple Langmuir probe will be discussed separately in Chapter III. The experimental results will be discussed in Chapter IV.

CHAPTER II

EXPERIMENTAL SETUP: PART I

The plasma source system used in this experiment is identical to the PEC system which is being researched concurrently at Texas Tech University, with the exception of the time-of-flight measurement portion. An evacuated Pyrex chamber contains a plasma gun, a drift chamber, an accelerating gap, a second drift chamber, and a particle detector at the downstream end. As the plasma moves away from the source, it encounters diagnostic probes which are inserted into the vacuum through Cajon fittings. The probe and detector signals are recorded by a computer controlled Hewlett Packard digital oscilloscope. The structure is evacuated to a pressure of 1 x 10^{-6} Torr with a Varian diffusion pump. The system arrangement is shown in Fig. 2.

Plasma Gun

Six parallel .05 μF capacitors were arranged in a coaxial configuration between two aluminum plates. At the center, a solid copper rod holds a pressurized spark gap in line with a spark plug. The capacitors were charged to voltages between $\pm$30 kV by a Hippotronics high voltage supply. The spark gap, Physics International Model 670, is triggered using a Pacific Atlantic PT-55 Trigger Generator which converts a 300 V input pulse into an output trigger of approximately 50 kV. The source arrangement is depicted in Fig. 3.

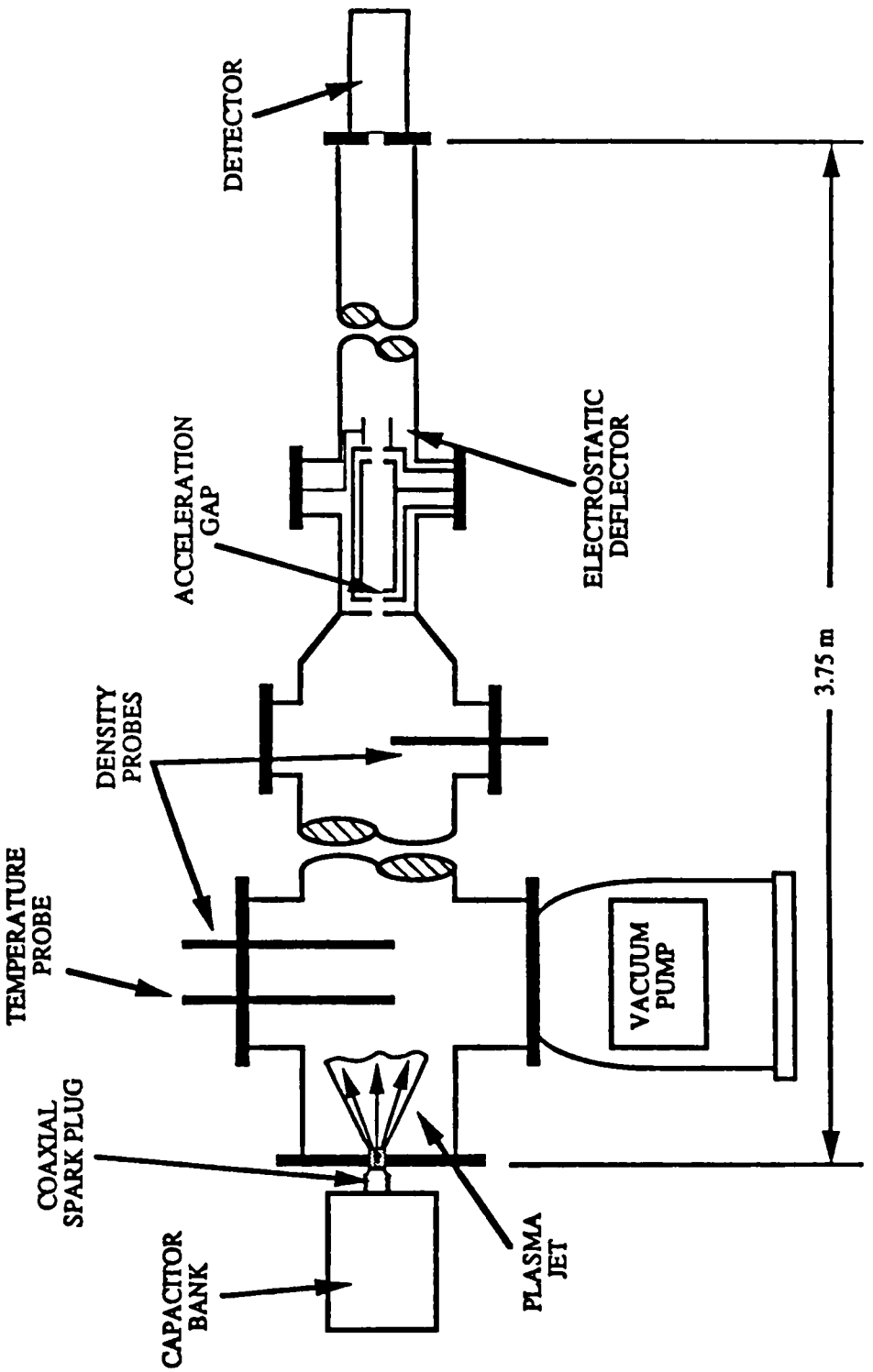

Fig. 2
Experimental Arrangement

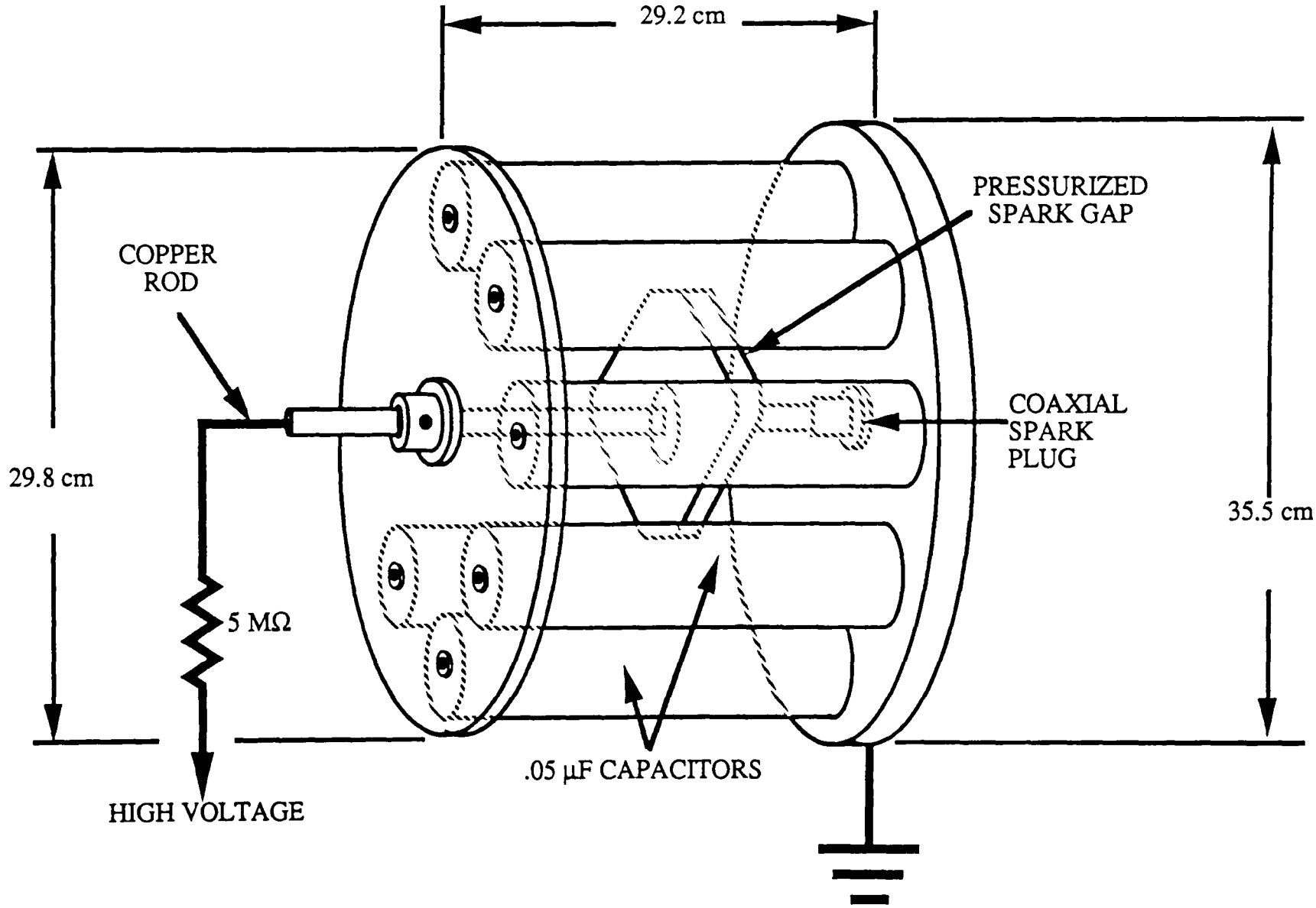

Fig. 3
Plasma Source Configuration

The source circuit can be analyzed as an RLC circuit. The current through the loop is given by

$$I(t) = \frac{V(0)}{\omega_o L} e^{-\alpha t} \sin(\omega_o t) \quad , \tag{2.1}$$

where ω_o is the ringing frequency and α is the damping factor.

The ringing discharge was detected using a dB/dt probe terminated into 50 ohms. The discharge is underdamped and the circuit inductance and resistance were calculated from the waveform. The resistance and inductance were calculated for each source configuration. The ringing frequency calculated from the measured curves remained the same for all charging voltages. Since,

$$\omega_o = \left(\frac{1}{L C}\right)^{.5} , \tag{2.2}$$

for an RLC circuit, the inductance is constant for each source configuration considered. The damping factor was also constant for each set-up, indicating a constant resistance.

As previously mentioned, the plasma source is a coaxially arranged spark plug. More specifically, the spark plug used is a Champion L76V with an insulator composed of 90% Al_2O_3, 7% SiO_2, and unspecified small percentages of MgO, CaO, and Zr. The outer conductor is made of carbon steel and the inner conductor is composed of 91% W, 6% Ni, and 3% Cu [5]. For geometry variation, a conical coil was attached to the outer conductor of the spark plug. A physical representation of the coil is shown in Fig. 4. It was indicated in experimental findings by C. Mendel

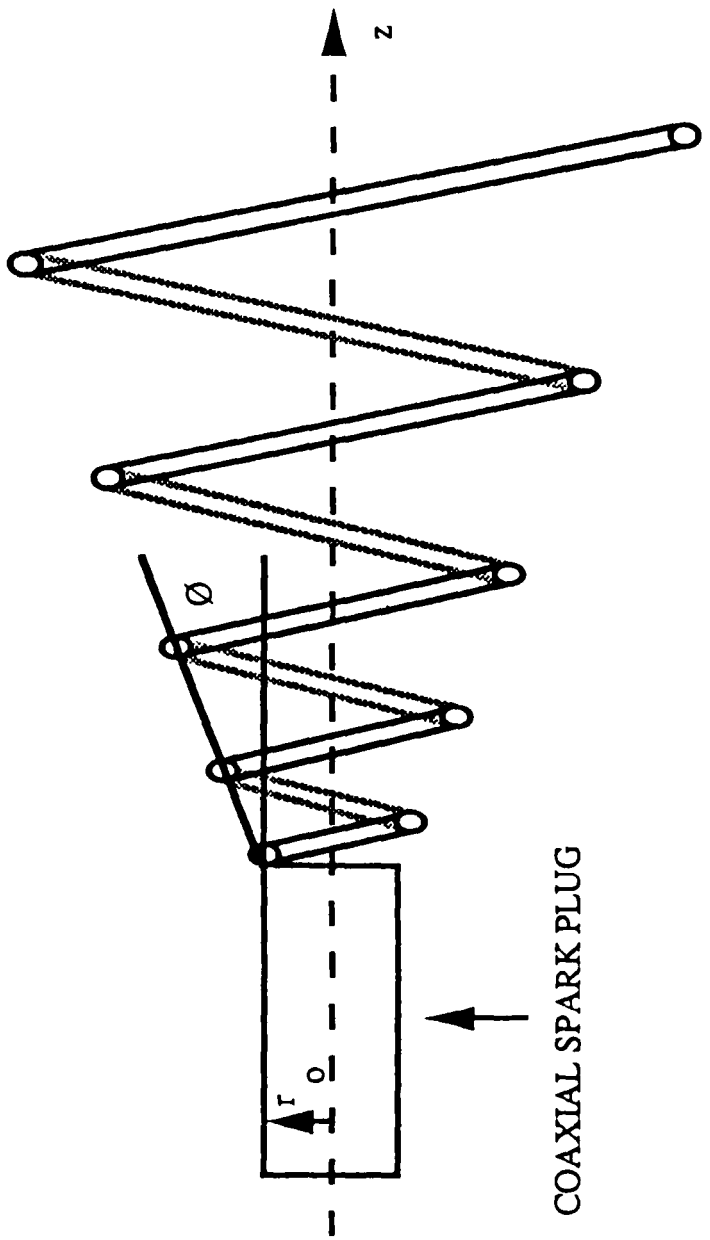

Fig. 4
Conical Gun Geometry

that the coil could generate a faster and more directed plasma flow [6,7]. The coil used in this experiment consisted of 8 turns on a cone with a pitch of 15°. The spacing between turns was approximately .4 cm for a total length of 3.2 cm.

Density Probes

The two Faraday Cup probes used in this experiment were made of 1/2" copper tubing housing a brass center conductor rod held in place by nylon washers. The collecting aperture of each probe was 1 mm in diameter to allow the ions to enter the probe. A 4 mm diameter collector cavity is drilled in the brass rod. A BNC connector was attached to the end of the probe to allow for biasing and measurement connections. The bias voltage of the ion collector must be negative enough to repel electrons. In this case, -50 V was used and the probe dimensions and bias circuit are shown in Fig. 5. The 33 kΩ resistor insulates the current signal from the DC power supply. Also, the 1 μF capacitor isolates the DC bias from the scope. The 50 Ω termination together with the coupling capacitance, results in a 50 μs time constant which is sufficient for the duration of plasma in this experiment. The first probe was placed at 25.4 cm from the source and the second at 131.4 cm. The velocity can be determined by measuring the time the plasma takes to reach each probe. The ion density, n_i, of the plasma is related to the collected current by,

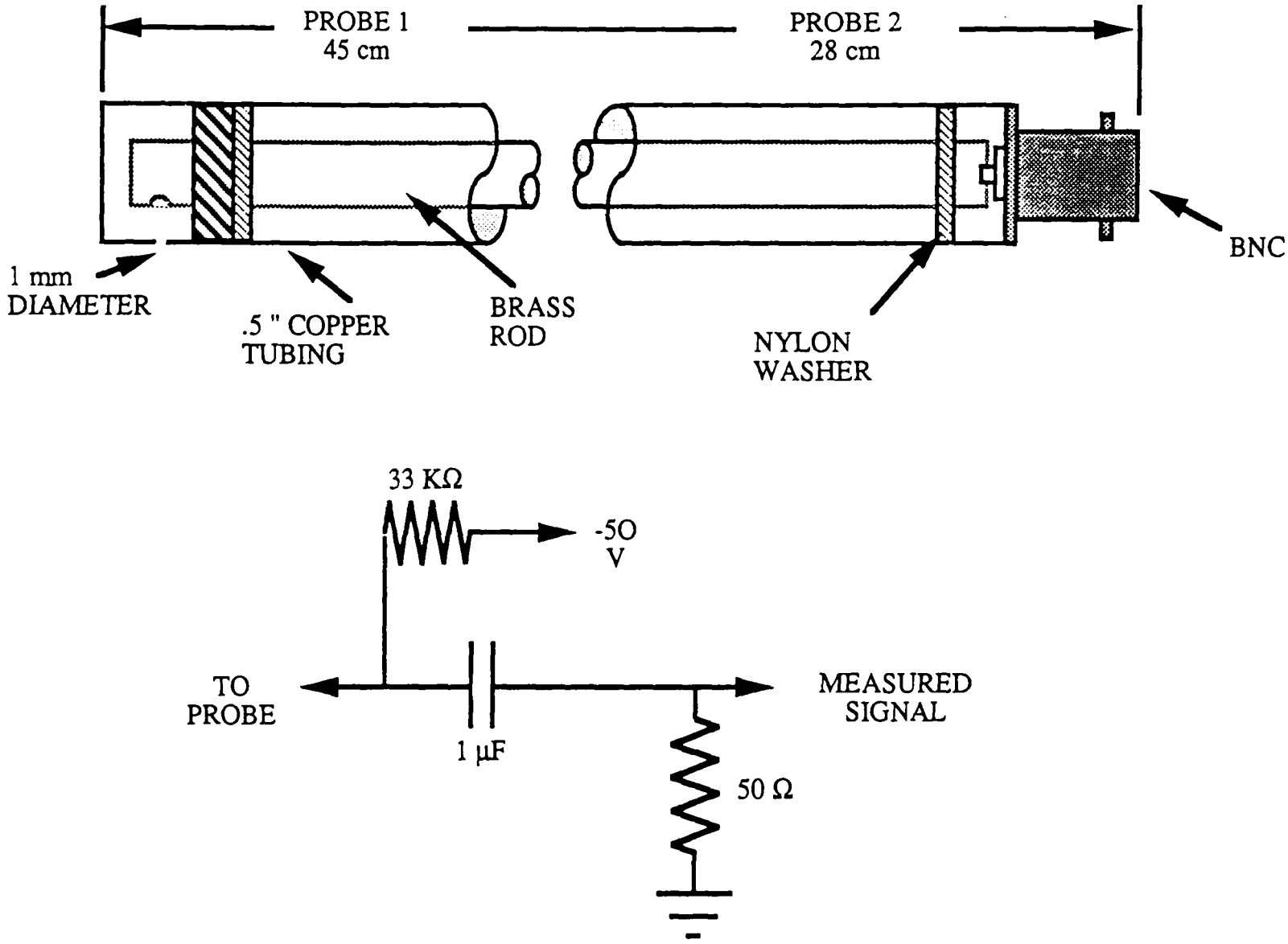

Fig. 5
Faraday Cup Flux Probes
(a) Probe Dimensions (b) Probe Biasing Circuit

$$I = n_i \, z \, A \, e \, v \quad , \tag{2.3}$$

where z is the charge state, A is the probe aperture, e is the charge of an electron and v is the velocity of the detected plasma. The plasma ions in this experiment are multiply ionized so a particular value of z cannot be used to represent the entire plasma. However, since $n = n_e = z\, n_i$, the equation can be rewritten as

$$n_e = \frac{I}{Aev} \quad . \tag{2.4}$$

Plasma probes are somewhat inaccurate due to secondary electron emission. Neglecting this occurrence results in a relatively small error, less than 20% [8,9].

Species Detection by Time-of-Flight Measurements

The method chosen to determine the ion species was a time-of-flight mass spectrometer, which was adopted from a previous experiment [5]. At a distance of 181 cm from the source, the plasma ions encounter an acceleration gap. The gap is formed by two concentric cylinders (Fig.2). The inner cylinder is pulsed with a negative 3000 V pulse for a duration of 110 ns. A 13 m cable is charged to -6000 V in order to produce the acceleration pulse. A delay generator, which is triggered by a trigger monitor output located on the PT-55, discharges the stored cable energy through a KN-6B Krytron tube into a 50 Ω load at the set delay time. In order to ensure that plasma ions and electrons do not reach the detector before and after the acceleration pulse, an electrostatic deflector is incorporated into the system. The open end of the -6000 V charged line is used to create an electric field between the

deflection plates behind the acceleration cylinders. The resulting qE force will deflect the plasma off center. During the acceleration pulse, the deflector is turned off and the accelerated ions pass safely.

The detector is located 193.6 cm away from the acceleration gap. The detector is an EMR Model 510W-16-03900-M2 Particle Detector/Electron Multiplier. The output voltage from the detector is amplified by a factor of 12 in order to display the species induced spikes on the oscilloscope.

Now that the species have been accelerated and detected, the signal must be analyzed to determine which ions were detected. The group of particles which are entering the acceleration gap at a given time, will all have approximately the same initial velocity, v_i, and will be accelerated by the same potential. After acceleration, the time, t, it will take an ion with a mass, m_i, and a charge, q, to traverse a given distance is

$$t = L \sqrt{\frac{m_i}{2\,q\,U + m_i\,v_i^2}} \quad , \tag{2.5}$$

where U is the accelerating potential. Since the particles in this case have different ionization states, the energy imparted to them will be proportional to their charge state. In other words, a particle will gain qU = zeU energy as it passes through the acceleration gap. One can replace m with M x amu. From Eq. (2.5) and the substitutions just mentioned, one can derive the mass to charge ratio as

$$\frac{M}{z} = \frac{e}{amu} \frac{2\,U}{\frac{L^2}{t^2} - v_i^2} \quad . \tag{2.6}$$

The initial velocity is calculated from the delay time. By measuring the time the spikes are detected, the mass to charge ratio can be calculated. The travel time and output voltage are calculated and printed by the program that controls the oscilloscope. These data are then input into a program which allows the user to vary the initial velocity and the acceleration voltage in order to calculate the most accurate ratio. Neither of these quantities were varied by more than 1%.

CHAPTER III

EXPERIMENTAL SETUP: PART II

Temperature Measurements

In addition to density, velocity and composition, the plasma temperature was determined. The method of measuring temperature which was used was a Langmuir probe. A Langmuir probe is typically a wire biased negative with respect to the plasma. A sheath forms around the probe into which ions will enter [10]. If the probe surface area, A, is known and the ions are assumed to have a drift velocity $\geq (kT_e/M_i)^{1/2}$, the ion current which will be collected is

$$I = n_s\, e_o\, A \left(\frac{kT_e}{M_i}\right)^{\frac{1}{2}} , \tag{3.1}$$

where n_s is the plasma density at the edge of the sheath. The sheath density is approximated by $\frac{1}{2}\, n_o$ [10]. When this substitution is incorporated into in Eq. (3.1) the result is referred to as the Bohm current, or ion saturation current:

$$I_B \simeq \frac{1}{2}\, n_o\, e_o\, A \left(\frac{k\, T_e}{M_i}\right)^{\frac{1}{2}} . \tag{3.2}$$

For a single wire, the saturation ion current density to the probe (Eq. (3.2)) is nearly independent of the probe potential as long as the probe is biased negative with respect to the space potential.

Most often, Langmuir probes are constructed with one or two electrodes. For a symmetrical probe two wires must have equal areas. With a floating double probe, one of the wires is biased negatively with respect to the second wire and the probe housing is allowed to float relative to the plasma. By varying the potential difference, v_d, and recording the corresponding waveforms, a curve of probe current vs. potential difference can be obtained. From a semi-log plot of ln I vs v_d the electron temperature can be calculated form the slope of the curve. Generating this curve requires a series of shots at each bias voltage. Since the plasma density varies from shot to shot, the measured current for several shots are averaged together for each potential difference. In order to get a smooth curve, the bias increment should be small. Typically, 100 shots are required to generate a smooth curve of averaged values. In addition, each of these shots must be measured at the same point in the plasma envelope.

Since the idea in this project was to see how plasma parameters change with changes in the source configuration, it would be inefficient to take around 100 shots for each set-up just to get the temperature. In order to reduce this time consuming process, the Langmuir probe theory was extended to a triple probe method discussed by Sin-Li Chen [11,12]. In the triple probe configuration, three parallel wires are placed into the plasma. The outer two wires are biased negatively with respect to the center wire at different potentials. The current signals on the outer electrodes are recorded on the oscilloscope. This is analogous to recording two points on the double probe curve simultaneously. This allows for the temperature to be calculated

from the data of a single shot with accuracy comparable to the double probe measurements.

Triple Probe Theory

The theory is similar to that of the double probe. Again, the probe areas are taken to be equal. The three electrodes were placed in a parallel orientation with separation between each wire on the order of 1 mm or less. The spacing turns out to be quite important to the measured results as will be discussed later. The arrangement is shown in Fig. 6. By placing negative bias voltages on the outer probes with respect to the center probe, the potentials of those probes will be lower than the floating potential. Thus, the currents which flow into them will be mainly positive ion current. On the other hand, the inner probe will collect electron current. Using the assumed current directions shown in Fig. 6 [p. 21] the following relationship is obtained

$$I_1 = I_2 + I_3 \quad . \tag{3.3}$$

As usual with probe theory, the electron distribution in the plasma is assumed to be Maxwellian, the mean free path of the electrons is significantly larger than the ion sheath thickness as well as the probe radius, and the ion sheath thickness is smaller than the probe separation distance [11]. In this experiment, the probe radius was 3.81×10^{-2} cm. The mean free path was calculated to be 2.4 cm and the ion sheath thickness is 7.4×10^{-4} cm. These values make the aforementioned assumption valid.

The instantaneous probe currents flowing into the probes can now be written as [11]

$$-I_1 = -S J_e e^{\left(-\frac{e_o V_{P1}}{k T_e}\right)} + S J_i (V_{P1}) \quad , \tag{3.4}$$

$$I_2 = -S J_e e^{\left(-\frac{e_o V_{P2}}{k T_e}\right)} + S J_i (V_{P2}) \quad , \tag{3.5}$$

and

$$I_3 = -S J_e e^{\left(-\frac{e_o V_{P3}}{k T_e}\right)} + S J_i (V_{P3}) \quad , \tag{3.6}$$

where

$$J_e = n_e \left(\frac{k T_e}{2 \pi m_e}\right)^{\frac{1}{2}} \quad . \tag{3.7}$$

In the equations above, J_e is the electron saturation current density, J_i is the ion saturation current density, and S is the surface area of the probe. As mentioned previously, it is assumed that the ion saturation current density is constant with respect to changes in the bias potential. In actuality, there is some error associated with this assumption. For an electron temperature measurement, the error is negligible for temperatures less than 10 eV [11]. Since it was known from Ref. 3 that the expected temperatures were on the order of 1 eV, the measurement should have little error. The measured results confirm that the triple probe measurement is within the expected temperature range. These results will be discussed in a following section.

By setting Eq. (3.4) equal to Eq. (3.5) and Eq. (3.6) and solving the two resulting equations for S, along with

$$V_{P2} - V_{P1} = V_2, \text{ and } V_{P3} - V_{P1} = V_3, \tag{3.8}$$

the following relationship is found

$$\frac{I_1 + I_2}{I_1 + I_3} = \frac{1 - e^{\left(-\frac{e_o V_2}{k T_e}\right)}}{1 - e^{\left(-\frac{e_o V_3}{k T_e}\right)}} \quad . \tag{3.9}$$

Since the relationship is known between I_1 and the outer probe currents, I_2 and I_3, the temperature can be determined from a measurement of any two of the three currents. In Eq. (3.9) T_e cannot be solved for explicitly. A table look-up method was employed in the analysis program to match measured ratios with calculated ratios in order to find T_e. Fig. 7 shows a graphed version of the table showing the correlation between T_e and the left side of Eq. (3.9) for V_2=2.5 V and V_3=4 V. The analysis program is listed in the Appendix.

Practical Considerations

The probe dimensions are shown in Fig. 8. This probe was constructed in a similar manner to that of the density probes. The probe housing is, again, ½". Three tungsten wires were arranged in parallel and held in place with epoxy at the vacuum end of the probe. Since tungsten cannot be soldered to copper wire, crimp connectors were used to attach the wires to insulated copper wire for circuit connections. Instead of attaching a single BNC connector onto the tubing, an

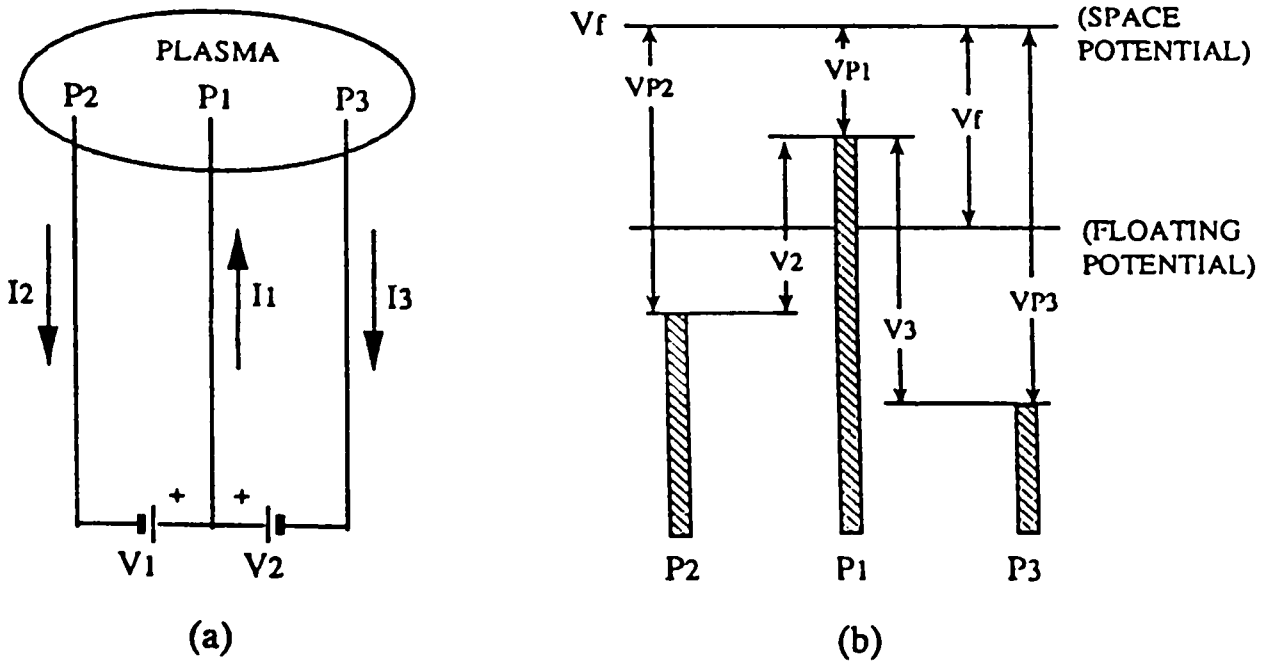

Fig. 6
Triple Probe Current and Voltage Orientation
(a) Current Directions (b) Potential Relations

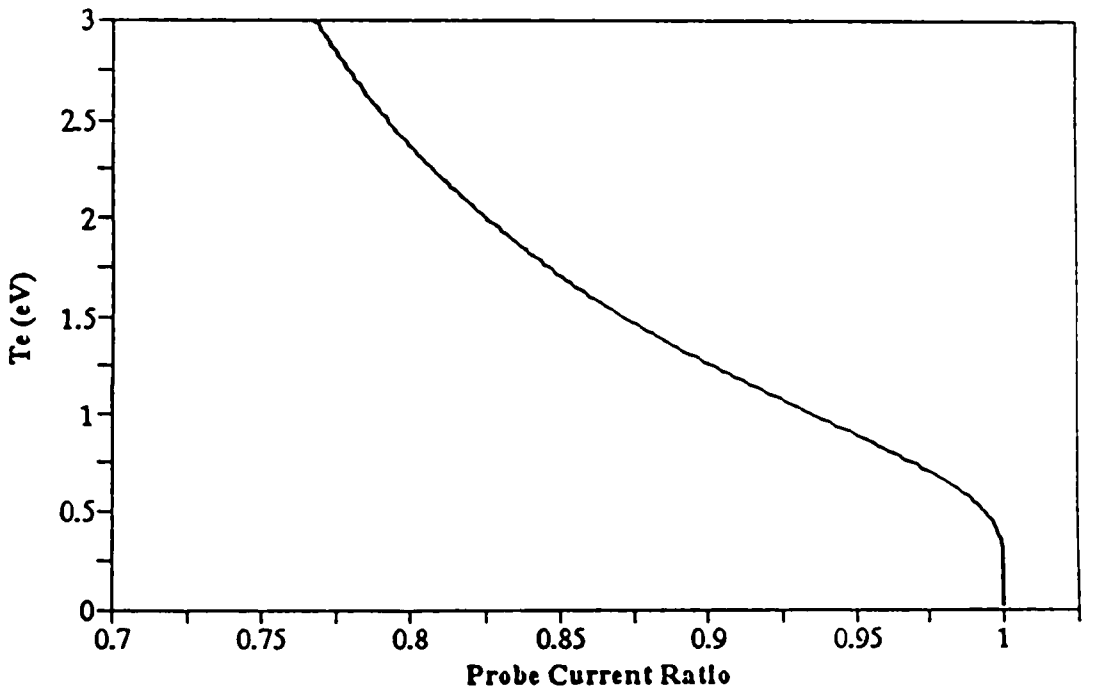

Fig. 7
Relationship Between T_e and the Current Ratio for V_1=2.5 V and V_2=4.0 V

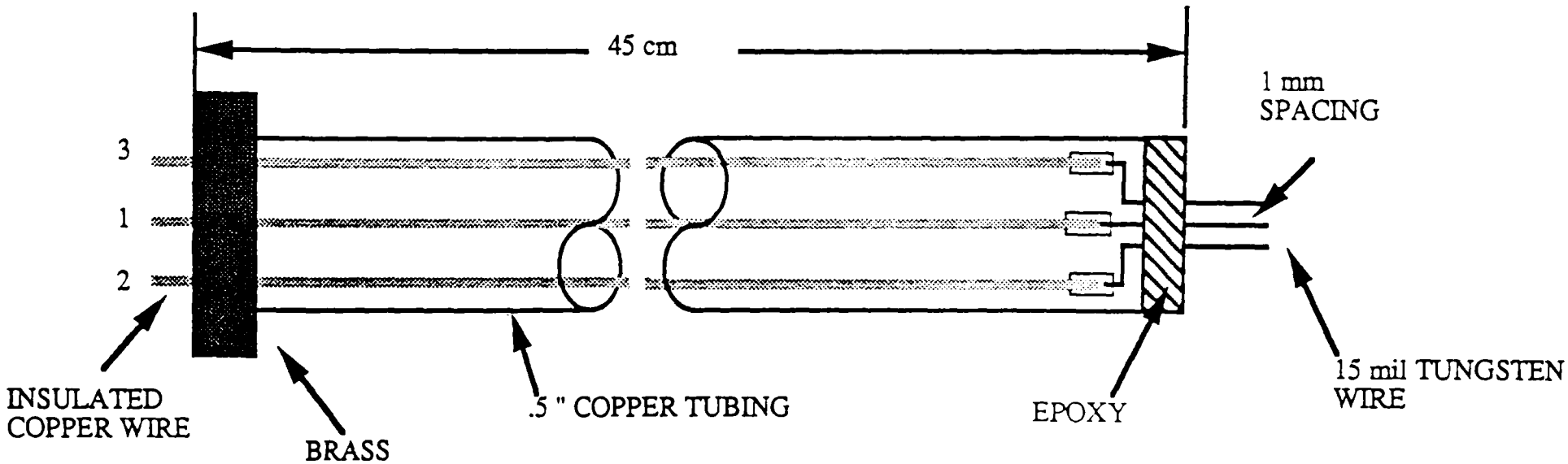

Fig. 8
Triple Langmuir Probe Construction

aluminum box with two isolated BNC feedthrough connectors was used for scope connections. Isolated BNC's are required since the probe housing must be allowed to float with the plasma and not be grounded through the box. Each of the output terminals connects to another box which holds the current sensing circuit. The complete circuit is shown in Fig. 9. A 1:1 Mini Circuits T1-6T transformer was used to monitor the current collected by the probes. The bias voltage was generated by using a battery and a 50 kΩ potentiometer in parallel with a capacitor. The capacitor provides for a time constant of 27.6 μs, with the 13.8 Ω load, so that the bias voltage will be constant throughout the pulse. The transformers have a frequency range of .003 MHz to 300 MHz. The bandwidth was the most important consideration in selecting a transformer. The rise time of the plasma pulse is on the order of 100 ns and the pulse duration is generally 25 μs at 25.4 cm from the source. Thus, the necessary frequency range was 40 KHz to 10 MHz. For the chosen transformer, the insertion loss is less than 1 dB for 20 KHz to 50 MHz.

When the probe was placed in the system for the first time, a significant undershoot was seen at the end of the pulse. It was suspected that the R/L time constant of the circuit was not long enough to allow the entire signal to be measured. By introducing a square current pulse, the transformer inductance was calculated by measuring the time that it took for V_o/V to reach 1/e. The resulting inductance of the transformer was found to be 1.2 mH. Although, it was not possible to simulate a pulse exactly like that of the plasma pulse to test the transformer output versus the input, a square pulse would show the dependence of circuit performance on the load

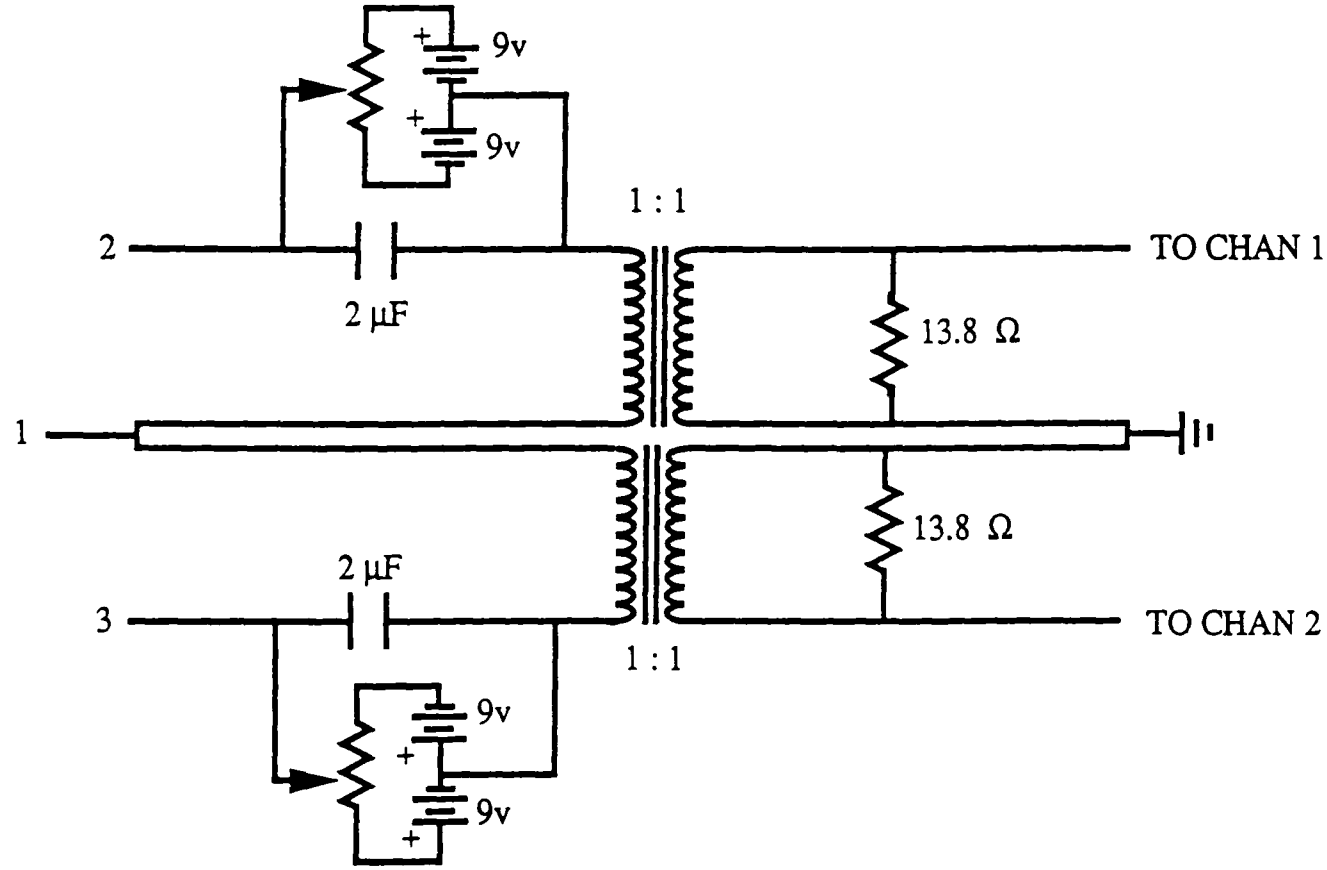

Fig. 9
Triple Langmuir Probe Circuit Schematic

resistance. Using PSPICE, a simulation with a square input pulse as the probe current source was implemented to see how the output resistance affected the circuit output voltage. The results of this simulation are shown in Fig. 10. It is obvious that lower load resistances significantly reduce the undershoot. The lowest resistance which can be used in the secondary of the transformer, according to the Mini Circuits data sheet, is 12.5 Ω. So, two 25 Ω, 10% tolerance, resistors were placed in parallel as the load. The actual resistance value turned out to be 13.8 Ω. When measuring the temperature, it is important to remember that even though the undershoot is reduced, some information may still be lost towards the end of the pulse as the waveform decays. As a result, the measurement may be more accurate for the faster portion of plasma. Thus the most accurate segment of the measured current pulse is expected to be around 15 μs, which will give an ample amount of temperature data.

Another problem which was encountered in the first trial measurements involved the spacing of the probe wires. If the same bias voltage is established at each probe, they should each collect the same amount of current. Initial tests showed that this was not the case. By examining Eq. (3.2), the only variable which would likely cause different currents on symmetrical probes is the plasma density. In this case, the probes were separated by approximately 3 mm, resulting in a separation between the two outer probes on the order of 6 mm. In Ref. 5, D. Buraczyk found that the density 1 cm from the center of the plasma jet was 80% of

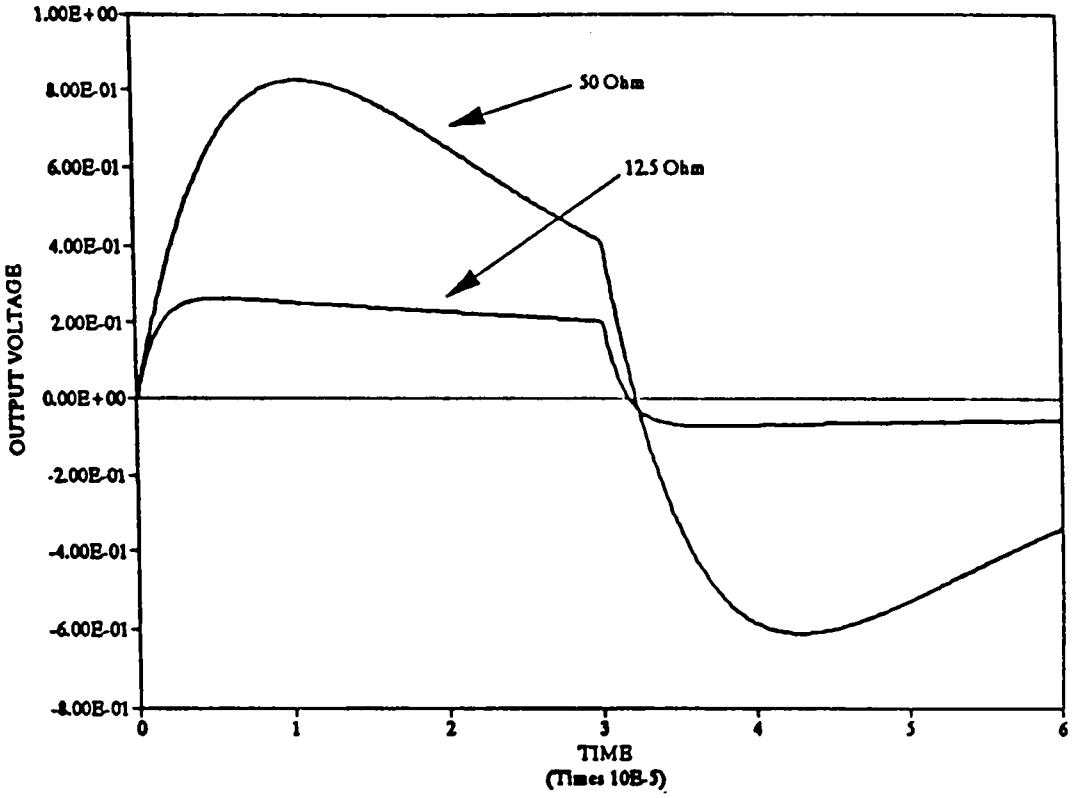

(a)

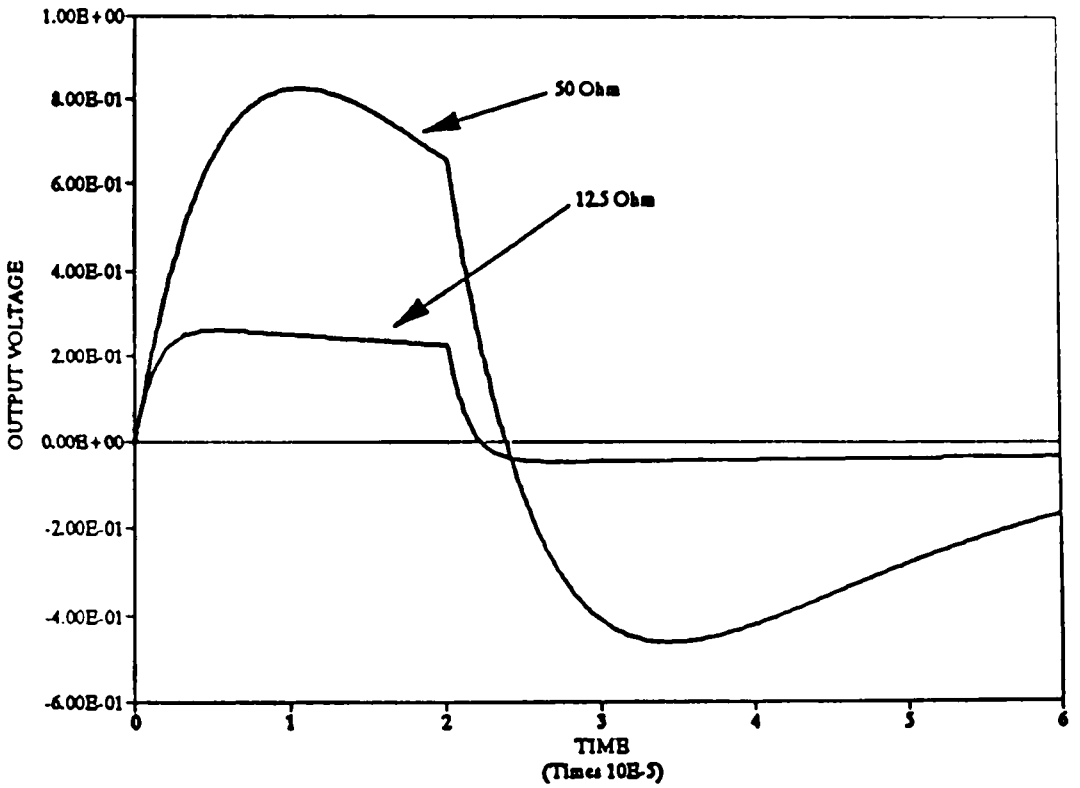

(b)

Fig. 10
SPICE Simulation Output
(a) 30 μsec Input Pulse (b) 20 μsec Input Pulse

the density at the center. With this type of gradient, the measured currents may also vary. For example, if the density across the probe is considered constant, typical currents of 24 mA and 33 mA would give a ratio of .9. For bias potentials of 2.5 V and 4 V, this corresponds to a temperature of 1.2 eV. If the density varies across the probes with the mentioned gradient, the probe located in the higher density could draw a current of 1.06 times greater. Likewise, the probe positioned in the lower density might draw only .94 times as much current. Using 24 mA and 33 mA as the currents for an ideal case and the numerical factors just mentioned, the new ratio would be .93. This value corresponds to a temperature of 1.02. Thus, the density gradient observed in this system could cause temperature measurement variations for probe separations approaching 1 cm. When the spacing was reduced to 1 mm, the currents collected for identical biasing were equal. Since the triple probe method relies upon the ratio of the two measured currents, it is crucial that the probes be subjected to identical plasma conditions. A typical probe current measurement from the final probe is shown in Fig. 11.

One important consideration with a diagnostic probe is reproducibility. Also in this case, it was necessary to make sure that the probes were really symmetrical. First, measurements were taken with the probe in an orientation transverse to the plasma flow and then the probe was turned 180° for a second measurement. The biasing potentials were left in the same spatial orientation as with the first measurement. For all cases, the calculated temperature was equal within <5%, illustrating the symmetry of the probe. Fig. 12 shows two temperature curves, one

PROBE #1 2.5 VOLTS. PROBE #2 4 VO
TIME DELAY OF 2 μSEC SHOT # 8M

TIMEBASE- 5 uSEC/DIV

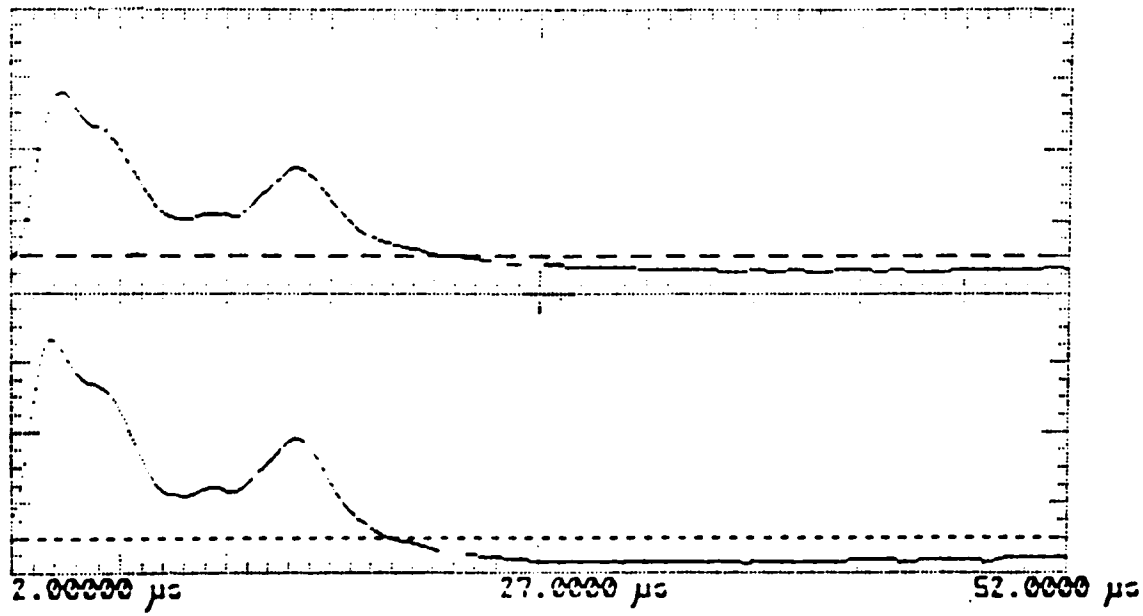

Ch. 1	-	300.0 mVolts/div	Offset	-	450.0 mVolts
Ch. 2	-	300.0 mVolts/div	Offset	-	450.0 mVolts
Timebase	-	5.00 μs/div	Delay	-	2.00000 μs

Fig. 11
Typical Triple Probe Current Measurement

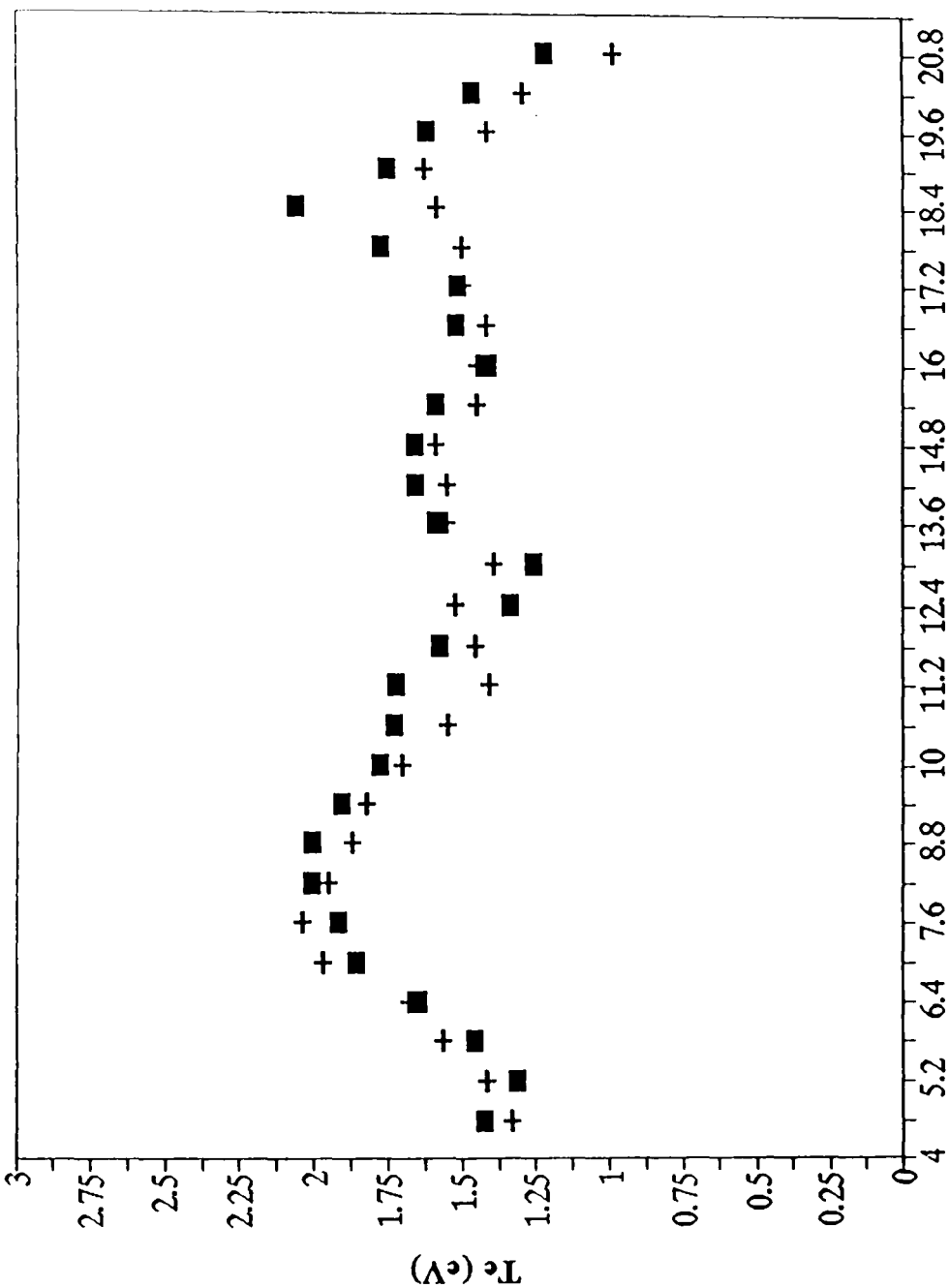

Fig. 12
Langmuir Probe Results for Opposite Spatial Orientations

for each probe orientation. The values are close early in time and fluctuate later in time, as was predicted earlier. The variation observed from shot to shot was typically within $10 \pm 2\%$. For another set the probes were left in place and the bias potentials were varied. The temperature was not dependent upon changes in the bias voltages for values between 2 and 4 V. Again, the agreement was good throughout the curve with the best consensus early in time. Finally, the orientation of the potential (right or left side of the plasma jet) was tested. It was seen that when the higher of the two bias voltages was on the right side of the jet, the calculated temperature was higher. The curves in Fig. 13 show this observation. Again, density gradients could account for this difference. The results of each of the mentioned tests were quite reproducible, indicating a systematic inhomegeniety in the plasma which was also observed in previous experiment [5].

For the temperature measurements which will be discussed in the next chapter, the bias voltages were 2.5 V on the right probe and 4 V on the left probe. This arrangement was not varied throughout the entire series of measurements, allowing for comparative analysis of the data.

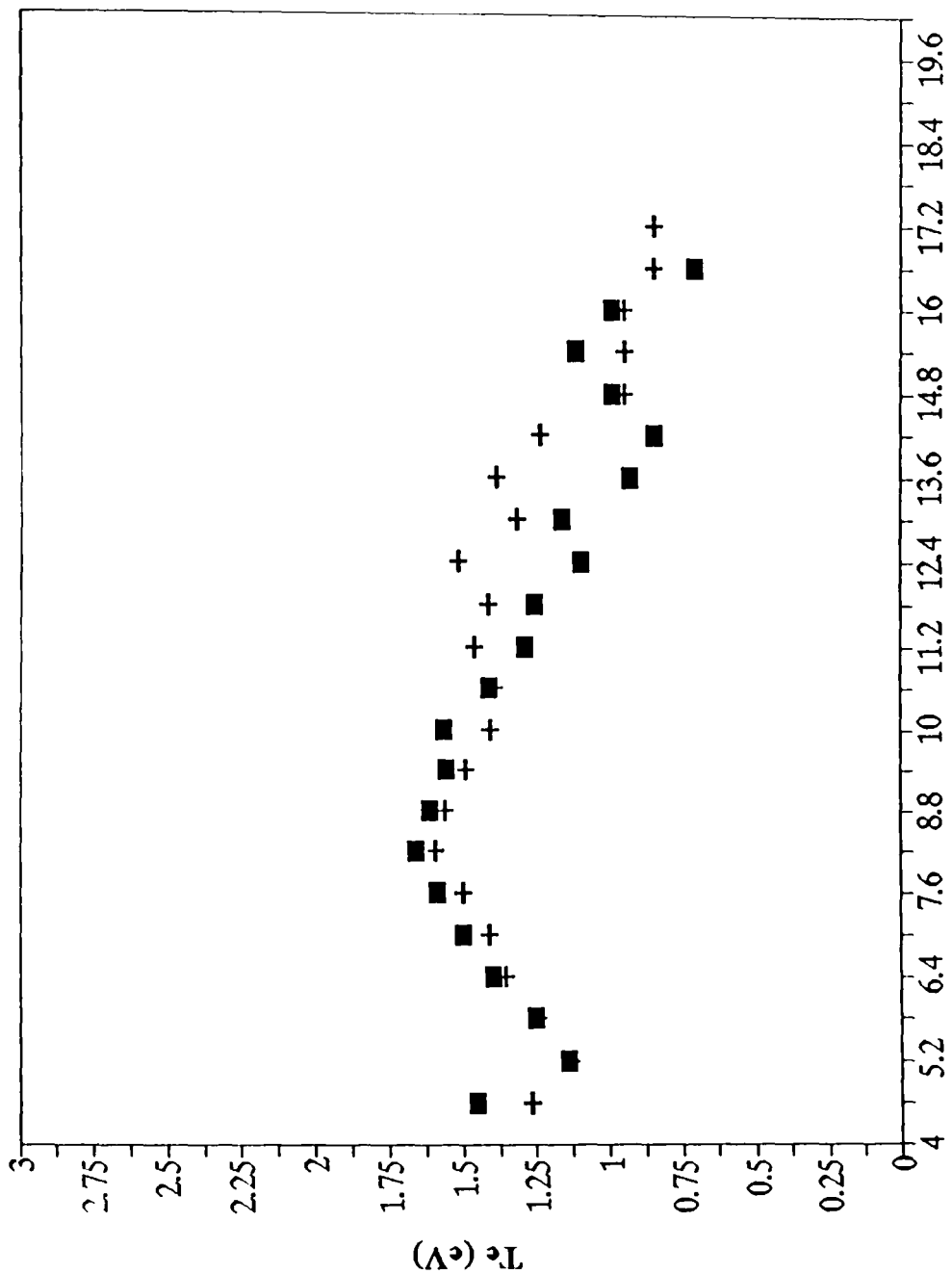

Fig. 13
Langmuir Probe Results for Opposite Potential Orientations

CHAPTER IV

EXPERIMENTAL MEASUREMENTS

The goal of this experimental work was to gather information about the relationship between the plasma and the source parameters. The plasma parameters of interest were density, velocity, temperature, and ion species composition. The source parameters which were varied were charging potential, gun geometry, and arc polarity. The data acquisition involved the use of 54111D HP and 54200A HP digital oscilloscopes. The 54111D was programmed to record the time-of-flight signals for three shots at each delay setting. Next, the program prompted the user to change scope inputs to acquire temperature data. This process was repeated for each delay setting from 13 μs to 103 μs in increments of 5 μs. The program allowed the user to skip the temperature measurement after three such measurements were made for each source configuration. Three measurements allowed for reproducibility verification, and since the temperature does not depend upon the delay setting it was not necessary to record any more temperature information. The flux probe results were recorded on the 54200A. The amplitude and time information of each peak was measured and then the traces were printed. Again, three flux measurements were made for the different source arrangements. The results were then graphed using QUATRO PRO.

Density and velocity measurements made with the flux probes are included for all of the charging voltages which were used in the experiment. As the charging

voltage was increased, the dominant effect on species measurements was that a greater particle flux was detected for each species. However, the actual composition remained the same. The detected plasma composition at various charging voltages results will be presented graphically for both positive and negative polarity without coil geometry. The species measurements will be discussed most completely for an example charging voltage of ±24 kV.

Density Results

Typical flux curves for each source configuration are shown in Figs. 14 and 15. In these curves noticeable differences can be seen for the varying source configurations. The flux measurement for positive arc polarity shows three to four distinct peaks whereas the negative counterpart has only two peaks. In order to make comparisons, two of the four peaks were selected for measurements. The two peaks evident with negative polarity travel at approximately 7 to 8 cm/μs and 4 to 5 cm/μs, respectively. The peaks chosen for the positive polarity, have close to the same velocities. The peaks measured for positive gun polarity occur earlier in time and are lower in magnitude than those measured for negative polarity.

Equation (4.1) shows the relationship between the initial density at the source and the density at a selected distance from the source.

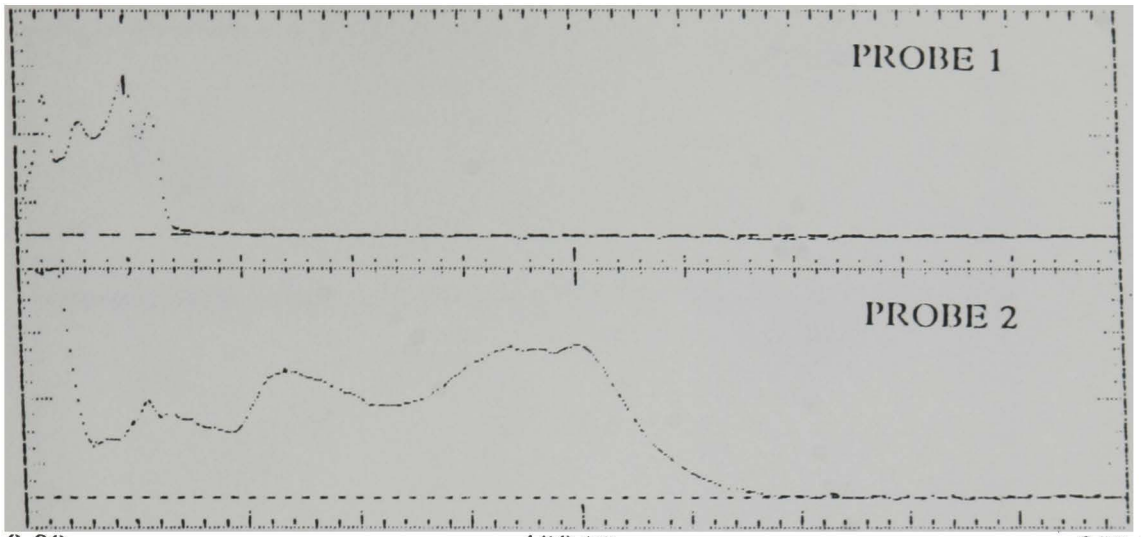

Ch. 1 = 300.00 mVolts/div
Ch. 2 = 4.00 mVolts/div
Timebase = 20 μsec/div

Offset = 450.00 mVolts
Offset = 6.00 mVolts
Delay = 0.0 sec

(a)

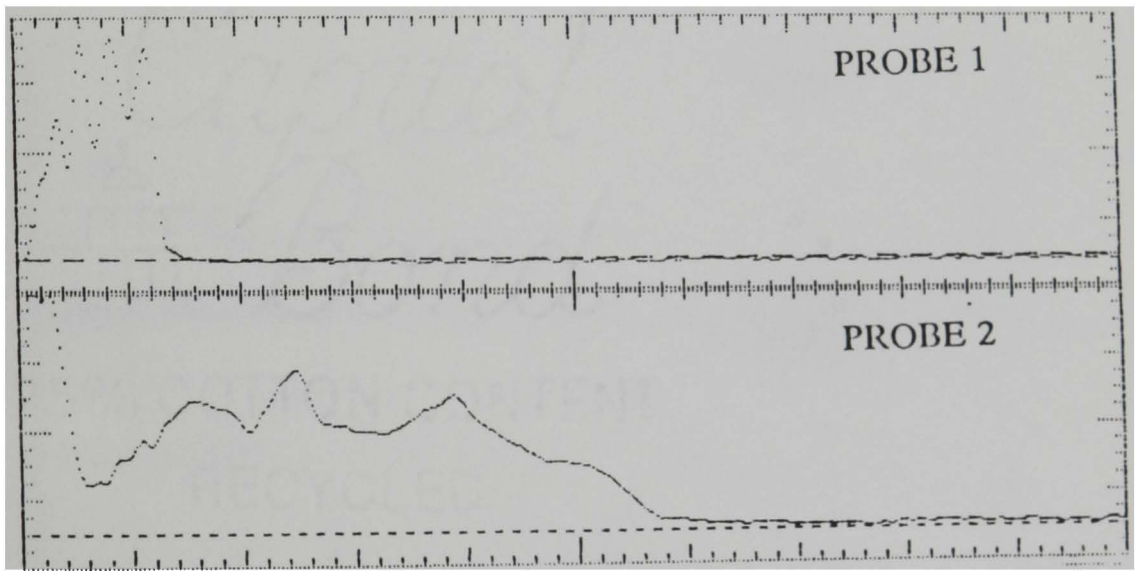

Ch. 1 = 300.00 mVolts/div
Ch. 2 = 4.00 mVolts/div
Timebase = 20 μsec/div

Offset = 450.00 mVolts
Offset = 6.00 mVolts
Delay = 0.0 sec

(b)

Fig. 14
Typical Flux Probe Measurements for Positive Gun Polarity
(a) No Coil (b) With Coil

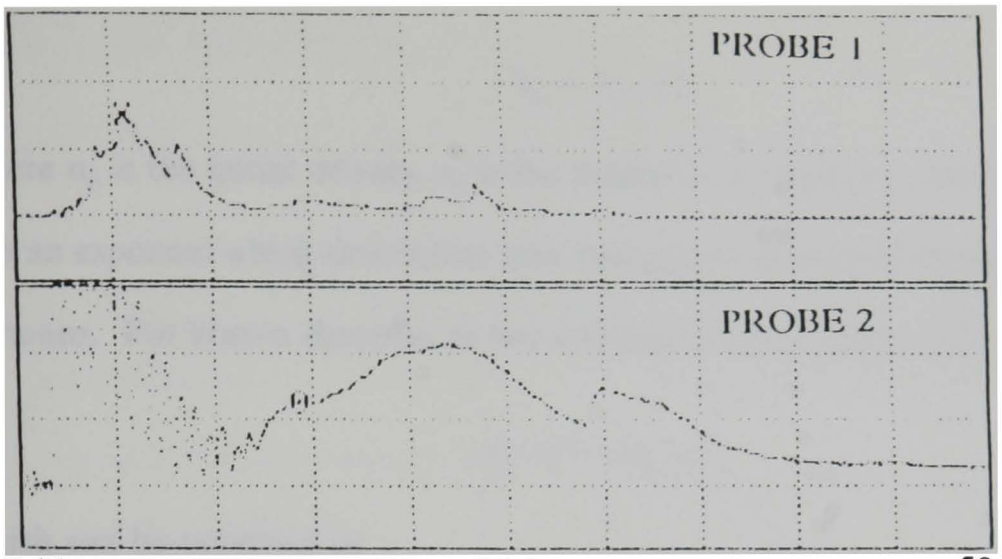

0.00 μs 25.00 μs 50.00 μs

Ch. 1 = 4.00 Volts/div Offset = 4.00 Volts
Ch. 2 = 10.00 mVolts/div Offset = 10.00 mVolts
Timebase = 5 μsec/div Delay = 0.0 sec

(a)

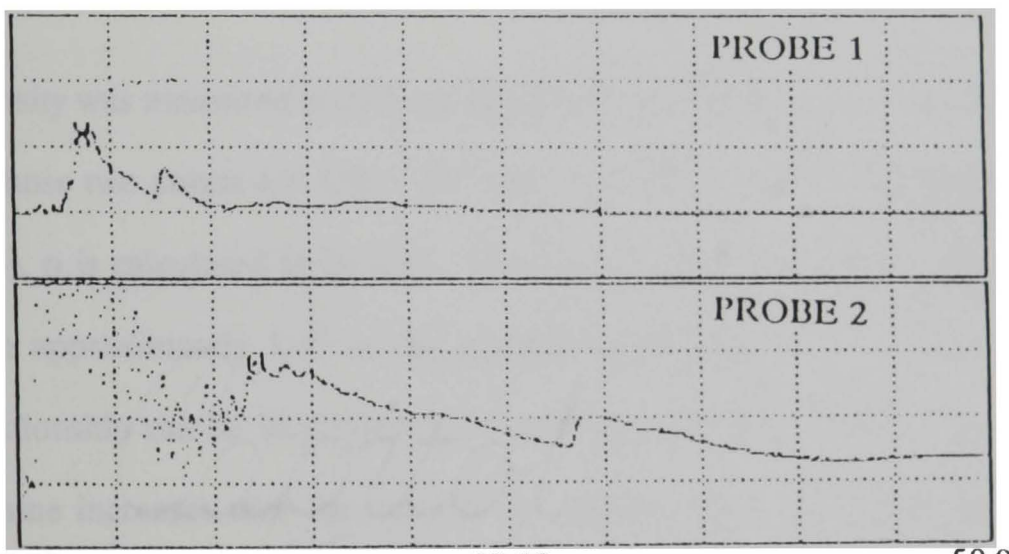

0.00 μs 25.00 μs 50.00 μs

Ch. 1 = 4.00 Volts/div Offset = 4.00 Volts
Ch. 2 = 10.00 mVolts/div Offset = 10.00 mVolts
Timebase = 5 μsec/div Delay = 0.0 sec

(b)

Fig. 15
Typical Flux Probe Measurements for Negative Gun Polarity
(a) No Coil (b) With Coil

$$n_o = n_1 r_1^p, \tag{4.1}$$

where n_o is the initial density, n_1 is the density at a distance r_1 from the source and p is an exponent which determines how strongly the density decreases relative to the distance. For known densities at two different distances, Eq. (4.2) can be derived.

$$n_1 r_1^p = n_2 r_2^p, \tag{4.2}$$

which can be rewritten as

$$p = \frac{\log \frac{n_1}{n_2}}{\log \frac{r_2}{r_1}}. \tag{4.3}$$

Density was measured at 25.4 cm and 131.4 cm in this experiment. Typical densities at those two points are 1.06×10^{12} cm^{-3} and 1.04×10^{10} cm^{-3}, respectively. From Eq. (4.3), p is calculated to be 2.81. Thus, calculations reveal that the density falls off with approximately $1/r^3$, as the plasma moves away from the source. The cubic relationship can be illustrated by considering a sphere. As the sphere expands, the volume increases with the cube of the radius. For a spherically expanding plasma volume, the density, assuming no particles are added, will exhibit an relation between density and distance of, $n \propto 1/r^3$. This requires that the plasma expand both radially and longitudinally. The longitudinal expansion can be clearly seen in the flux curves by comparing the pulse width of the curve at the two probe distances and is a result of the velocity spread. The time range of flux at 131.4 cm, approximately 30 μs, is

much greater than that at 25.4 cm, approximately 15 μs. The magnitude is smaller as well, which represents the effect of radial expansion.

It was expected that the plasma flux would increase as the charging potential of the capacitor bank increased. Figs. 16-19 show the particle density for different charging voltages at the first two peaks for each probe. All measurements but one show an increase in particle density with respect to charging voltage. The density calculated from the second probe for negative polarity and no coil remains fairly constant for each voltage level. In general, the coil has a greater effect on density when the charging voltage is negative. For example, close to the source and early in the plasma envelope, the coil geometry creates a plasma which is 24% lower in density than that without the coil for negative polarity; see Fig. 16. However, Figs. 17-19 show that the plasma density due to a negative gun is increased by as much as 43% with the coil in place, most noticeably at the probe located farther from the source. With positive polarity, the coil geometry has more effect on early portions of the plasma than on the later. From Fig. 16, the density without the coil geometry is 59% less than that with the coil at +24 kV. Farther away, the coil appears to have actually reduced the density. In Fig. 19, the density at 24 kV is 41% lower with the coil during positive arc polarity. These effects are not easily explained. Without further investigation of the plasma, no detailed explanation can be made. Since electrons in the PEC arrangement are extracted at a distance of 18 cm downstream from the plasma gun, the density information calculated from the probe closest to the source will be more significant to further PEC research. At that location, in general,

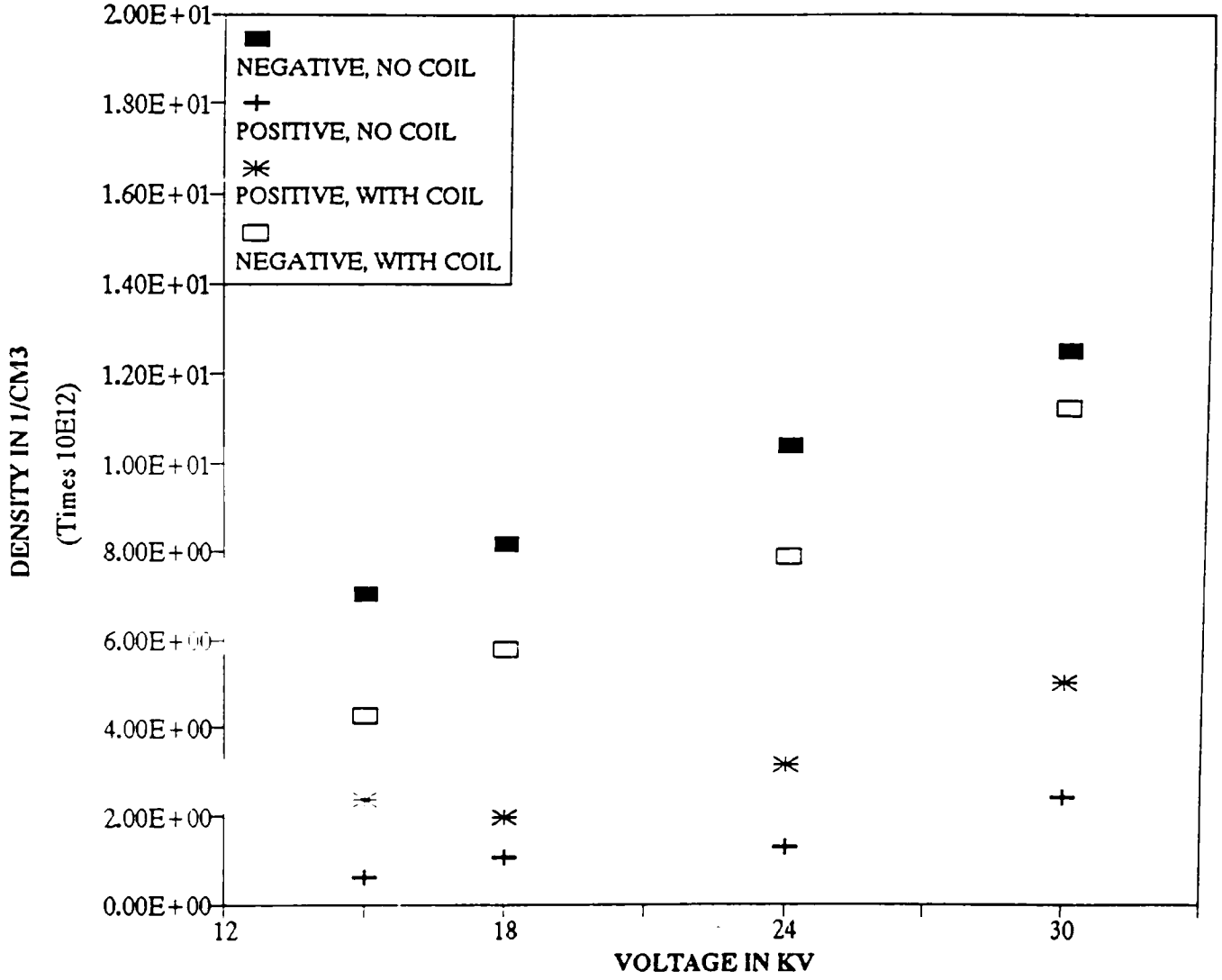

Fig. 16
Calculated Density for the First Peak of Probe 1

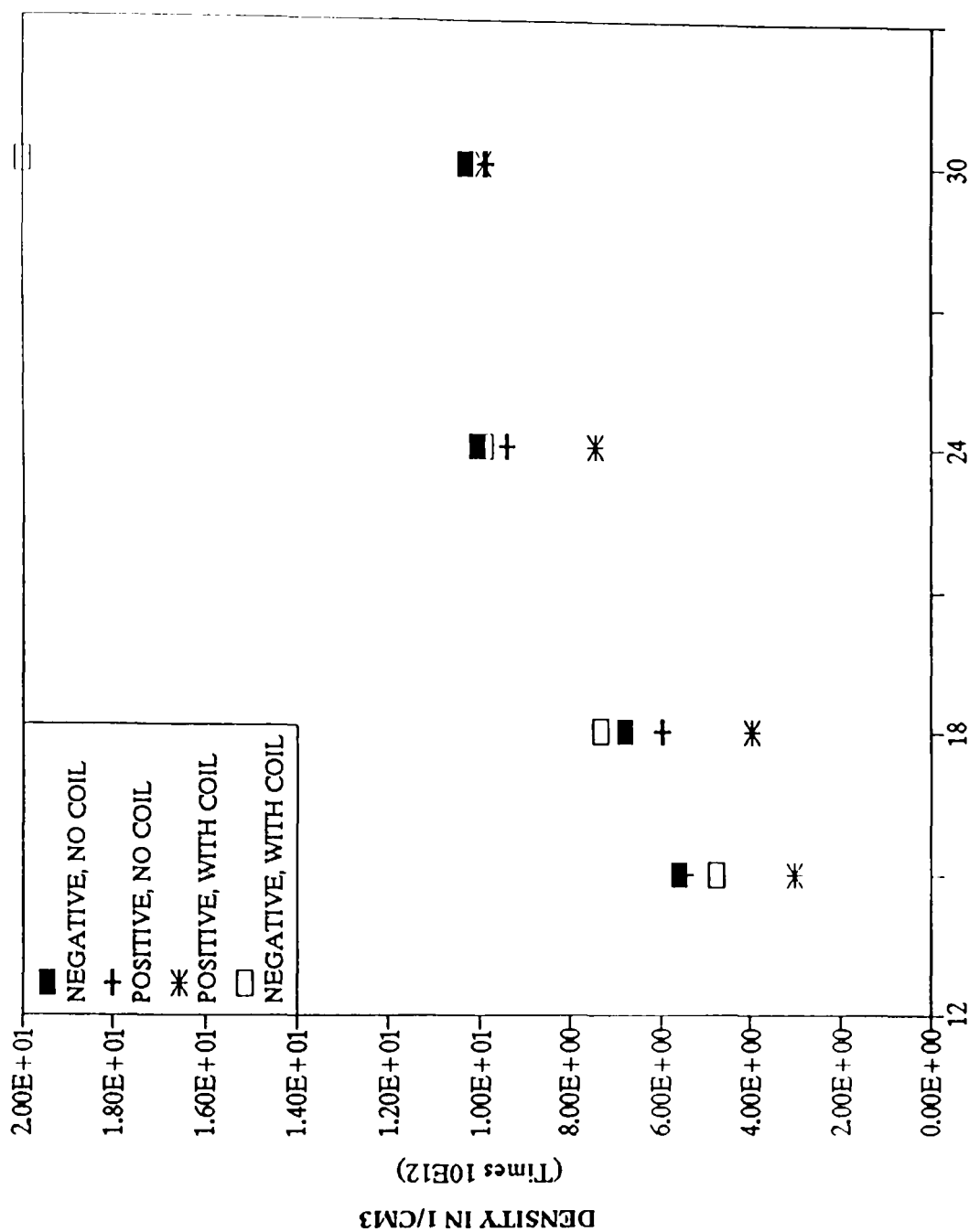

Fig. 17
Calculated Density for the Second Peak of Probe 1

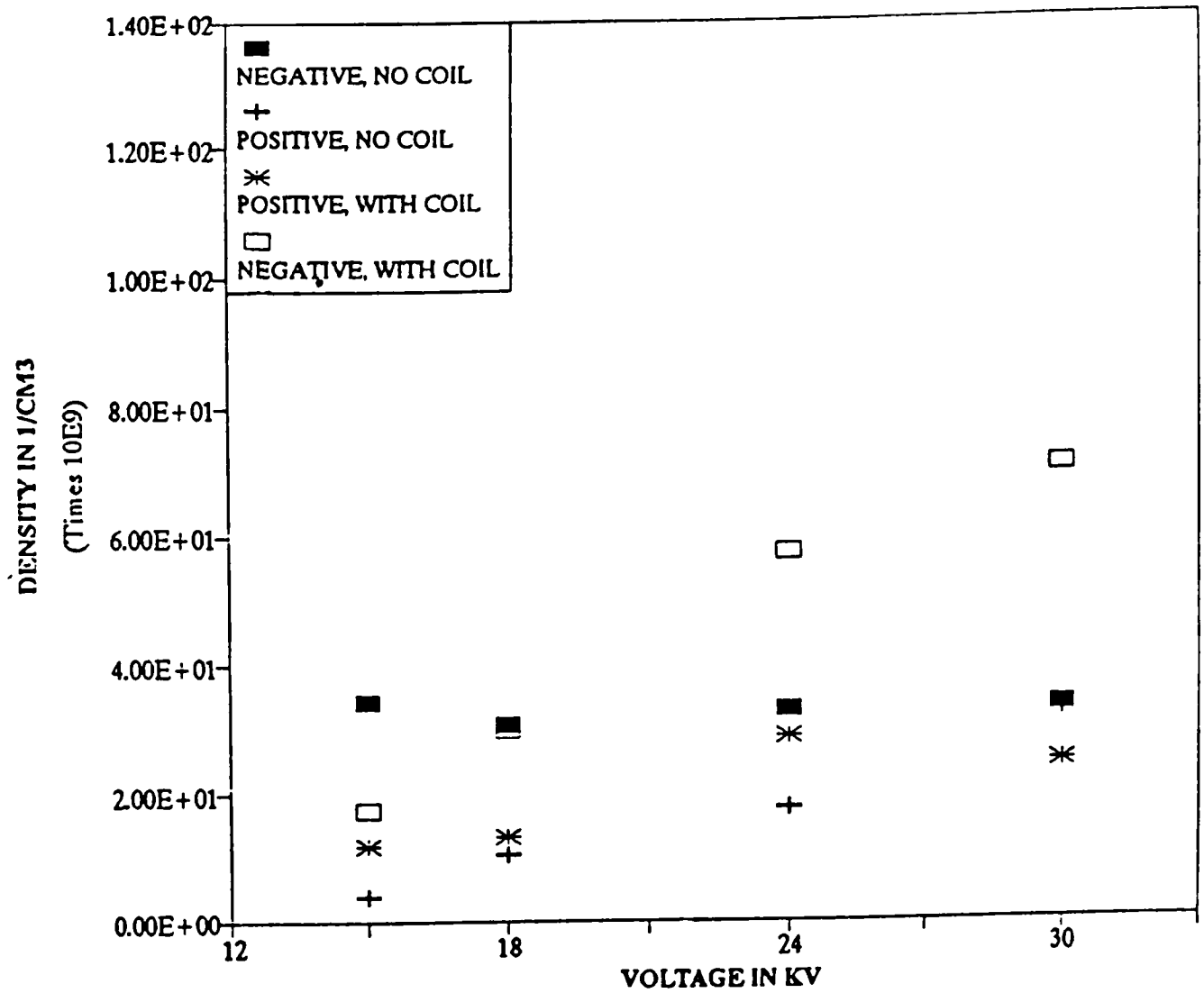

Fig. 18
Calculated Density for the First Peak of Probe 2

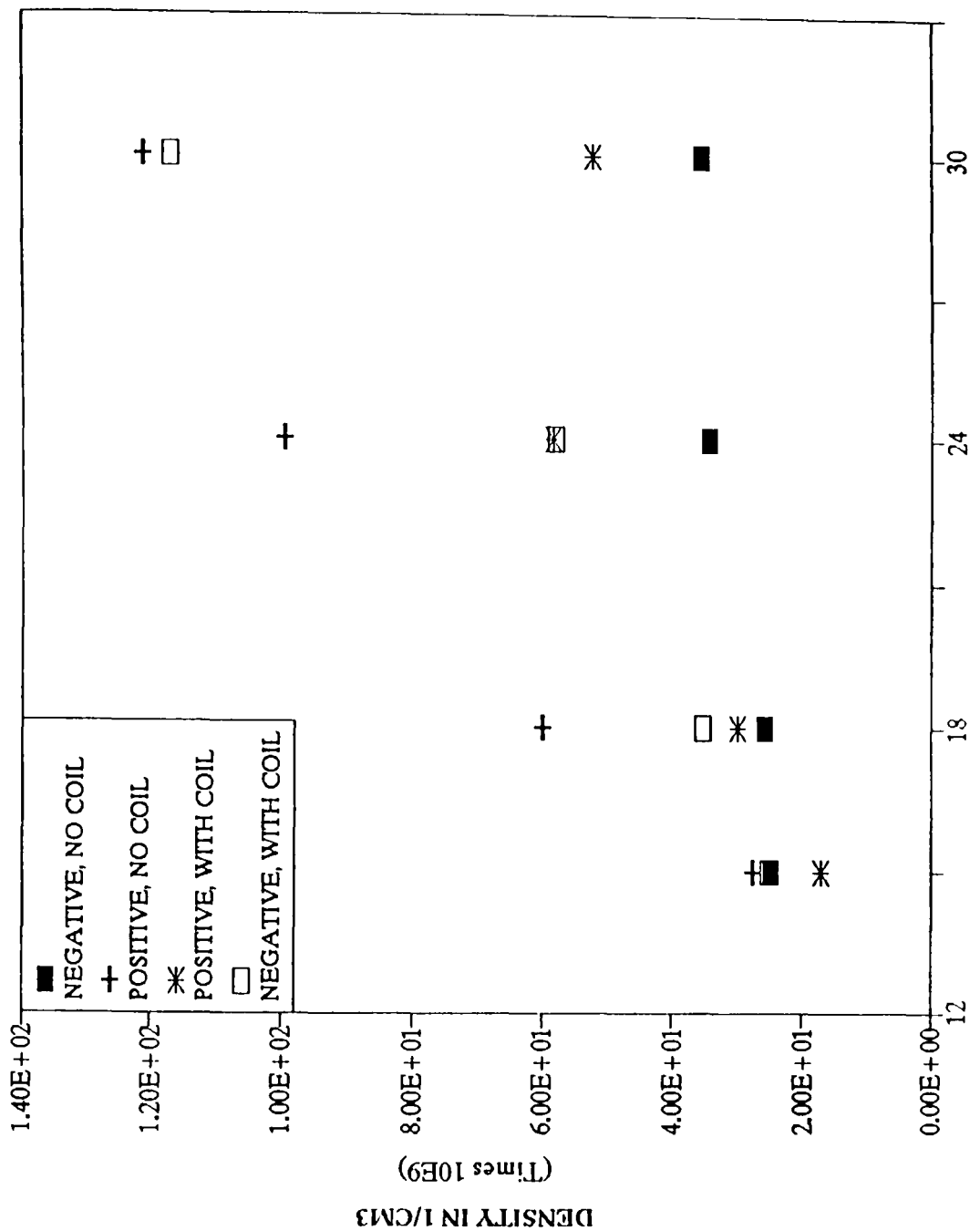

Fig. 19
Calculated Density for the Second Peak of Probe 2

the coil has a greater effect in early portions of the plasma, for both positive and negative polarity where the density for negative polarity is lowered and the density for positive polarity is increased. During the second peak, the effect of the coil is inconsistent. Negative polarity creates a more dense plasma than positive polarity regardless of whether or not the coil is in place. In conclusion, since the coil does not have a profound beneficial effect on a negatively charged gun, the best configuration with respect to density is the negative gun without the external coil.

Velocity Results

The velocity of the plasma is measured in two ways. First, the velocities of the fast and slow components of the plasma are determined from the flux probe information. By dividing the probe distance by the time the peak is measured, the velocity of the peak is calculated. It is known from previous measurements that the plasma is created early in the flashover, up to 2 μs after the trigger. As a result, some error in initial velocity calculation may ensue by using d/t, since the flight time might not be equal to the measured time [5]. The farther from the source, the smaller this error becomes. This fact leads to the second type of velocity measurement used in this experiment. The acceleration gap is 181 cm from the source, by measuring the initial velocity at this point, greater accuracy is achieved. Since the species which will be detected for a particular delay setting reach the acceleration gap at the given time, the initial velocity for the detected particles can be calculated by s_a/t_d, where s_a is the distance from the source to the acceleration

gap and t_d is the delay time. By using both of these measurements, a general idea of overall plasma speed and specific ion species velocity can be obtained.

Figs. 20-23 show the relationship between velocity and charging voltage for each source configuration. For each set of measurements, velocity does not seem to depend upon charging voltage. The highest velocity results when the gun is charged negatively without the coil geometry. It was mentioned in Chapter I that C. Mendel used the coil geometry as an acceleration device. Thus, a greater velocity would be expected. However, in this experiment the coil appears to slow the plasma down rather than accelerate it. The only condition in which the coil geometry produces a greater velocity is for positive voltage. Even for positive polarity, the late plasma is the only portion which shows and increase in velocity. Thus, it does not appear that the coil greatly affects the velocity for this type of plasma source.

As mentioned previously, the delay setting of the acceleration pulse for the time-of-flight measurement was varied from 13 μs to 103 μs in increments of 5 μs. These delay settings correspond to initial velocities of 13.92 cm/μs to 1.76 cm/μs, respectively. For a negative polarity, species were detected with the early delay setting of 13 μs. These detected species are O^{6+}, O^{5+}, O^{4+}, O^{3+}, O^{2+}, Al^{6+}, and Al^{5+}. With positive polarity, however, the species do not appear consistently until 23 to 28 μs delays. The most probable initial velocities of each species for the configurations with a charging voltage of $\pm$24 kV are shown in Table 1. The lower voltages exhibit generally the same velocities as 24 kV, again showing that the velocity is not strongly

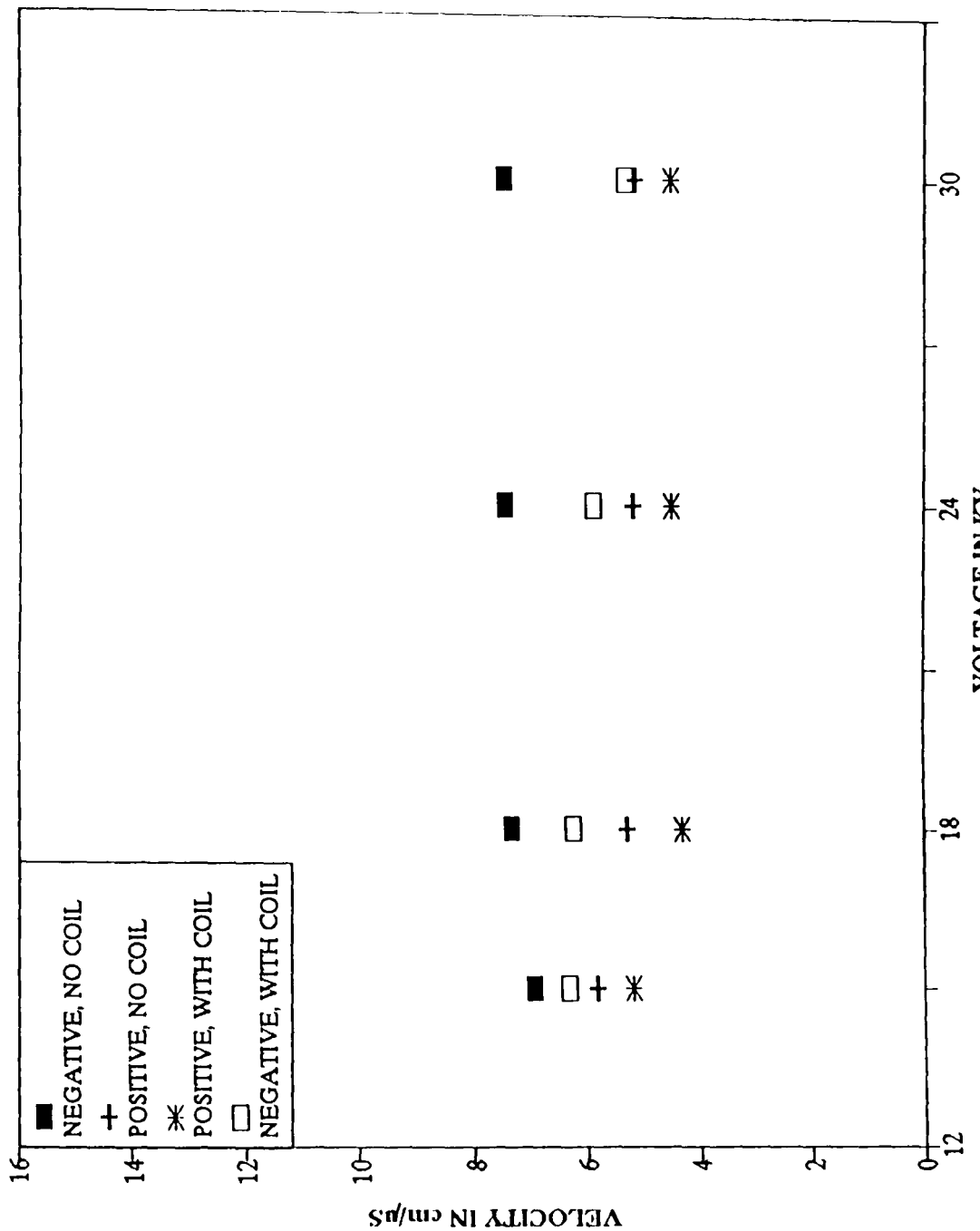

Fig. 20
Calculated Velocity for the First Peak of Probe 1

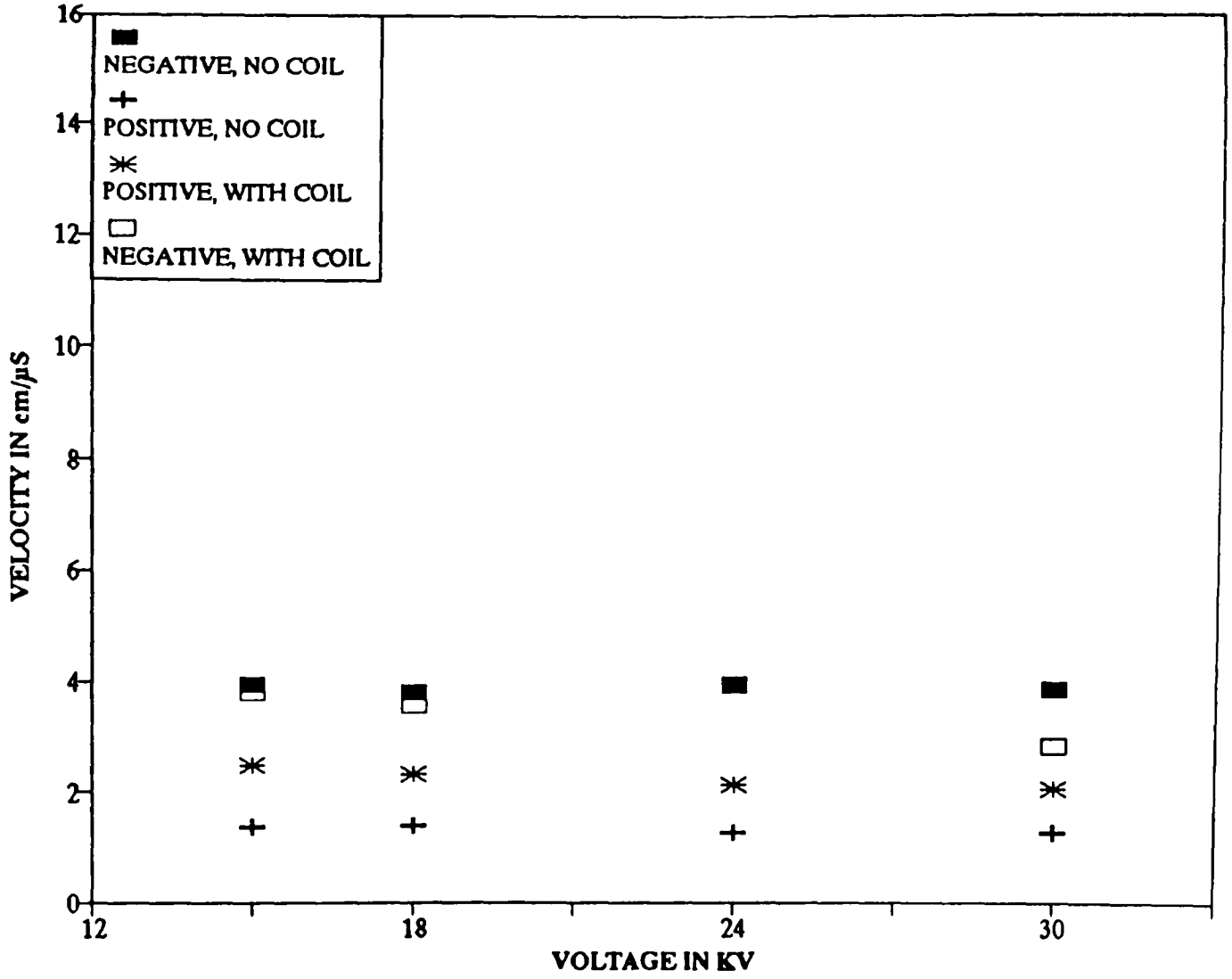

Fig. 21
Calculated Velocity for the Second Peak of Probe 1

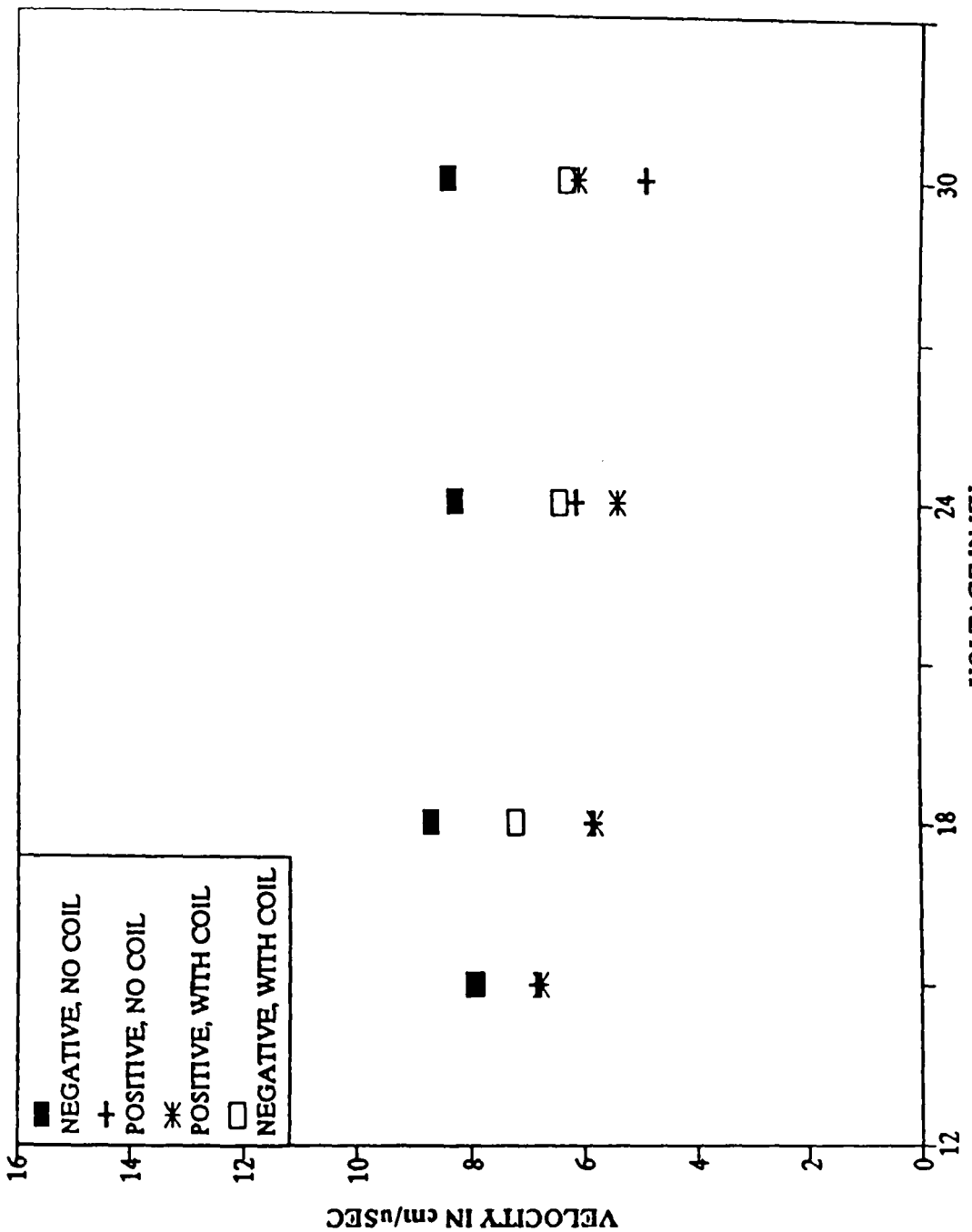

Fig. 22
Calculated Velocity for the First Peak of Probe 2

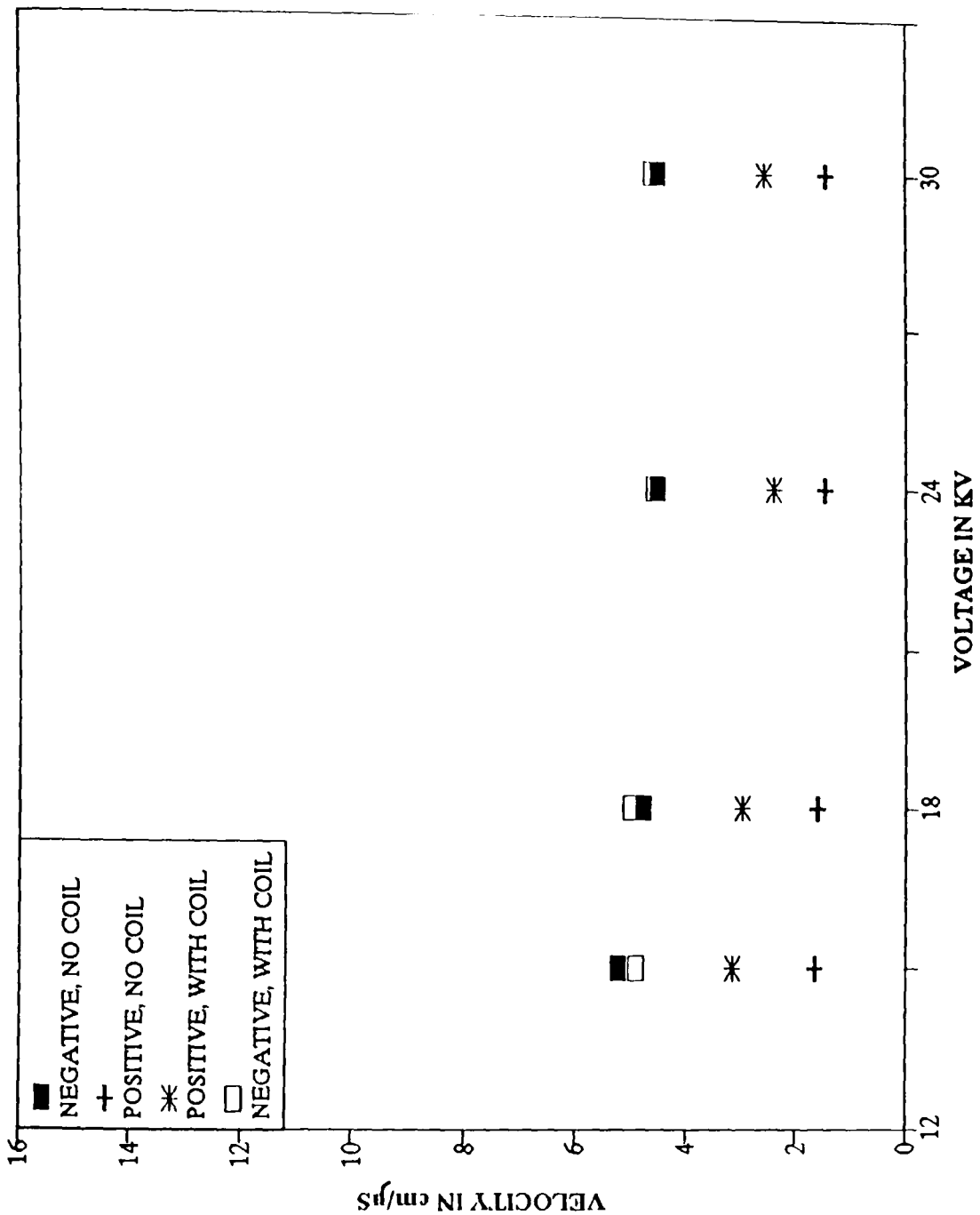

Fig. 23
Calculated Velocity for the Second Peak of Probe 2

Table 1: Initial Velocity of Species for Different Source Arrangements

	-24 kV WITH COIL	-24 kV NO COIL	+24 kV WITH COIL	+24 kV NO COIL
O^{6+}	13.9 cm/μs	13.9 cm/μs	13.9 cm/μs	-
O^{5+}	10.1 cm/μs	10.1 cm/μs	10.1 cm/μs	6.5 cm/μs
O^{4+}	10.1 cm/μs	10.1 cm/μs	10.1 cm/μs	6.5 cm/μs
Al^{6+}	10.1 cm/μs	13.9 cm/μs	10.1 cm/μs	-
O^{3+}/Al^{5+}	7.9 cm/μs	7.9 cm/μs	10.1 cm/μs	4.8 cm/μs
Al^{4+}	7.9 cm/μs	10.1 cm/μs	10.1 cm/μs	6.5 cm/μs
O^{2+}	5.5 cm/μs	4.2 cm/μs	5.5 cm/μs	4.2 cm/μs
Al^{3+}	7.9 cm/μs	5.4 cm/μs	5.5 cm/μs	4.8 cm/μs
Al^{2+}	4.2 cm/μs	4.2 cm/μs	4.2 cm/μs	4.2 cm/μs
O^{+}	3.4 cm/μs	3.8 cm/μs	2.3 cm/μs	2.9 cm/μs
Al^{+}	3.8 cm/μs	4.2 cm/μs	2.3 cm/μs	2.9 cm/μs

dependent on the charging voltage. The most probable initial velocity was calculated from the delay setting where the greatest number of each particular species was detected. A corresponding 3-dimensional graph which also includes this information will be discussed in a later section. With the exception of positive polarity without the coil, no configuration provides significantly faster or slower ions in terms of initial velocity. The positive configuration without the coil yields slower ions by an average of 28%. O^{6+} and Al^{6+} are not detected for this configuration.

In a previous chapter, an equation was derived which determined the velocity required for ions to traverse the extraction gap in the PEC. Table 2 shows this minimum required initial velocity for the different charge states of Aluminum and Oxygen calculated from Eq. (1.8). The most likely initial velocity of each species is high enough to satisfy the necessary condition. For positive polarity, O^{+}, O^{2+}, Al^{+}, and Al^{2+} are detected with a delay setting of as long as 103 μsec, which indicates initial velocities down to 1.76 cm/μs. So, even for the slowest particles which are detected, their velocity exceeds the minimum which is required. This section focused primarily on the most probable initial velocity of each species. Figs. 24-31 show the current detected by the multiplier by the different species at various delay settings.

Temperature Results

The temperatures measured for the different source arrangements varied between .9 eV and 1.4 eV. As mentioned previously, four measurements were made

Table 2: Minimum Required Velocity for Oxygen and Aluminum Ions to Traverse the Extraction Gap

	1	2	3	4	5	6
O	.99 cm/μs	1.22 cm/μs	1.41 cm/μs	1.58 cm/μs	1.73 cm/μs	1.87 cm/μs
Al	.77 cm/μs	.94 cm/μs	1.09 cm/μs	1.22 cm/μs	1.33 cm/μs	1.44 cm/μs

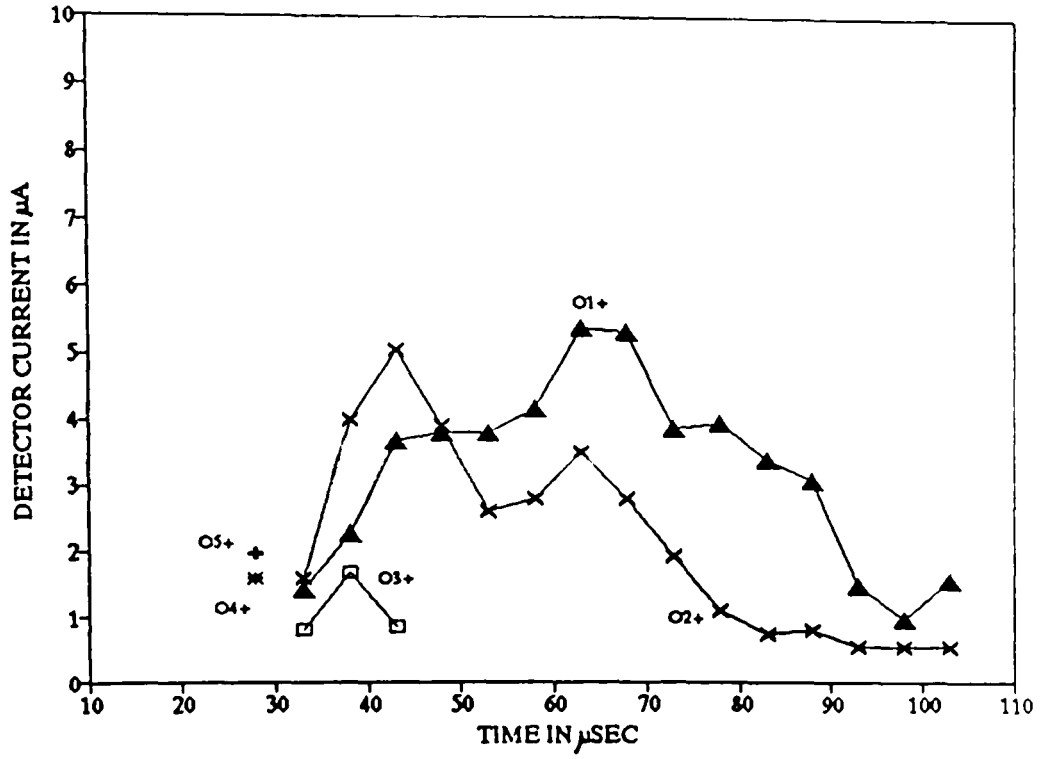

(a)

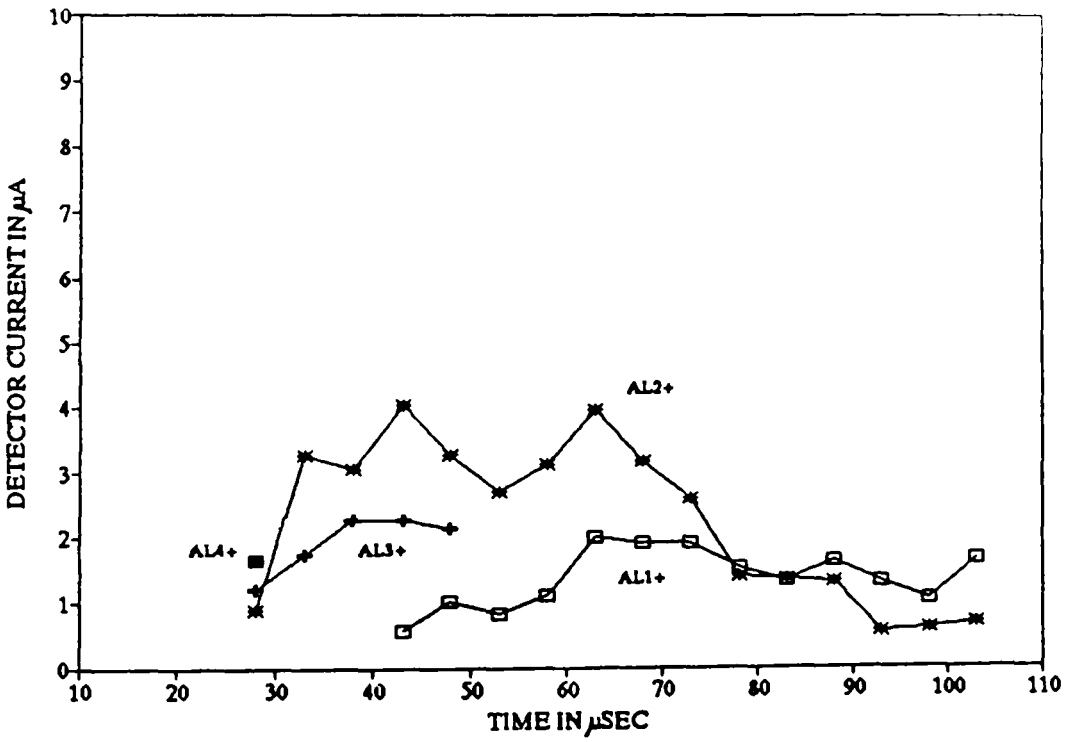

(b)

Fig. 24
Ion Species Detected for +24 kV, No Coil
(a) Oxygen (b) Aluminum

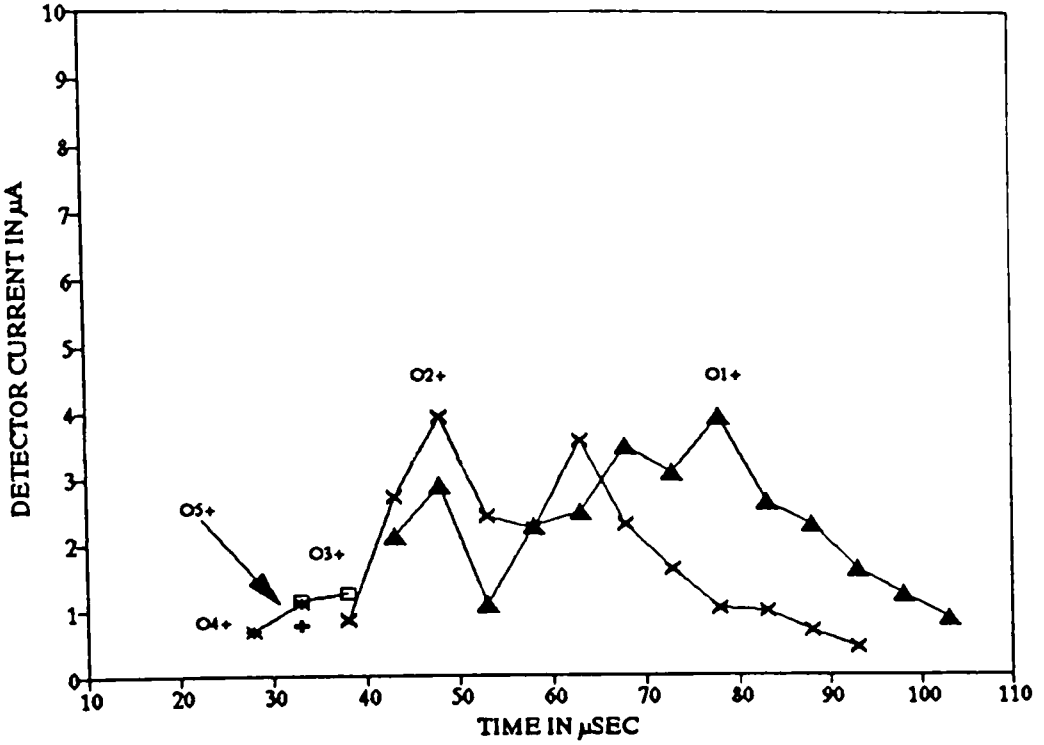

(a)

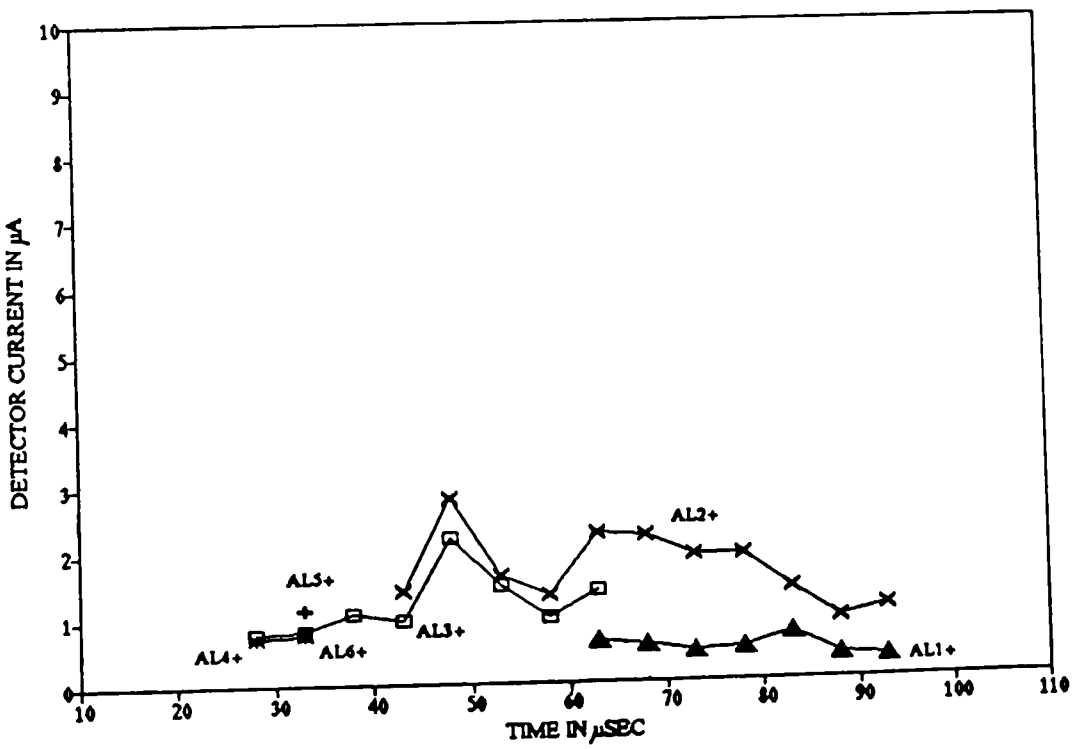

(b)

Fig. 25
Ion Species Detected for +18 kV, No Coil
(a) Oxygen (b) Aluminum

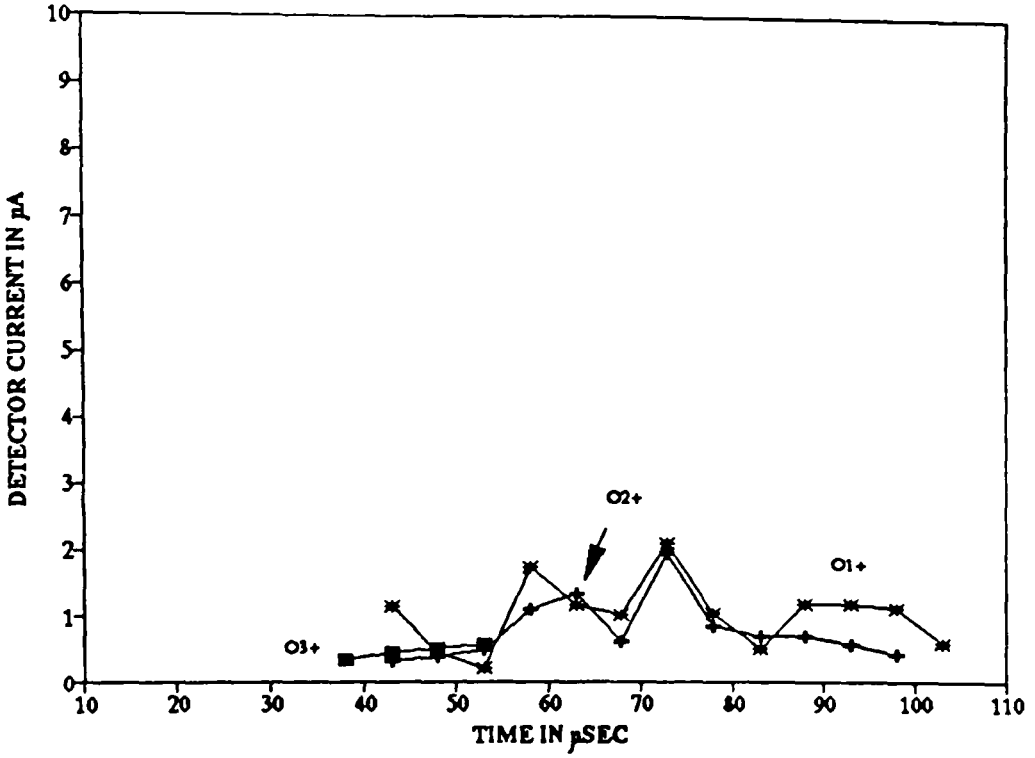

(a)

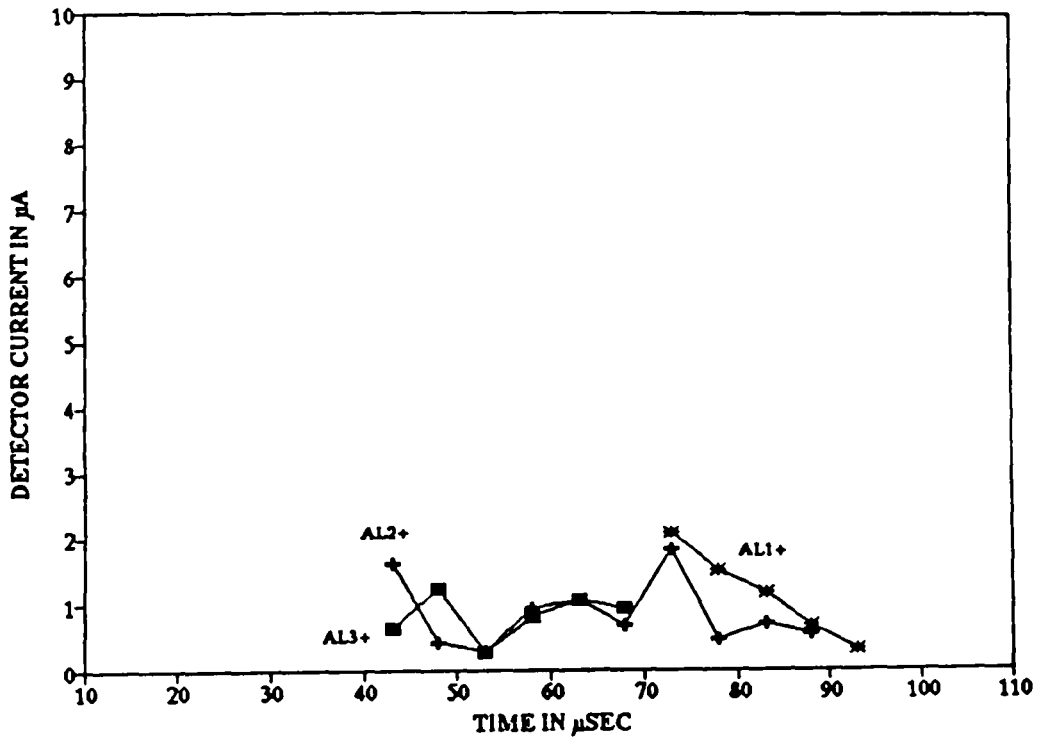

(b)

Fig. 26
Ion Species Detected for +15 kV, No Coil
(a) Oxygen (b) Aluminum

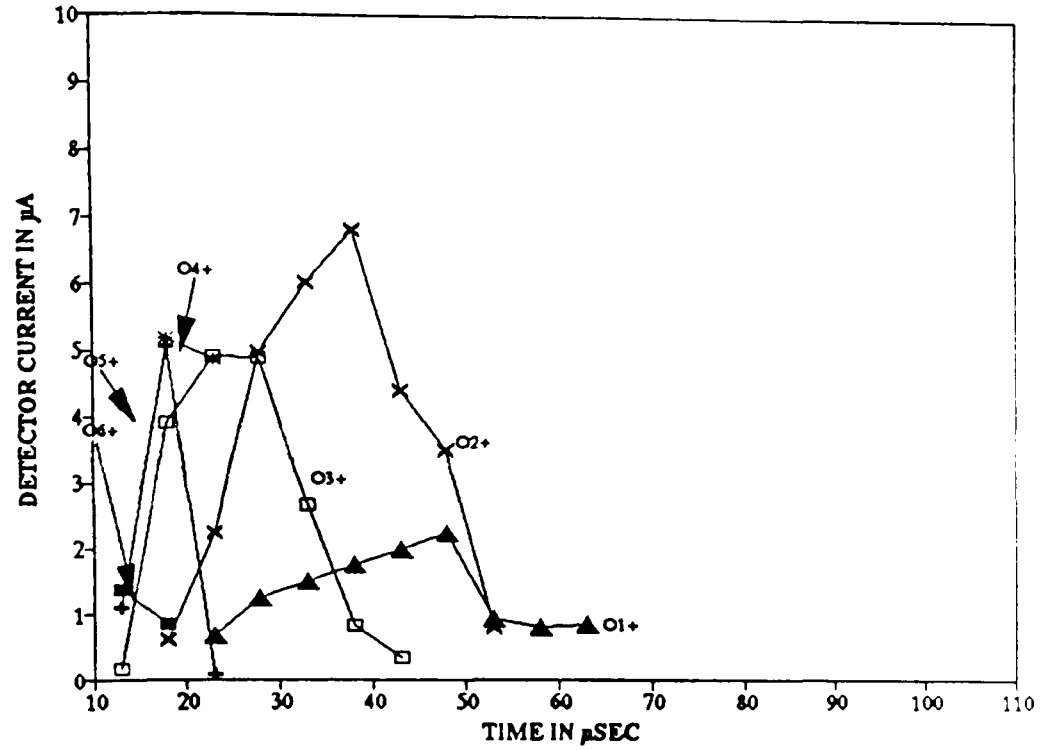

(a)

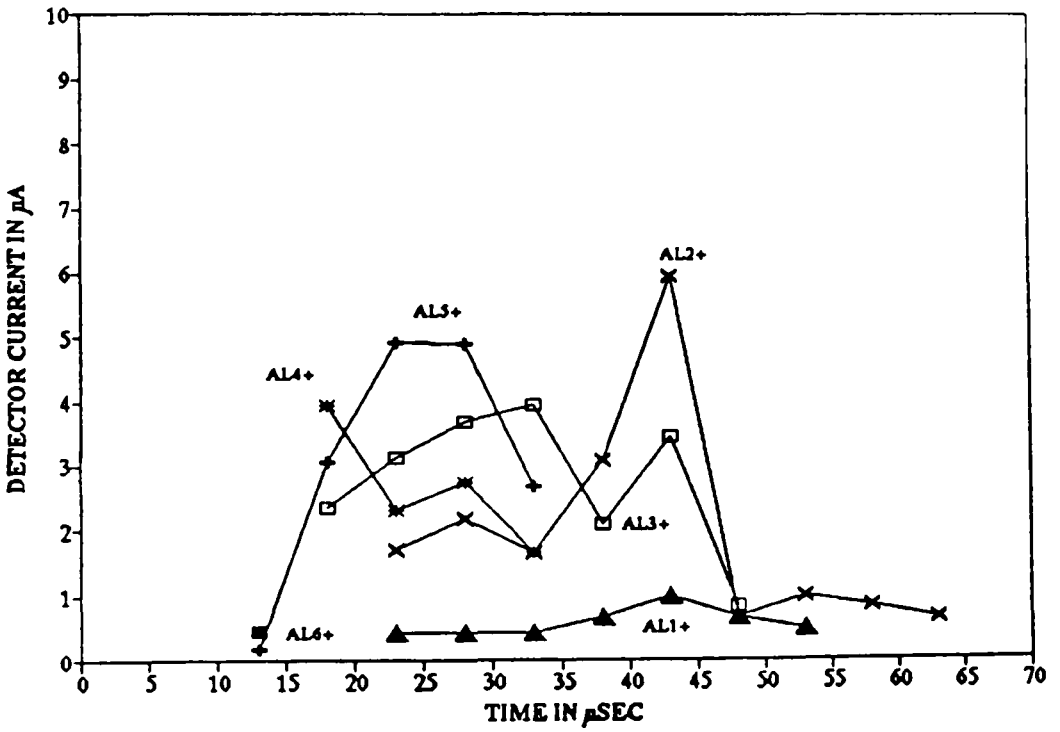

(b)

Fig. 27
Ion Species Detected for -24 kV, No Coil
(a) Oxygen (b) Aluminum

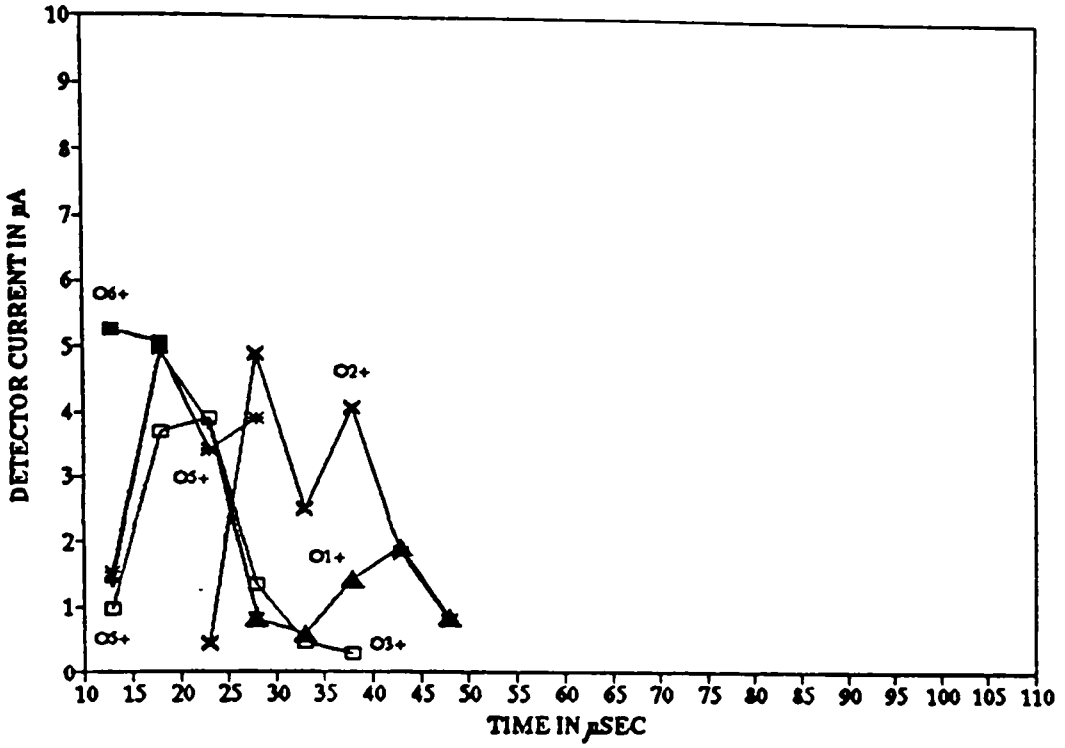

(a)

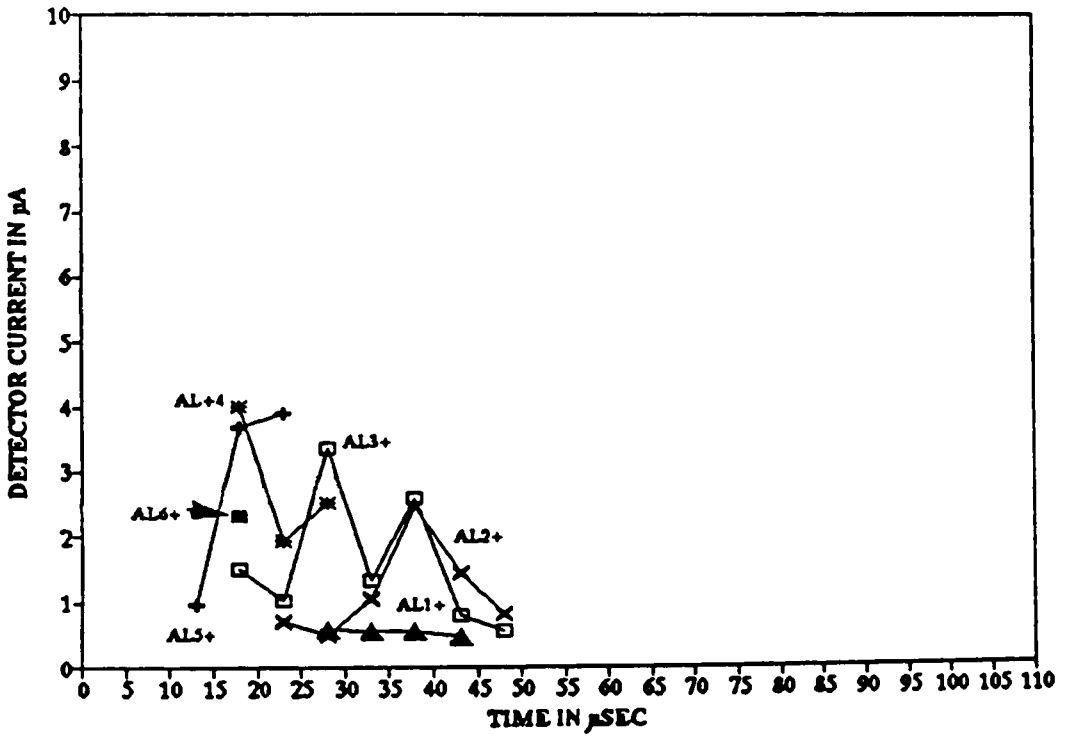

(b)

Fig. 28
Ion Species Detected for -18 kV, No Coil
(a) Oxygen (b) Aluminum

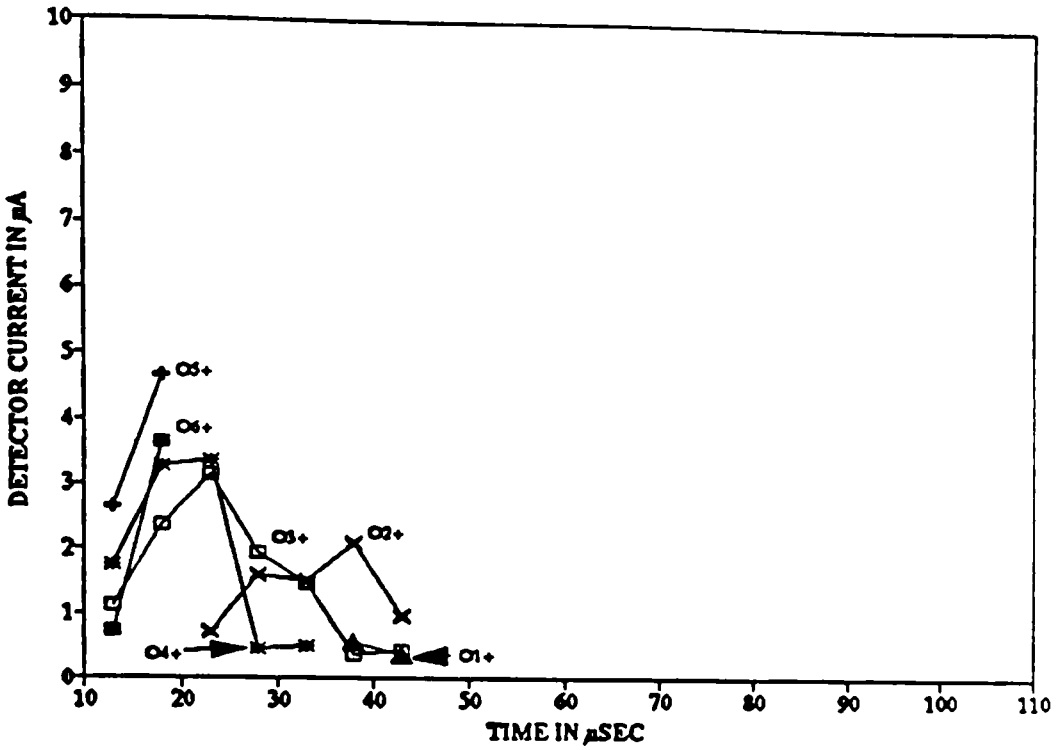

(a)

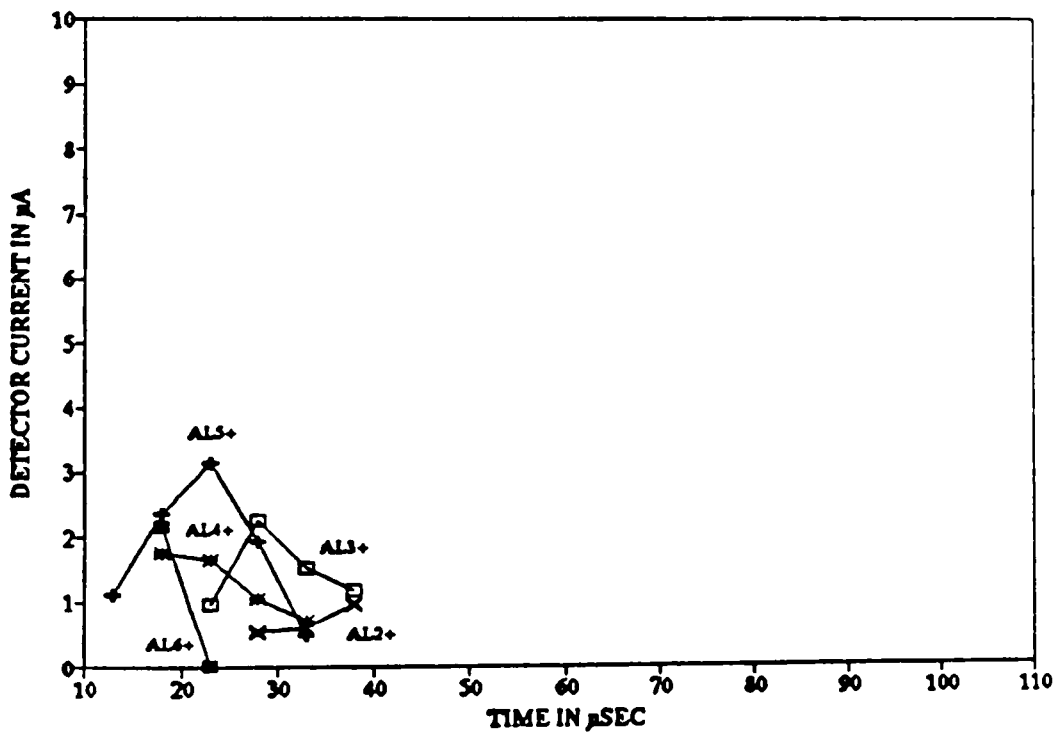

(b)

Fig. 29
Ion Species Detected for -15 kV, No Coil
(a) Oxygen (b) Aluminum

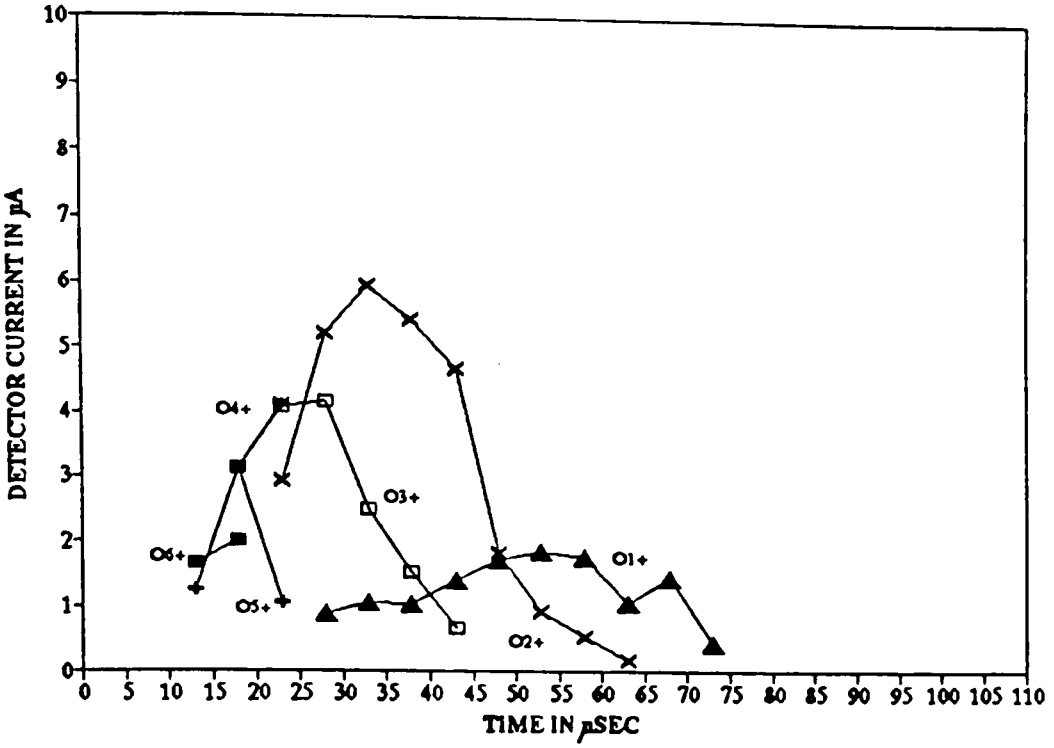

(a)

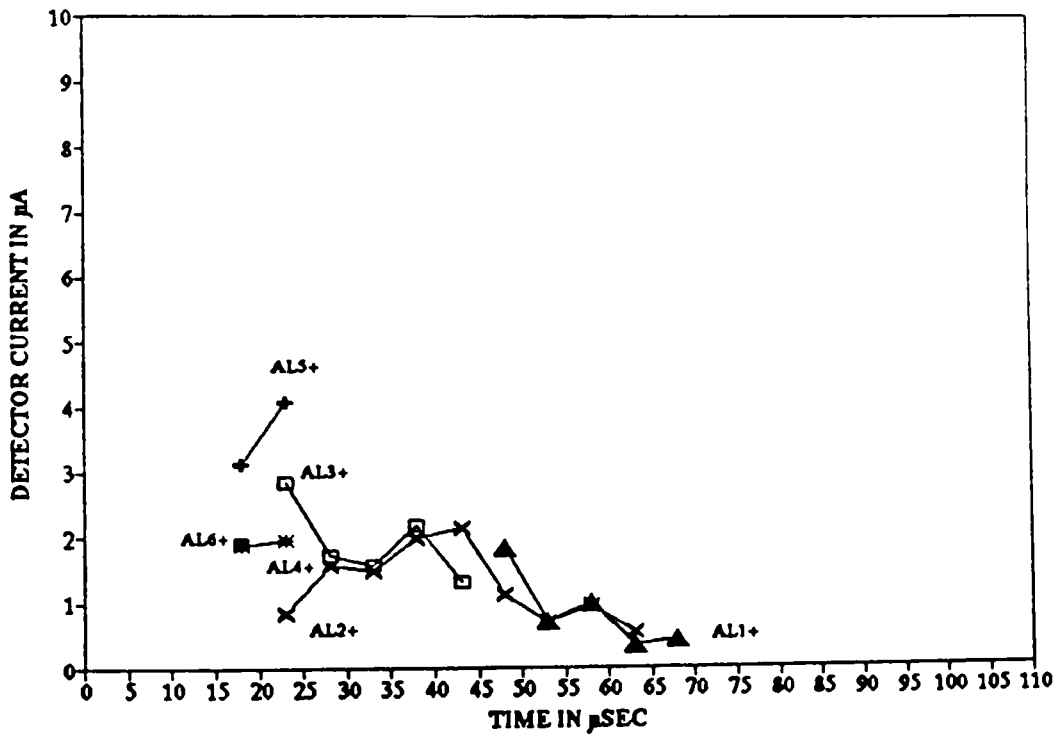

(b)

Fig. 30
Ion Species Detected for -24 kV, With Coil
(a) Oxygen (b) Aluminum

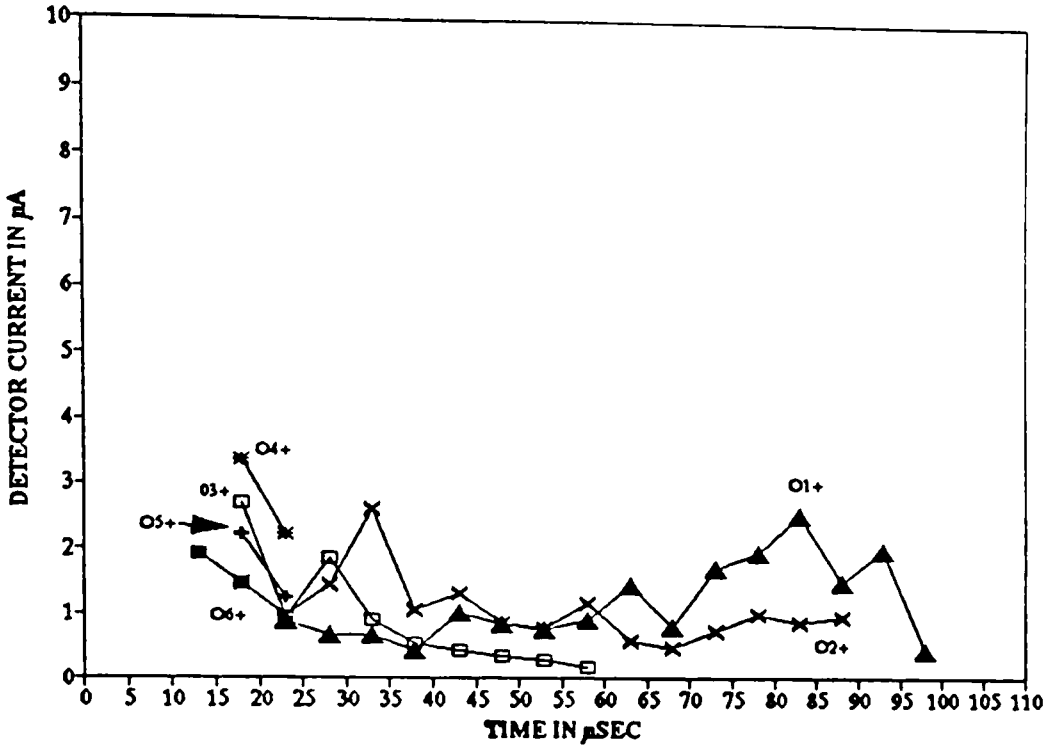

(a)

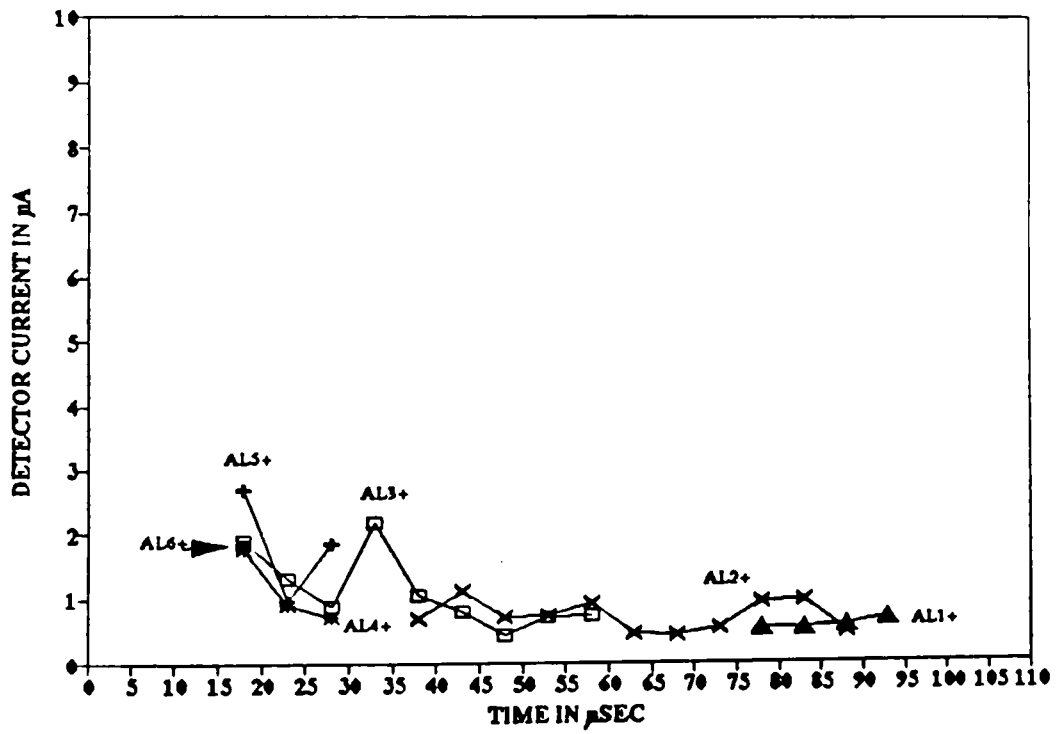

(b)

Fig. 31
Ion Species Detected for +24 kV, With Coil
(a) Oxygen (b) Aluminum

for each arrangement. For all configurations, the four temperature measurements resulted in the same values within ± 15%. The greatest differences appear towards the end of the plasma pulse. At the end of the probe measurement, the signal becomes smaller, decreasing the signal to noise ratio. In addition, the transformer circuit time constant has an adverse influence on the later parts of the measurement. Fig. 32 shows the four temperature measurements for one set of conditions to show the reproducibility and low measurement variation from shot to shot.

With respect to charging voltage, the temperature had very little, if any, dependence. The temperature curves for each charging voltage are shown for the different source configurations in Figs. 33-36. The coil geometry affects the temperature more significantly than the other plasma parameters. The temperature measured when the coil was present is much more constant throughout the entire shot. Also, with the coil geometry, the measured temperatures for both positive and negative polarities are essentially equal. They are lower than that measured without the coil in place. Without the coil, positive polarity results in a slightly higher temperature than negative polarity.

The best configuration with respect to temperature cannot be based solely on temperature. The temperature affects the maximum theoretical extractible current density, as shown in Chapter I. Temperature will also affect the transverse expansion behind the material edge in a PEC configuration. The extractible current density is

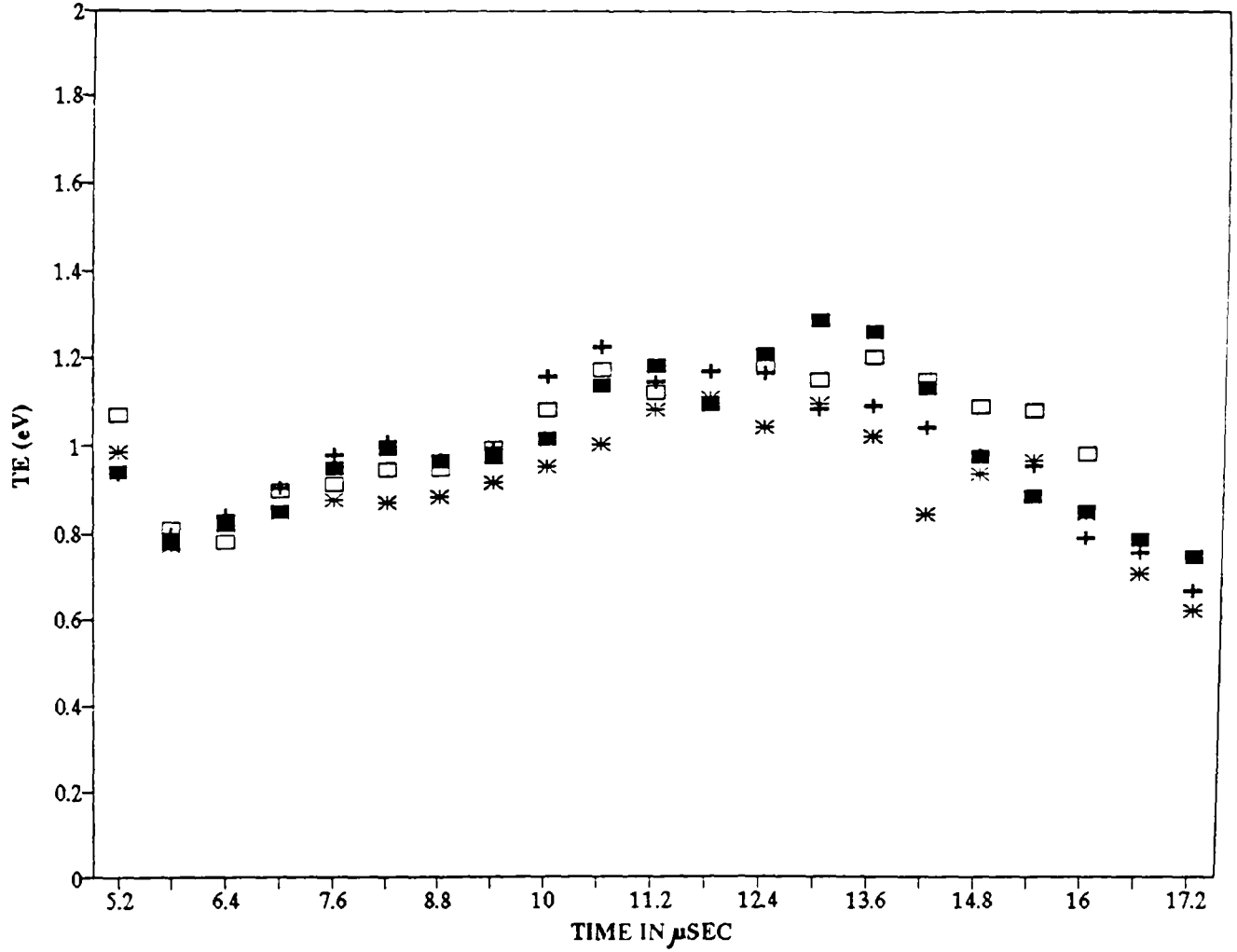

Fig. 32
Four Typical Temperature Measurements from One Source Configuration

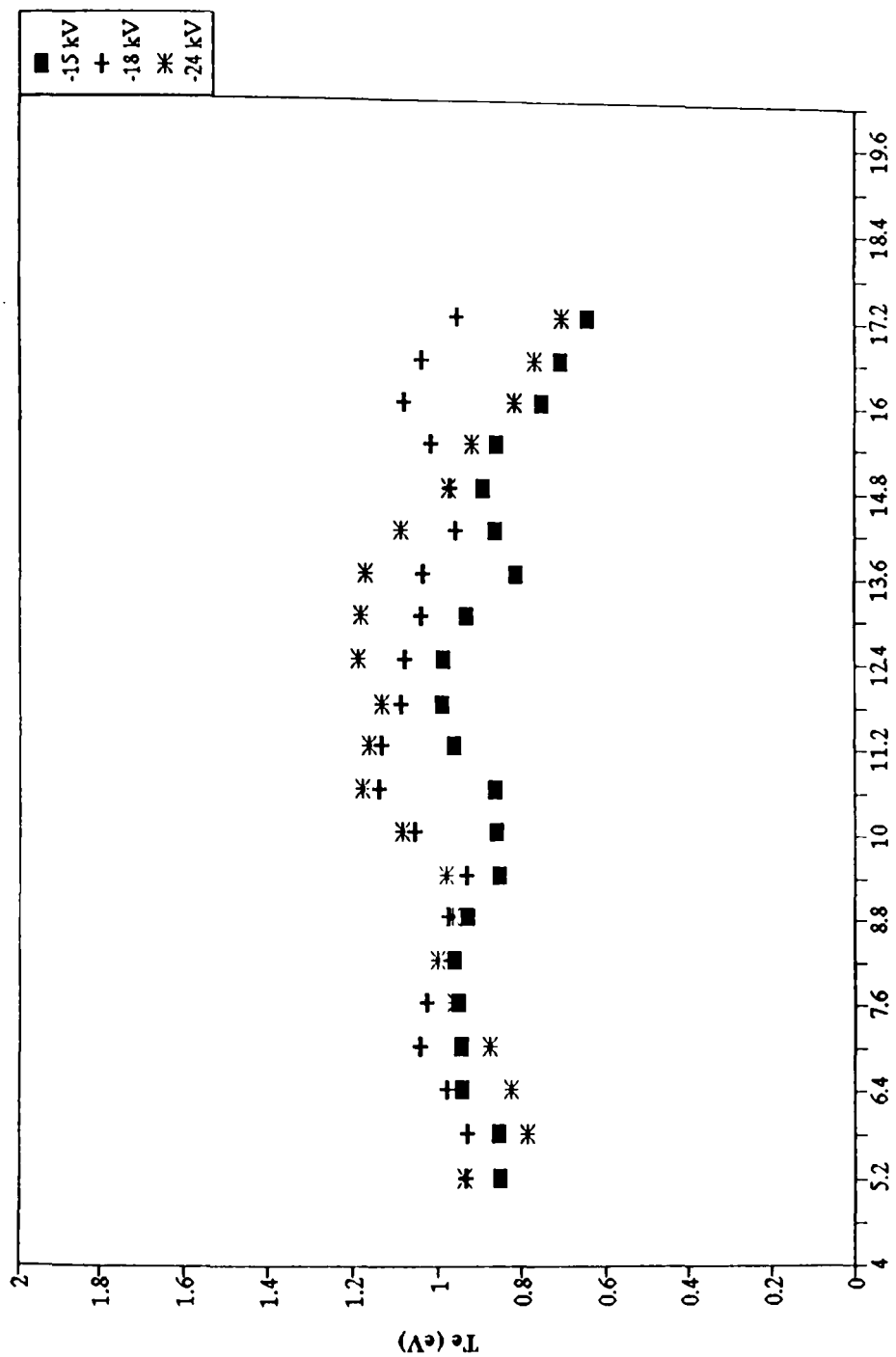

Fig. 33
Calculated Temperature for Negative Polarity, No Coil

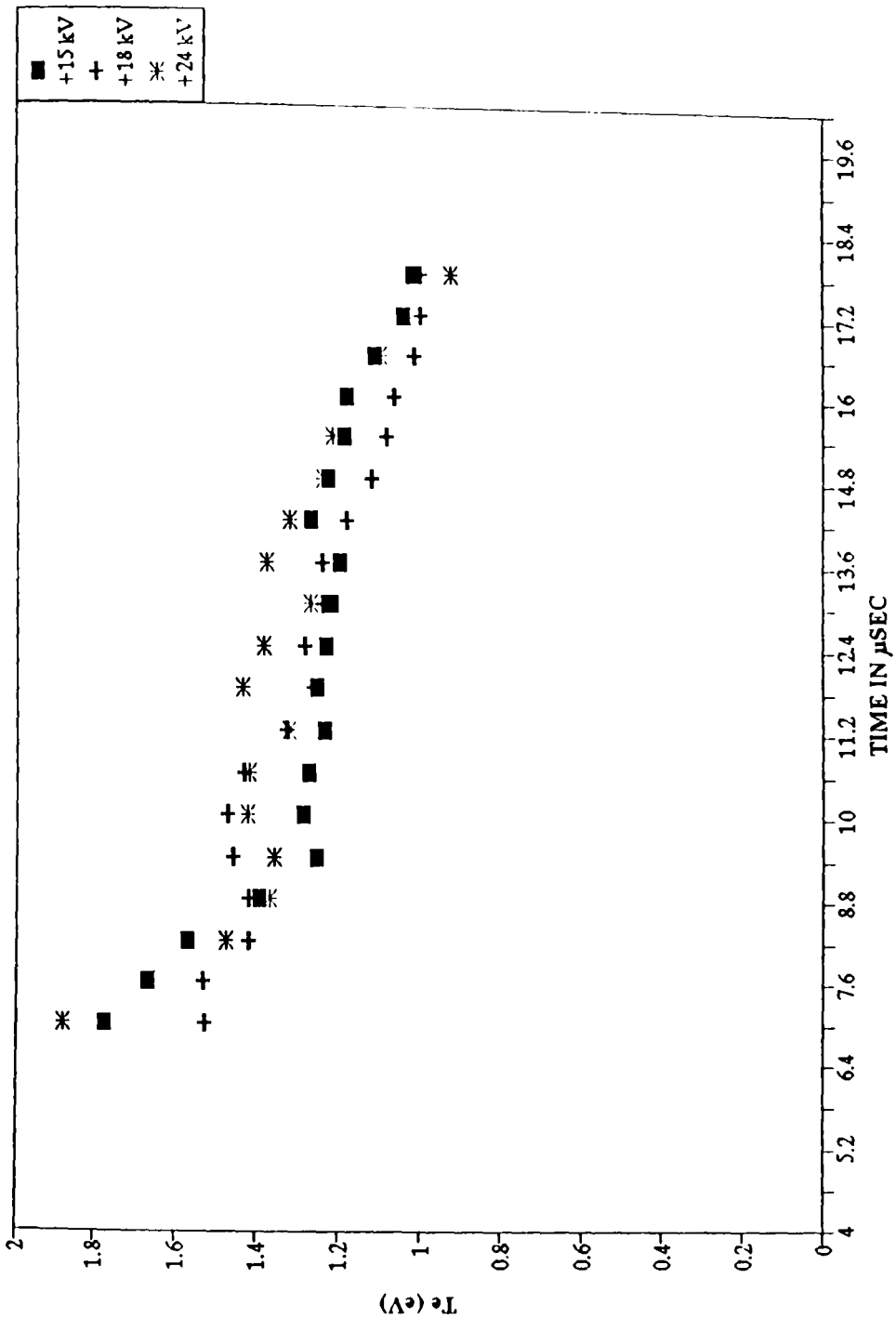

Fig. 34
Calculated Temperature for Positive Polarity, No Coil

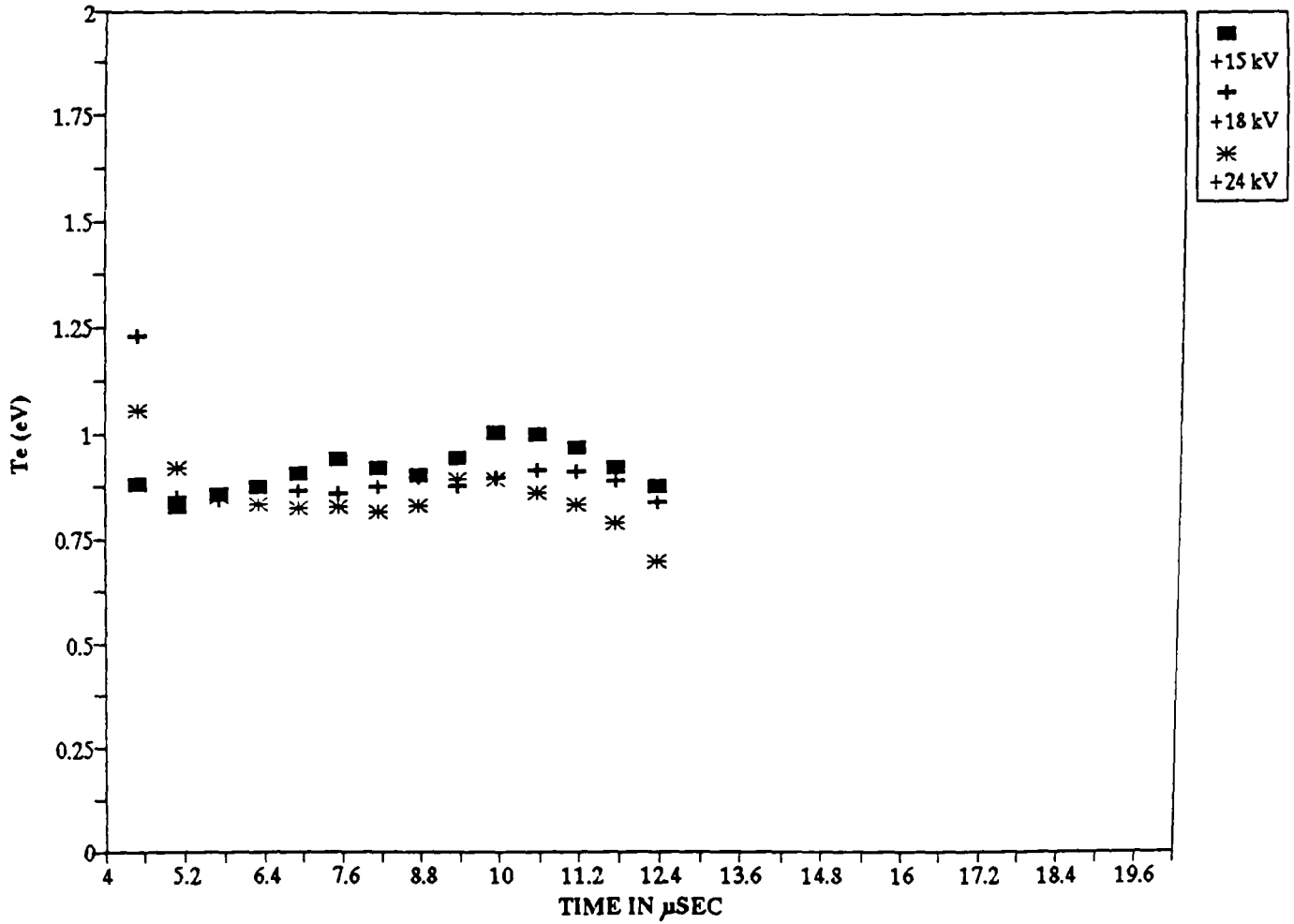

Fig. 35
Calculated Temperature for Negative Polarity, With Coil

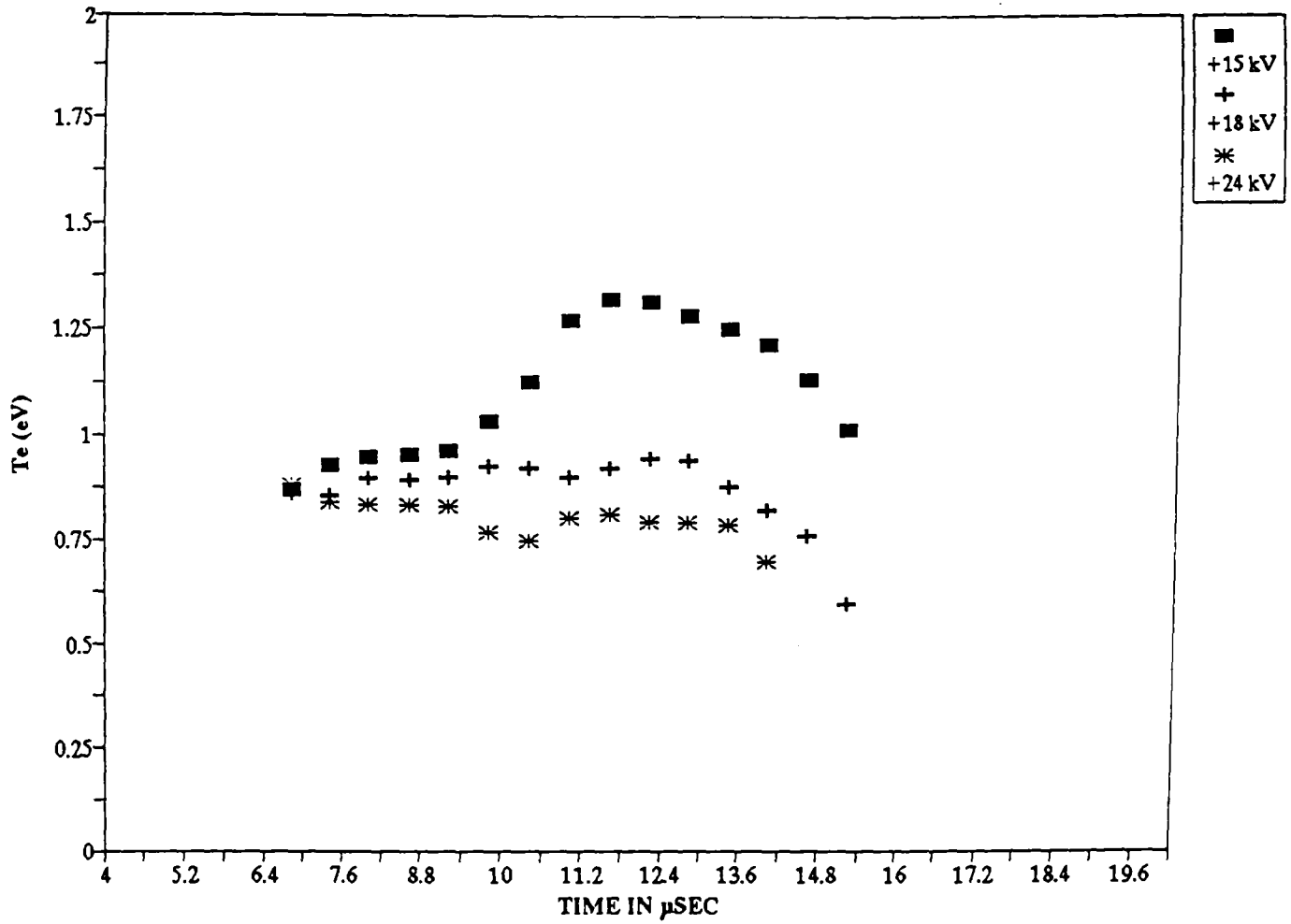

Fig. 36
Calculated Temperature for Positive Polarity, With Coil

also proportional to the plasma density. By simply choosing the arrangement with the smaller temperature, a set-up might be chosen which has a lower than desired density.

Time-of-Flight Results

The most abundant species detected were various oxygen and aluminum ions. Since the insulator is made up of 90% Al_2O_3, the presence of these ions makes sense. In some shots ions from the electrode were detected. These were Ni, Fe, C and W. Of these ions only Ni was detected fairly consistently. Nickel, Ni, from the inner electrode, only appeared for positive polarity. Iron, Fe, and W, from the outer electrode, were detected when the polarity was negative. These materials seems to come consistently from the anode.

As mentioned previously, the only dependence of the detected species on charging voltage was in abundance of the ions. The ions composition itself did not vary. Figs. 37-40 show the current detected, the ion velocity before the acceleration gap, and the mass to charge ratio of the oxygen and aluminum ions for the charging voltage of 24 kV. From these graphs, a similar effect to that mentioned in the section on density is seen with reference to the coil geometry. That is, the coil seems to have a greater effect on the positively charged arrangement. Without the coil, the time range in which the ions are detected is shorter but the magnitude is greater,

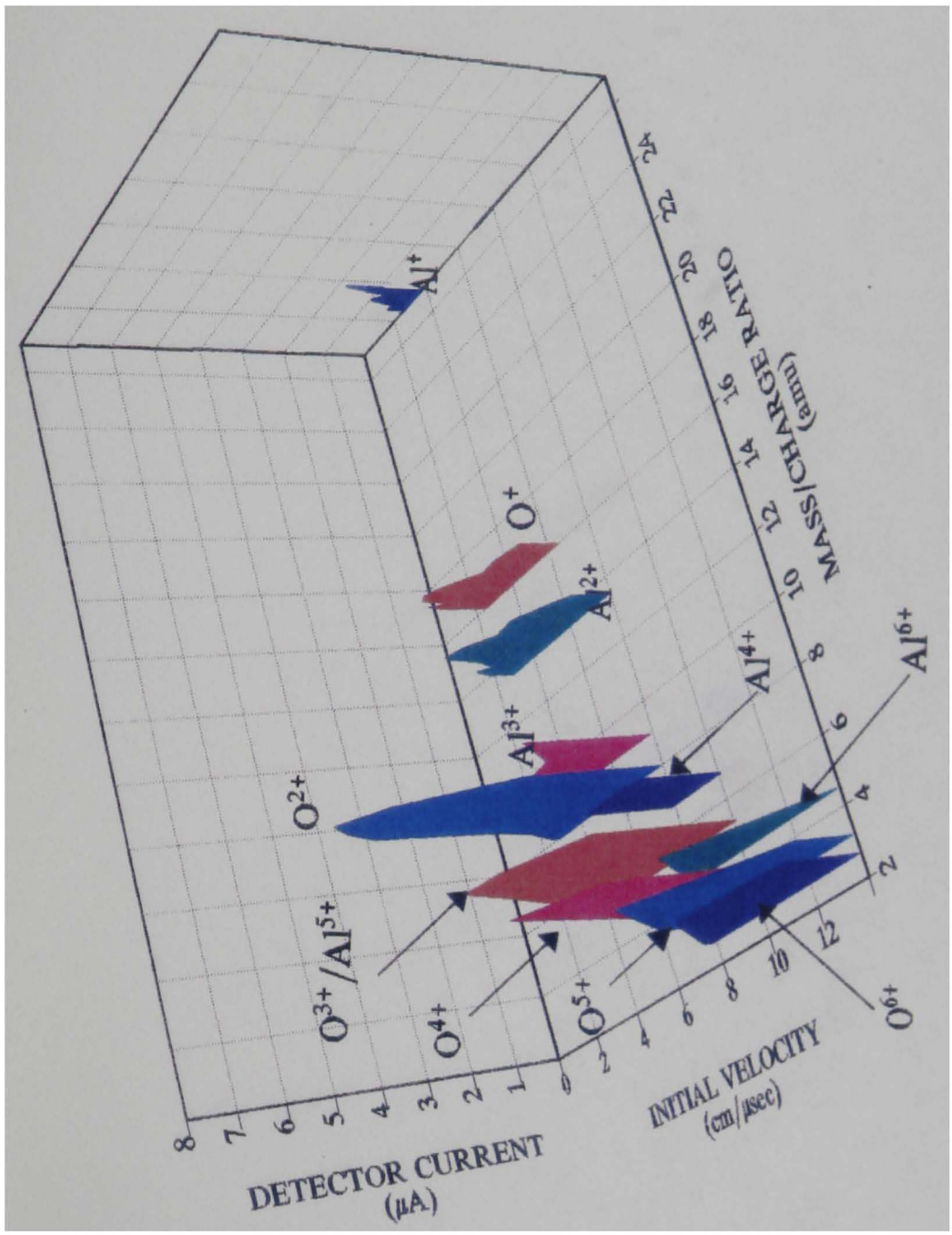

Fig. 37
3-Dimensional Representation of Time-of-Flight Results
Positive Polarity, No Coil

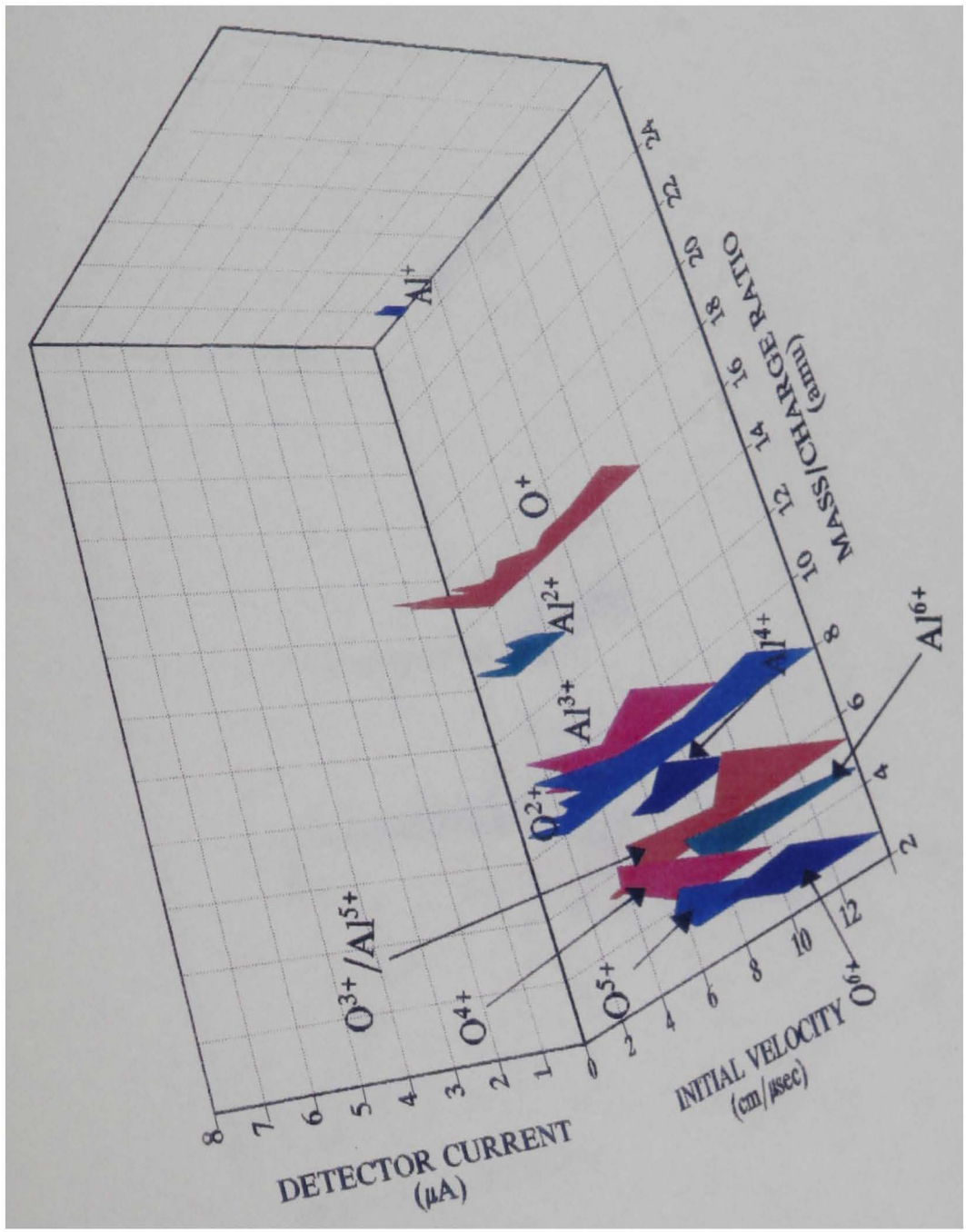

Fig. 38
3-Dimensional Representation of Time-of-Flight Results
Positive Polarity, With Coil

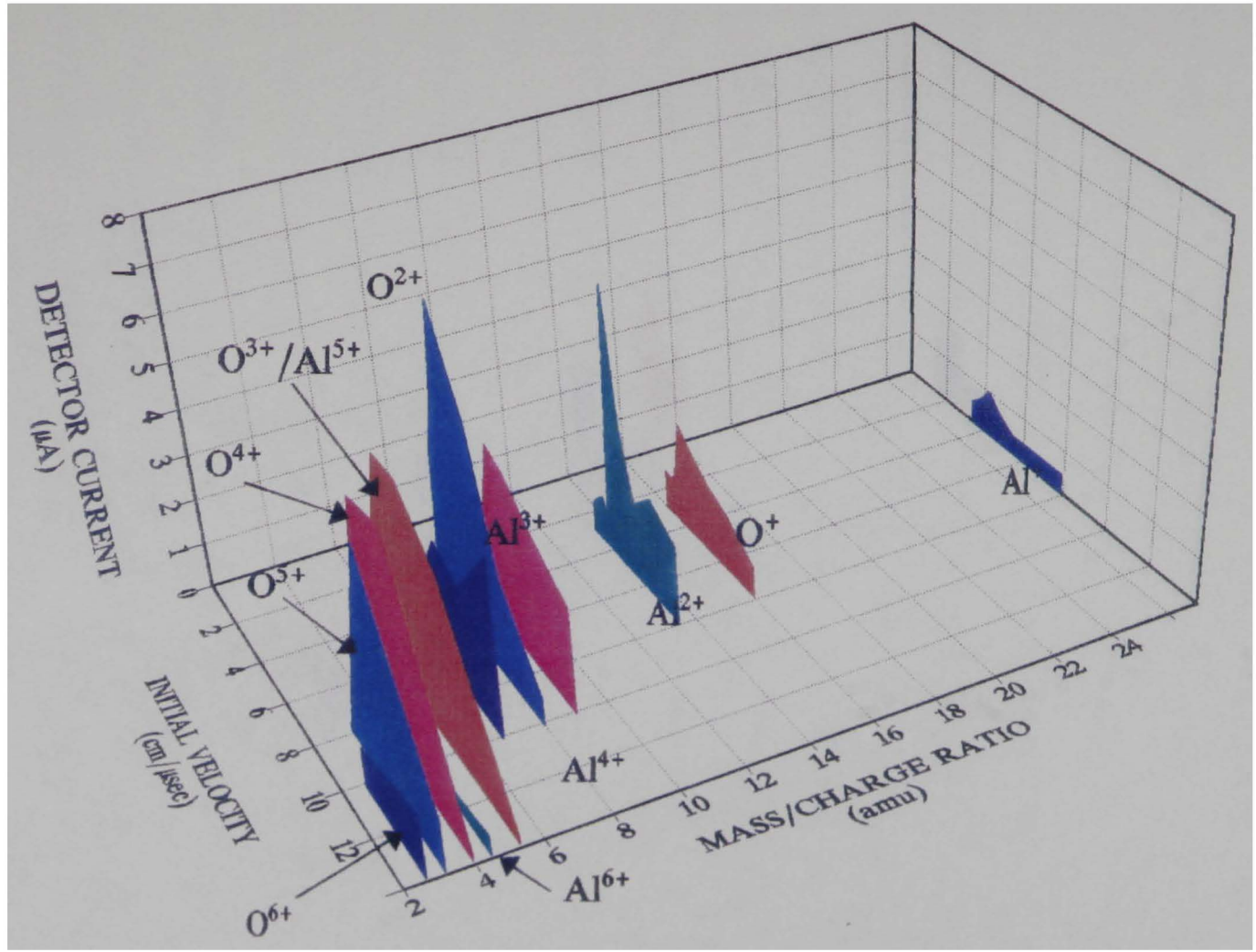

Fig. 39
3-Dimensional Representation of Time-of-Flight Results
Negative Polarity, No Coil

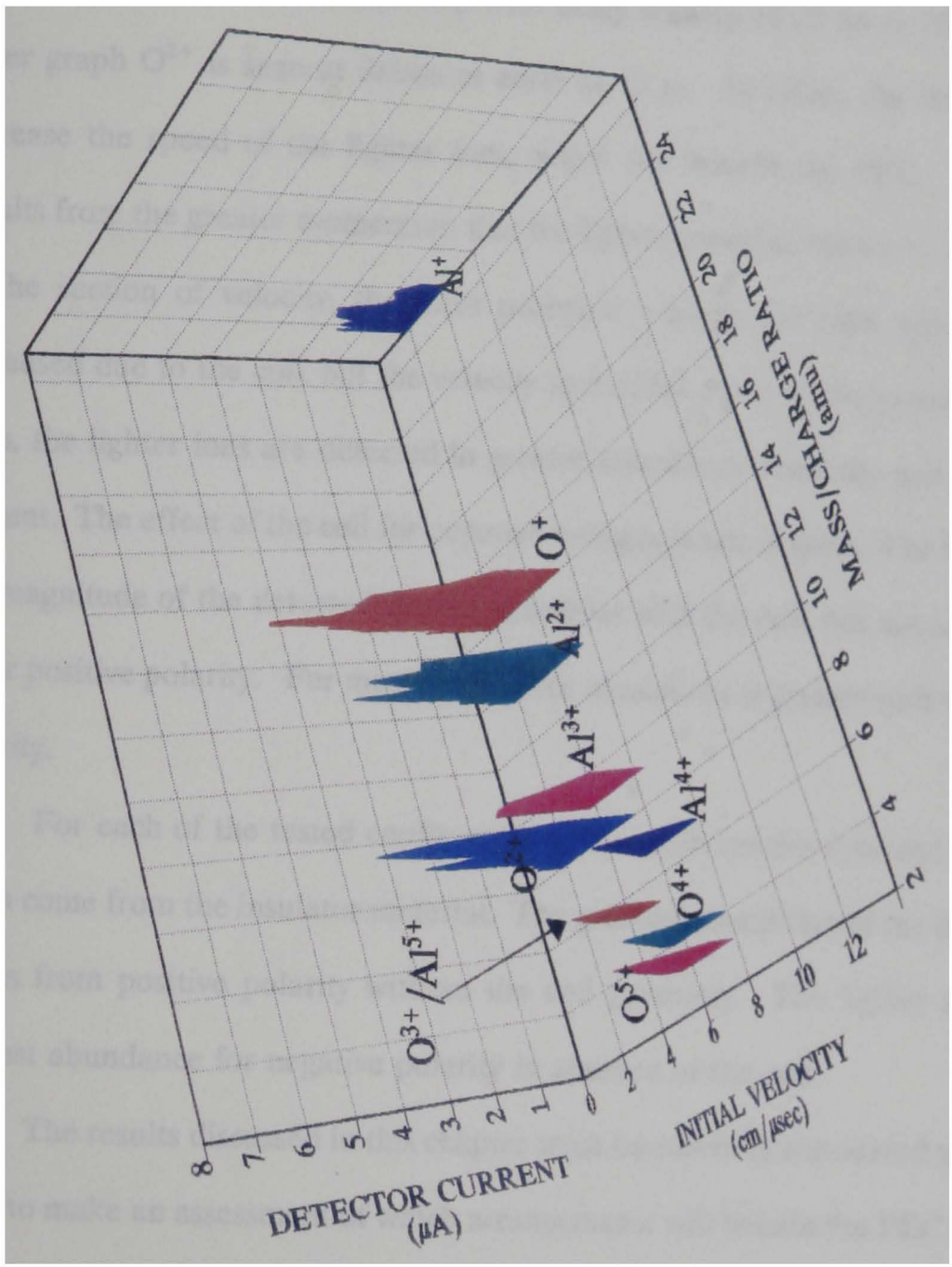

Fig. 40
3-Dimensional Representation of Time-of-Flight Results
Negative Polarity, With Coil

especially for slow ion species. The plasma seems to be more evenly distributed over time and, therefore, over velocity. For example, compare O^{2+} if Figs. 37 and 38. In Fig. 37 this species is detected only with delay settings of 33 μs to 103 μs. In the other graph O^{2+} is seen at delays as early as 13 μs. In effect, the coil appears to increase the speed of the lighter ions, which will benefit the PEC. This benefit results from the greater momentum that the lighter particles will have. As discussed in the section of velocity, the most probable velocity for each species was not increased due to the coil, but the velocity spread for many of the species increased. Also, the lighter ions are detected in greater abundance when the coil geometry is present. The effect of the coil for negative voltages is not as great. For this polarity, the magnitude of the detected species is smaller with the coil, but not as drastically as for positive polarity. For most species, the abundance is greater with the negative polarity.

For each of the tested configurations, the main species detected were those which come from the insulator material. The greatest abundance of the heavier ions results from positive polarity without the coil geometry. The lighter ions are in greatest abundance for negative polarity in absence of the coil.

The results discussed in this chapter must be carefully considered together, in order to make an assessment of which arrangements will benefit the PEC in the best ways. Density, velocity, temperature and species composition all affect the effectiveness of the PEC in different ways. It may be necessary to make further

measurements in the future to increase the understanding of the observed results to fully utilize the benefits of each configuration.

CHAPTER V

CONCLUSIONS

The characteristics of a surface flashover plasma have been measured for various source arrangements. The most desirable plasma for the PEC has high density and velocity and is composed of ions with sufficient momentum to pass the extraction region. The plasma temperature also plays a role in determining the maximum current density which can be extracted from the plasma.

The arrangement which results in the highest density, close to 1 x 10^{13} cm^{-3}, at the desired distance from the source, is a negatively charged gun without the coil geometry attached. This configuration also produces the fastest plasma with the peak flux traveling at around 7 cm/μsec. The coil does not have a significant effect on the density or the speed of the plasma. Perhaps the most noticeable effect of the coil can be seen in the species detection. The level of current measured in the detector is smaller for most all species when the coil is in place and the species appear to be more evenly spread throughout the plasma. Even though the coil does not increase the density or velocity, it might be desirable to have a plasma with a more consistent composition throughout the pulse. Further experimentation will have to be done to see if a benefit is achieved for the PEC in this respect.

The temperature did not depend greatly upon the charging voltage level for each source configuration. Actually, the temperature averaged between 1 eV and 1.2 eV for all configurations. A positive gun resulted in a higher temperature than a

negative gun. Also, the measured temperature was, in general, somewhat lower when the coil was in place. The temperature measurement in a single shot by use of a triple probe is one of the main accomplishments in this work. The agreement between the triple probe measurements made here and the double probe measurements by M. Grothaus [3] is good. For a positive gun and no coil, the double probe measured temperatures between .9 eV and 1.6 eV over time. The triple probe measurement results varied between 1 eV and 1.8 eV for the same configuration. Since, the triple probe method is reliable and saves a substantial amount of time in measurements and calculations, further development and use of this technique would be advantageous in future experimentation.

In conclusion, the ceramic plasma source produces highly charged aluminum and oxygen ions, which have sufficient momentum to pass the extraction region with tolerable deflection, for all source configurations. The density and temperature measurement show values which approach those mentioned in Chapter I for theoretical current extraction of 100 A/cm^2. It was mentioned that this current density could be achieved with a temperature of 1 eV and a density of 4×10^{13} cm^{-3}. Each configuration affects the plasma in different ways. The negative gun without the coil is the leading choice with the present knowledge.

REFERENCES

1. Zieher, K.W. "A Plasma Edge Cathode Scheme," 1986 IEEE Intl. Conf. on Plasma Science, May 19-21, IEEE Cat. No. 86CH2317-6, p.12.

2. Zieher, K.W. "Proposal of a Simple Plasma Edge Cathode," University of New Mexico, IAPBT 85-2, 1985, (unpublished).

3. Grothaus, M.G. "Experimental Investigation of a Plasma Edge Cathode Scheme for High Current Density, Long Pulse Electron Extraction," Phd. Dissertation, Texas Tech University, Lubbock, Texas, May, 1990.

4. Swift, J.D. and Schwar, M.J. Electrical Probes for Plasma Diagnostics, Am. Elsevier Pub. Co., N.Y., 1969.

5. Buraczyk, D. "Mass Spectrometry of a Fast Plasma Jet," Master's Thesis, Texas Tech University, Lubbock, Texas, May, 1990.

6. Mendel, C.W., Zagar, D.M., Mills, G.W., Humphries, Jr., S., and Goldstein, S.A. "Carbon Plasma Gun," Rev. Sci. Instr., 51(12), Dec., 1980, pp. 1641-1644.

7. Humphries, Jr., S., Mendel, C.W., Kuswa, G.W., and Goldstein, S.A. "High-Intensity Carbon Ion Injector," Rev. Sci. Instr., 50(3), Aug., 1979, pp. 993-996.

8. Baumhakel, R., "Elektromemenission von Intermetallischen Verbindungen bei IonenbeschuB," Zeitschrigt fur Physikk, no. 199, PP. 41-55, Sept. 1966.

9. Chung. P.M., Talbot, L., and Touryan, K.J. Electric Probes in Stationary and Flowing Plasmas: Theory and Application, Springer-Verlag, N.Y., 1975.

10. Chen, F.F. Introduction to Plasma Physics and Controlled Fusion, 2nd Ed., Plenum Press, N.Y., 1985.

11. Chen, Sin-Li, and Sekiguchi, T. "Instantaneous Direct-Display System of Plasma Parameters by Means of a Triple Probe," J. Appl. Phys., 36(8), Aug. 1965, pp. 2362-2375.

12. Kunieda, S., Kawashima, N. and Mori, S. "Research Notes: Electron Temperature Measurement of a Plasma from a Plasma Gun by Means of a Triple Probe," Journal of Nuclear Energy: Part C, Vol. 7, pp. 175-177.

APPENDIX

COMPUTER PROGRAM LISTING

```
10    !*****************************************************************************
20    !******
30    !******                                                                  *******
40    !******                    DATA ACQUISITION PROGRAM                      *******
50    !*****************************************************************************
60    PRINTER IS CRT
70    !
80    !DIMENSION ARRAYS AND SET UP PATH NAMES
90    !
100   FOR R=1 TO 3
101   CLEAR SCREEN
110   OPTION BASE 1
120   DIM V1(8192,2),V2(8192,2),X1(1:8),X2(1:8),X(1:8),X3(1:8),X4(1:8)
130   DIM I1(1000,2),I2(1000,2),Ir(500,2),Ir(1500,2),T(300,2),Spike(15,3,2)
140   INTEGER Func1(1:8192) BUFFER
150   INTEGER Func2(1:8192) BUFFER
180   Jk=0
190   I=0
200   Z=0
210   ASSIGN @Buff1 TO BUFFER Func1(*);FORMAT OFF
220   ASSIGN @Buff2 TO BUFFER Func2(*);FORMAT OFF
250   ASSIGN @Scope2 TO 707
270   ASSIGN @Printer TO 701
280   !
281   INPUT "DO YOU WANT TO ACQUIRE SPECIES DATA?",Sd$
282   IF Sd$="N" THEN GOTO 1900
290   !SET UP SCOPE TO DO MEASUREMENTS
300   !
310   INPUT "ENTER CHARGING VOLTAGE",Cv$
320   INPUT "ENTER SHOT NUMBER",N$
330   PRINT "SETTING UP SCOPE TO DO COMPOSITION MEASUREMENTS"
340   CLEAR 707
350   OUTPUT @Scope2;"STOP"
360   OUTPUT @Scope2;"RECALL 8"
370   INPUT "DELAY SETTING IN USEC FOR SPECIES DETECTION? ",Susec$
380   U$=Susec$&"E-6"
390   OUTPUT @Scope2;"TIM DEL "&U$
400   OUTPUT @Scope2;"ACQ TYPE NORM RESO 6"
410   OUTPUT @Scope2;"WAV SRC MEM1,2 FORM WORD HEAD OFF EOI OFF"
420   OUTPUT @Scope2;"DIG1,2"
430   CLEAR SCREEN
440   PRINT TABXY(25,7),"AFTER TRIGGER HAS OCCURRED,"   ! ADJUST
450   PRINT TABXY(25,8),"  INPUT TIME/DIV IN USEC"      ! TIME PER
460   OUTPUT @Scope2;"TIM SENS .5E-6"                    ! DIVISION
470   INPUT Tds$                                         ! AS NEEDED
480   OUTPUT @Scope2;"TIM SENS "&Tds$&"E-6"              ! TO VIEW
490   INPUT "OK? (Y/N)",Tdyns$                           ! OUTPUT IN
```

```
500   IF Tdyns$="Y" THEN 560
510   IF Tdyns$="N" THEN                                    ! BEST
520     CLEAR SCREEN                                        ! POSSIBLE
530     GOTO 450                                            ! FASHION
540   END IF
550   GOTO 450
560   INPUT "SAVE SPECIES DATA? (Y/N)",A$
570   CLEAR SCREEN
580   !
590   !TRANSFER DATA AND PARAMETERS FROM SCOPE TO BUFFERS AND CONVERTS
600   !DATA TO VOLTAGE TIME PAIRS
610   !
620   IF A$="Y" THEN
630     PRINT "AQUIRING CHANNEL 1 FROM SCOPE2 FOR SPECIES "
640     OUTPUT @Scope2;"WAV SRC MEM1 FORM WORD HEAD OFF EOI OFF"
650     Ch$="CHAN1"
660     GOSUB Scope_setup
670     MAT X1= X
680     OUTPUT @Scope2;"WAV SRC MEM1 FORM WORD HEAD OFF EOI OFF"
690     OUTPUT @Scope2;"DATA?"
700     TRANSFER @Scope2 TO @Buff1;COUNT 8192,WAIT
710     ASSIGN @Buff1 TO *
720     PRINT "AQUIRING CHANNEL 2 FROM SCOPE2 FOR SPECIES"
730     OUTPUT @Scope2;"WAV SRC MEM2 FORM WORD HEAD OFF EOI OFF"
740     Ch$="CHAN2"
750     GOSUB Scope_setup
760     MAT X2= X
770     OUTPUT @Scope2;"WAV SRC MEM2 FORM WORD HEAD OFF EOI OFF"
780     OUTPUT @Scope2;"DATA?"
790     TRANSFER @Scope2 TO @Buff2;COUNT 8192,WAIT
800     ASSIGN @Buff2 TO *
810     GOSUB Convert
820     !
830     !SET HALF OF ACCELERATOR PULSE WIDTH AS TIME ZERO REFERENCE
840     !
850     PRINT "FINDING TIME ZERO REFERENCE"
860 Find_time0:!
870     I=I+1
880     IF V2(I,2)<-2 AND V2(I+1,2)<-2 AND V2(I+2,2)<-2 THEN Calc_time0
890     GOTO Find_time0
900     INPUT "DO YOU WANT A HARDCOPY OF SPECIES INFORMATION?",Hc$
910     IF Hc$="N" THEN GOTO 1100
920 Calc_time0:  !
930     Time0=V2(I,1)+5.2E-8                    !APPROX. HALF WIDTH OF PULSE
940     D$=VAL$(Time0)                          !CONVERT TO STRING$ DATA
950     OUTPUT @Scope2;"TIM DEL "&D$             !SET SCOPE TO THIS DELAY
960     OUTPUT @Printer;CHR$(27)&"(s1B";CHR$(27)&"&l1S"
961     OUTPUT @Printer;"CHARGING VOLTAGE IS  ";Cv$;"KVOLTS"
970     OUTPUT @Printer;"TIME DELAY OF APPROX. ";Susec$;" uSEC";"  SHOT # ";N$
```

```
980     OUTPUT @Printer;CHR$(10);CHR$(13);"TIMEBASE= ";Td$;" uSEC/DIV"
990     OUTPUT @Printer;CHR$(10);CHR$(27)&"&l0S"
1000    WAIT 1
1010    CLEAR @Scope2
1020    OUTPUT @Scope2;"PRINT"                          !PRINT OUT
1030    SEND 7;UNL UNT                                  !A HARDCOPY
1040    SEND 7;LISTEN 1                                 !OF THE SCOPE
1050    SEND 7;TALK 7                                   !SCREEN ON THE
1060    SEND 7;DATA                                     !THINK JET
1070    CLEAR SCREEN
1080    PRINT TABXY(25,8);"HARDCOPY IN PROGRESS..."
1090    !
1100    !
1110    !FIND SPIKES AND LOCATE 50% POINT ON FRONT OF SPIKE
1120    !
1130    CLEAR SCREEN
1140    PRINT "ANALYZING WAVEFORM FOR SPECIES INDUCED SPIKES"
1150    Time1=VAL(Susec$)                 ! USE DELAY TIME ENTERED EARLIER
1160    Vel1=1.81/(Time1*1.E-6)           ! TO CALCULATE APPROX. PLASMA VELOCITY
1170    Time2=1.9/Vel1                    ! AND FIND TIME WHEN IT ENTERS THE EMP
1180 Calc_spike_time: !
1190    Z=Z+1
1200    IF Z>8100 THEN End_spike
1210    IF V1(Z,1)>Time0+Time2 THEN
1220      PRINT "PLASMA ENTERS EMP AT ";V1(Z,1)-Time0
1230      WAIT 1
1240      GOTO End_spike
1250    END IF
1260    Y=Z
1270    IF V1(Z+15,2)-V1(Z,2)<-2.8E-3 THEN Find_half      ! CHECK dV/dt
1280    GOTO Calc_spike_time
1290 Find_half: !
1300    IF (V1(Z,1)-Time0)<2.E-6 THEN Calc_spike_time     ! SPIKE IS TOO EARLY
1310    Y=Y+1                                             ! SO IGNORE IT
1320    K=0
1330    FOR K=0 TO 10                                   ! MAKE SURE SLOPE IS
1340      IF V1(Y+K,2)>V1(Y+K+1,2) THEN Find_half       ! NEGATIVE UNTIL A LOCAL
1350    NEXT K                                          ! MIN IS FOUND, THEN
1360    !PRINT "LOCATED SPIKE AT",V1(Y,1)-Time0         ! THIS IS TIME OF SPIKE
1370    Vhalf=(V1(Y,2)+V1(Z,2))/2                 ! FIND 50% POINT OF SPIKE
1380    IF ABS(V1(Y,2)-Vhalf)<.0025 THEN      ! IF 50% IS TOO SMALL, IGNORE SPIKE
1390 Ignore:    !
1400      !PRINT "SPIKE IGNORED"
1410      GOTO Calc_spike_time
1420    END IF
1430    FOR J=Z TO Y
1440      IF V1(J,2)<Vhalf THEN Calc_time    ! FIND TIME CORRESPONDING TO 50%
1450    NEXT J
1460!
```

```
1470!FILL ARRAYS WITH VOLTAGE TIME PAIRS OF SPIKE MIN, MAX, AND 50% POINT
1480!
1490 Calc_time: !
1500     IF V1(Y,1)-V1(J,1)<1.5E-8 THEN Ignore
1510     Jk=Jk+1
1520     Spike(Jk,1,1)=V1(Z,1)-Time0
1530     Spike(Jk,1,2)=V1(Z,2)
1540     Spike(Jk,2,1)=V1(J,1)-Time0
1550     Spike(Jk,2,2)=Vhalf
1560     Spike(Jk,3,1)=V1(Y,1)-Time0
1570     Spike(Jk,3,2)=V1(Y,2)
1580     Z=Y+15                                  !GO TO OTHER SIDE OF THE SPIKE
1590     GOTO Calc_spike_time                    !LOOK FOR THE NEXT SPIKE
1600 End_spike:!
1610     !
1620     !OUTPUT SPIKE DATA TO THE PRINTER
1630     !
1640     CLEAR SCREEN
1650     PRINT TABXY(10,8);"STRIKE ENTER KEY IF HARDCOPY IS COMPLETE"
1660     INPUT Null$
1670     PRINTER IS 701
1680     PRINT ""
1690     PRINT ""
1700     PRINT ""
1710     PRINT ""
1720     PRINT "                                                 **********"
1730     PRINT "SPIKE              MIN                           **      50%      **
    MAX "
1740     PRINT "NUMBER        TIME      VOLTS                    **TIME      VOLTS**          T
IME      VOLTS"
1750     PRINT "                                                 **********"
1760     PRINT CHR$(27)&"&l2S"
1770     PRINTER IS 701;WIDTH 142
1780     IMAGE  4X,K,17X,MD.DDDESZZ,8X,MD.DDDESZZ,16X,MD.DDDESZZ,8X,MD.DDDESZZ,18
X,MD.DDDESZZ,8X,MD.DDDESZZ
1790     FOR Jm=1 TO J1
1800       PRINT USING 1780;Jm,Spike(Jm,1,1),Spike(Jm,1,2),Spike(Jm,2,1),Spike(Jm
,2,2),Spike(Jm,3,1),Spike(Jm,3,2)
1810     NEXT Jm
1820     PRINT CHR$(27)&"&l0S"
1830     PRINT USING "@,#"
1840     PRINTER IS CRT
1850     GOTO 1881
1860   ELSE
1870     GOTO 1881
1880   END IF
1881   NEXT R
1900   PRINT "SETTING UP SCOPE FOR TEMPERATURE MEASUREMENTS"
1910   INPUT "HAVE YOU CHANGED SCOPE INPUTS?",C1$
```

```
1920  IF C1$="Y" THEN GOTO 1980
1930     PRINT "CHANGE SCOPE INPUTS"
1940     GOTO 1910
1980  !
1981  K1=0
1982  Kj=0
1983  K1=0
1990  INTEGER Func3(1:1000) BUFFER
1991  INTEGER Func4(1:1000) BUFFER
1992  ASSIGN @Buff3 TO BUFFER Func3(*);FORMAT OFF
1993  ASSIGN @Buff4 TO BUFFER Func4(*);FORMAT OFF
1995  OUTPUT @Scope2;"RECALL 7"
1996  INPUT "TEMPERATURE PROBE1 VOLTAGE SETTING?",P1
1997  INPUT "TEMPERATURE PROBE2 VOLTAGE SETTING?",P2
1998  OUTPUT @Scope2;"ACQ TYPE NORM RESO 7"
1999  OUTPUT @Scope2;"WAV SRC MEM1,2 FORM WORD HEAD OFF EOI OFF"
2000  OUTPUT @Scope2;"DIG 1,2"
2001  !
2002  CLEAR SCREEN
2003  PRINT TABXY(25,7),"AFTER TRIGGER HAS OCCURRED"
2004  INPUT "KEEP THIS SHOT?",S$
2005  IF S$="Y" THEN GOTO 2007
2006  IF S$="N" THEN GOTO 1990
2007  PRINT TABXY(25,8),"INPUT DESIRED TIM/DIV IN uSEC FOR TEMP"
2008  INPUT Dt$
2009  OUTPUT @Scope2;"TIM SENS "&Dt$&"E-6"
2010  INPUT "OK? (Y/N)",Ok$
2011  IF Ok$="Y" THEN 2017
2012  IF Ok$="N" THEN
2013     CLEAR SCREEN
2014     GOTO 2007
2015  END IF
2016  !
2017  INPUT "ENTER DESIRED TIME DELAY IN uSEC",De$
2018  OUTPUT @Scope2;"TIM DEL "&De$&"E-6"
2019  INPUT "OK? (Y/N)",Ok2$
2020  IF Ok2$="Y" THEN 2025
2021  IF Ok2$="N" THEN
2022     CLEAR SCREEN
2023     GOTO 2017
2024  END IF
2025  !
2026  !TRANSFER TEMPERATUERE DATA
2027  PRINT "ACQUIRING CHANNEL 1 FOR TEMPERATURE"
2028  OUTPUT @Scope2;"WAV SRC MEM1 FORM WORD HEAD OFF EOI OFF"
2029  Ch$="CHAN1"
2030  GOSUB Scope_setup
2031  MAT X3= X
2032  OUTPUT @Scope2;"WAV SRC MEM1 FORM WORD HEAD OFF EOI OFF"
```

```
2033  OUTPUT @Scope2;"DATA?"
2034  TRANSFER @Scope2 TO @Buff3;COUNT 1000,WAIT
2035  ASSIGN @Buff3 TO *
2036  PRINT "ACQUIRING CHANNEL 2 FOR TEMPERATURE"
2037  OUTPUT @Scope2;"WAV SRC MEM2 FORM WORD HEAD OFF EOI OFF"
2038  Ch$="CHAN2"
2039  GOSUB Scope_setup
2040  MAT X4= X
2041  OUTPUT @Scope2;"WAV SRC MEM2 FORM WORD HEAD OFF EOI OFF"
2042  OUTPUT @Scope2;"DATA?"
2043  TRANSFER @Scope2 TO @Buff4;COUNT 1000,WAIT
2044  ASSIGN @Buff4 TO *
2045  GOSUB Current
2046  GOSUB Temp
2047  OUTPUT @Scope2;"LOCAL"
2048  PRINT "ADJUST WAVEFORM FOR PRINTING. PRESS ENTER WHEN READY"
2049  INPUT Null$
2051  OUTPUT @Scope2;"REMOTE"
2052  INPUT "DO YOU WANT A PRINT OUT OF TEMPERATURE WAVEFORMS?",W$
2053  IF W$="N" THEN GOTO 2071
2054  OUTPUT @Printer;CHR$(27)&"(s1B";CHR$(27)&"&l1S"
2055  OUTPUT @Printer;"PROBE #1  ";P1;"  VOLTS.  PROBE #2  ";P2;"  VOLTS."
2056  OUTPUT @Printer;"TIME DELAY OF  ";De$;" uSEC";"  SHOT # ";N$
2057  OUTPUT @Printer;CHR$(10);CHR$(13);"TIMEBASE- ";Dt$;" uSEC/DIV"
2058  OUTPUT @Printer;CHR$(10);CHR$(27)&"&l0S"
2059  WAIT 1
2060  CLEAR @Scope2
2061  OUTPUT @Scope2;"PRINT"
2062  SEND 7;UNL UNT
2063  SEND 7;LISTEN 1
2064  SEND 7;TALK 7
2065  SEND 7;DATA
2066  CLEAR SCREEN
2067  PRINT TABXY(25,7);"HARDCOPY IN PROGRESS"
2068  !
2069  !PRINT RESULTS
2070  !
2071  INPUT "PRESS ENTER WHEN HARDCOPY IS COMPLETE",A$
2072  !
2073  PRINTER IS 701
2074  PRINT ""
2075  PRINT ""
2076  PRINT ""
2077  PRINT ""
2078  PRINT "                    CURRENT RATIOS & TEMPERATURES  VERSUS TIME"
2079  N1=((X3(8)-X3(5))/X3(1))+X3(3)
2080  N2=((X4(8)-X4(5))/X4(1))+X4(3)
2081  PRINT "      IR                    I                    TIME"
2082  FOR K=1 TO 105 STEP 3
```

```
2083     IMAGE 4X,MD.DDDESZZ,10X,MD.DDDESZZ,10X,MD.DDDESZZ
2084     PRINT USING 2083;Ir(K,2),I(K,2),Ir(K,1)
2085   NEXT K
2086   PRINTER IS CRT
2087   GOTO End_prog
2088   !!!!!!!!!!!!!!!!!!!!!!!!!!!!!!!!!!!!!!!!!!!!!!!!!!!!!!!!!!!!!!!!!!!!!!!!!
2089   !                   SUBROUTINES
2090   !!!!!!!!!!!!!!!!!!!!!!!!!!!!!!!!!!!!!!!!!!!!!!!!!!!!!!!!!!!!!!!!!!!!!!!!!
2091   !
2092 Scope_setup:                 ! LOADS IN PARAMETERS FROM THE O-SCOPE
2093   PRINT "PARAMETERS TRANSFERRING..."
2094   OUTPUT @Scope2;"XINC?"
2095   ENTER @Scope2;X(1)
2096   OUTPUT @Scope2;"YINC?"
2097   ENTER @Scope2;X(2)
2100   OUTPUT @Scope2;"XREF?"
2110   ENTER @Scope2;X(3)
2120   OUTPUT @Scope2;"YREF?"
2130   ENTER @Scope2;X(4)
2140   OUTPUT @Scope2;"XORG?"
2150   ENTER @Scope2;X(5)
2160   OUTPUT @Scope2;"YORG?"
2170   ENTER @Scope2;X(6)
2180   OUTPUT @Scope2;Ch$
2190   OUTPUT @Scope2;"RANGE?"
2200   ENTER @Scope2;X(7)
2210   OUTPUT @Scope2;"TIMEBASE"
2220   OUTPUT @Scope2;"DEL?"
2230   ENTER @Scope2;X(8)
2240   RETURN
2250   !
2260   !!!!!!!!!!!!!!!!!!!!!!!!!!!!!!!!!!!!!!!!!!!!!!!!!!!!!!!!!!!!!!!!!!!!!!!!!
2270   !
2280 Convert:                     ! CONVERT DATA TO VOLTAGE TIME PAIRS
2290   PRINT "CONVERTING TO VOLTAGE TIME PAIRS..."
2300   PRINT "                         CHAN1..."
2310   FOR Ki=1 TO 8192
2320     V1(Ki,2)=((Func1(Ki)-X1(4))*X1(2))+X1(6)
2330     V1(Ki,1)=((Ki-X1(3))*X1(1))+X1(5)
2340   NEXT Ki
2350   PRINT "                         CHAN2..."
2360   FOR Kk=1 TO 8192
2370     V2(Kk,2)=((Func2(Kk)-X2(4))*X2(2))+X2(6)
2380     V2(Kk,1)=((Kk-X2(3))*X2(1))+X2(5)
2390   NEXT Kk
2400   RETURN
2401 Current: !
2402   PRINT "CONVERTING DATA TO CURRENT ARRAYS..."
2403   PRINT "CHAN1"
```

```
2404  FOR Ki=1 TO 1000
2405  T1=((Ki-X3(3))*X3(1))+X3(5)
2406  IF T1<X3(8) THEN GOTO 2409
2407  I1(Ki,2)=((((Func3(Ki)-X3(4))*X3(2))+X3(6)))/13.8
2408  I1(Ki,1)=((Ki-X3(3))*X3(1))+X3(5)
2409  NEXT Ki
2410  PRINT "CHAN2"
2411  FOR Kk=1 TO 1000
2412  T2=((Kk-X4(3))*X4(1))+X4(5)
2413  IF T2<X4(8) THEN GOTO 2416
2414  I2(Kk,2)=((((Func4(Kk)-X4(4))*X4(2))+X4(6)))/13.8
2415  I2(Kk,1)=((Kk-X4(3))*X4(1))+X4(5)
2416  NEXT Kk
2417  N1=((X3(8)-X3(5))/X3(1))+X3(3)
2418  N2=((X4(8)-X4(5))/X4(1))+X4(3)
2419  FOR Kj=1 TO 500
2420  ON ERROR GOTO 2424
2422  Ir(Kj,2)=((2*I1(Kj+N1,2))+I2(Kj+N2,2))/(I1(Kj+N1,2)+(2*I2(Kj+N2,2)))
2423  Ir(Kj,1)=I1(Kj+N1,1)
2424  NEXT Kj
2425  RETURN
2426 Temp: !
2427  PRINTER IS CRT
2428  PRINT "CREATING TEMPERATURE RATIO ARRAY"
2429  Z=.01
2430  FOR G=1 TO 1500
2431  E1=(1-(EXP((-1.6E-19*P1)/(11600*1.38E-23*Z))))
2432  E2=(1-(EXP((-1.6E-19*P2)/(11600*1.38E-23*Z))))
2433  R=E1/E2
2434  Tr(G,1)=Z
2435  Tr(G,2)=R
2436  Z=Z+.01
2437  NEXT G
2438  !
2439  PRINT "MATCHING VALUES"
2440  FOR W=1 TO 300
2441  FOR Y=1 TO 1500
2442  IF Ir(W,2)>1 OR Ir(W,2)=1 THEN GOTO 2450
2443  IF Ir(W,2)=Tr(Y,2) THEN GOTO 2447
2444  IF Ir(W,2)<Tr(Y,2) THEN GOTO 2466
2445  IF I1(W,2)<0 OR I2(W,2)<0 THEN GOTO 2467
2446  GOTO 2453
2447  T(W,2)=Tr(Y,1)
2448  T(W,1)=Ir(W,1)
2449  GOTO 2467
2450  T(W,2)=-1.E-1
2451  T(W,1)=Ir(W,1)
2452  GOTO 2467
2453  A=Tr(Y-1,2)
```

```
2454  B=Tr(W,2)
2455  C=Tr(Y,2)
2456  D=Tr(Y-1,1)
2457  F=Tr(Y,1)
2458  Bc=B-C
2459  Ac=A-C
2460  Df=D-F
2461  Ef=(Bc/Ac)*Df
2462  E=Ef+F
2463  T(W,2)=E
2464  T(W,1)=Tr(W,1)
2465  GOTO 2467
2466  NEXT Y
2467  NEXT W
2468  RETURN
2469 End_prog: !
2470  OUTPUT @Scope2;"LOCAL"
2471  INPUT "ANOTHER SHOT?",Yn$
2472  IF Yn$="Y" THEN GOTO 100
2473  CLEAR SCREEN
2474  PRINT TABXY(30,8);"THANK YOU"
2475  STOP
2480  END
```